Université de Montréal

A Brain-Computer Interface for navigation in virtual reality

Bilal Alchalabi
Institut de Génie Biomédical
Université de Montréal

MÉMOIRE PRÉSENTÉ EN VUE DE L'OBTENTION
DU DIPLÔME DE MAÎTRISE ÈS SCIENCES APPLIQUÉES
(GÉNIE BIOMÉDICAL)

Janvie 2013

Université de Montréal
Institut de Génie Biomédical

Ce mémoire intitulé:

"A Brain-Computer Interface for navigation in virtual reality"

Présenté par:
Bilal Alchalabi

a été évalué par un jury composé des personnes suivantes:

Pr. Pierre Savard, président-rapporteur
Pr. Jocelyn Faubert, directeur de recherche
Pr. Mohamad Sawan, membre du jury

Résumé :

L'interface cerveau-ordinateur (ICO) décode les signaux électriques du cerveau requise par l'électroencéphalographie et transforme ces signaux en commande pour contrôler un appareil ou un logiciel. Un nombre limité de tâches mentales ont été détectés et classifier par différents groupes de recherche. D'autres types de contrôle, par exemple l'exécution d'un mouvement du pied, réel ou imaginaire, peut modifier les ondes cérébrales du cortex moteur. Nous avons utilisé un ICO pour déterminer si nous pouvions faire une classification entre la navigation de type marche avant et arrière, en temps réel et en temps différé, en utilisant différentes méthodes. Dix personnes en bonne santé ont participé à l'expérience sur les ICO dans un tunnel virtuel. L'expérience fut a était divisé en deux séances (48 min chaque). Chaque séance comprenait 320 essais. On a demandé au sujets d'imaginer un déplacement avant ou arrière dans le tunnel virtuel de façon aléatoire d'après une commande écrite sur l'écran. Les essais ont été menés avec feedback. Trois électrodes ont été montées sur le scalp, vis-à-vis du cortex moteur. Durant la 1re séance, la classification des deux taches (navigation avant et arrière) a été réalisée par les méthodes de puissance de bande, de représentation temporel-fréquence, des modèles autorégressifs et des rapports d'asymétrie du rythme β avec classificateurs d'analyse discriminante linéaire et SVM. Les seuils ont été calculés en temps différé pour former des signaux de contrôle qui ont été utilisés en temps réel durant la 2^{e} séance afin d'initier, par les ondes cérébrales de l'utilisateur, le déplacement du tunnel virtuel dans le sens demandé. Après 96 min d'entrainement, la méthode « online biofeedback » de la puissance de bande a atteint une précision de classification moyenne de 76 %, et la classification en temps différé avec les rapports d'asymétrie et puissance de bande, a atteint une précision de classification d'environ 80 %.

Mots-clés: Interface cerveau-ordinateur(ICO), synchronisation lié à l'événement, Moteur imaginaire, électroencéphalogramme (EEG), Réalité Virtuelle, Navigation, classification de EEG.

Abstract:

A Brain-Computer Interface (BCI) decodes the brain signals representing a desire to do something, and transforms those signals into a control command. However, only a limited number of mental tasks have been previously detected and classified. Performing a real or imaginary navigation movement can similarly change the brainwaves over the motor cortex. We used an ERS-BCI to see if we can classify between movements in forward and backward direction offline and then online using different methods. Ten healthy people participated in BCI experiments comprised two-sessions (48 min each) in a virtual environment tunnel. Each session consisted of 320 trials where subjects were asked to imagine themselves moving in the tunnel in a forward or backward motion after a randomly presented (forward versus backward) command on the screen. Three EEG electrodes were mounted bilaterally on the scalp over the motor cortex. Trials were conducted with feedback. In session 1, Band Power method, Time-frequency representation, Autoregressive models and asymmetry ratio were used in the β rhythm range with a Linear-Discriminant-analysis classifier and a Support Vector Machine classifier to discriminate between the two mental tasks. Thresholds for both tasks were computed offline and then used to form control signals that were used online in session 2 to trigger the virtual tunnel to move in the direction requested by the user's brain signals. After 96 min of training, the online band-power biofeedback training achieved an average classification precision of 76 %, whereas the offline classification with asymmetrical ratio and band-power achieved an average classification precision of 80%.

Keywords: Brain-Computer Interface, Event-Related Synchronization, Motor Imagery, electroencephalogram(EEG), Virtual Reality, Navigation, EEG classification

Table of Contents:

Chapter 8 Conclusions & future work

List of figures:

List of tables:

List of Abbreviations:

AAR	Adaptive Auto-Regression
AR	Auto-Regression
ARMA	Auto-Regression with Moving Average
ARMAX	Auto-Regression with Moving Average & exogenous output
As.R	Asymmetrical Ratio
ARX	Auto-Regression with exogenous input
BCI	Brain-Computer Interface
BP	Band-Power
CAR	Common Average Reference
CRBF	Cerebral Blood Flow
CSP	Common Spatial Pattern
ECG	Electrocardiogram
EEG	Electroencephalogram
EMG	Electromyogram
EOG	Electrooculogram
ERD	Event Related De-synchronization
ERS	Event Related Synchronization
ERP	Event Related Potential
FES	Functional Electrical Stimulation
Fs	Sampling Frequency
GA	Genetic Algorithm
ICA	Independent Component Analysis
IIR	Infinite Impulse Response
LDA	Linear Discriminant Analysis
LMS	Least Mean Square
MPNN	Multi Perceptron Neural Network
MRP	Movement Related Potential
OC	Operant Conditioning
PCA	Principle Component Analysis
PR	Pattern Recognition
PET	Positron Emission Tomography
PSD	Power Spectral Density
SCP	Slow Cortical Potential
SSAEP	Steady State Auditory Evoked Potential
SSVEP	Steady State Visual Evoked Potential
STDEV	Standard Deviation
STFT	Short Time Fourier Transform
SVM	Support Vector Machine
TFR	Time-Frequency Representation
TH	Threshold
VE	Virtual Environment
VEP	Visual Evoked Potential
VR	Virtual Reality

Remerciments :

Tout d'abord je tiens à remercier une personne spéciale qui m'a soutenu pendant deux ans pour préparer ce mémoire. Prof. Jocelyn Faubert, tu étais un directeur unique avec un magnifique sens de l'humour, qui m'a donné de son précieux temps et m'a motivé à atteindre mes objectifs, merci beaucoup professeur de m'avoir accepté et de m'avoir permis de faire ce projet, merci pour la bourse que tu m'as offerte. J'ai beaucoup appris de toi. Merci beaucoup Isabelle Legault, l'assistante de mon directeur, pour m'avoir aidé plusieurs fois, merci pour tous tes conseils et précieux efforts. Merci beaucoup à mes collègues Rémy Allard et Vadim Sutyushev, qui m'ont aidé dans la programmation.

Merci à mon collègue Frederick Poirier pour tes précieux conseils. Merci à toute l'équipe du laboratoire de Psychophysiques et perception visuelle, pour votre soutien, vos encouragements et pour l'ambiance d'amitié que j'ai trouvé au labo. J'ai vraiment eu beaucoup de plaisir à travailler avec vous.

Je tiens aussi à remercier les différents membres de mon jury d'avoir accepté de juger mon travail et mon mémoire.

Merci mes chers parents, Dr.Abdul Ghani Alchalabi et Dr. Khloud Sarraj, mes précieux cadeaux de dieu. Sans vous, sans votre soutien moral et financier, sans votre encouragement et sagesse, je ne serais pas devenu ce que je suis, je n'aurais pas été ici, et ce mémoire n'aurait jamais été écrit. Depuis l'enfance, vous m'avez toujours inspiré dans la recherche pour le savoir et la science. Je voulais vous rendre fières de moi.

Merci à mes frères et ma sœur, Dr.Omar Alchalabi, Besher Alchalabi et Dr.Maya Alchalabi, les fleurs de la famille, merci pour toutes les belles soirées et pour votre encouragement. Merci pour les succès Maya.

Des mercis très spéciaux à ma nouvelle famille, tant Aeda, oncle Issam, mes nouveaux frère et sœur Dr.Ahmad et Dr.Ola, merci de m'avoir accepté parmi vous et pour m'avoir offert cette très belle ambiance, honneur et le sentiment merveilleux de faire partie de votre famille. Avoir une famille come vous est une bénédiction.

Merci à mon premier directeur de thèse à l'université de Damas, Dr.Basel Douagi, qui m'a accepté au projet de l'année pré-finale du bac. Je ne t'oublierai jamais.

Mon ami Saria Mohammed, tu as été un vrai ami et frère, j'ai eu beaucoup de plaisir à te rencontrer et à passer les weekends avec toi. Merci pour ton encouragement, pour être mon ami et pour le joli poème tu m'as écrit à mon anniversaire.

Quand ce mémoire a été écrit, tu étais un bébé qui était en train de grandir doucement dans le ventre de sa mère, j'ai tellement pensé à toi. Merci mon fils Aboudeh pour venir et remplir notre vie de joie, et me donner le privilège de devenir ton papa.

Les derniers sont les premiers……Un merci spécial, un très gros merci à ma jolie femme adorable, mon amour et inspiration, Dr.Abir, je suis le plus heureux des hommes quand je suis avec toi, merci de m'aimer comme je suis, pour partager avec moi les plus beaux sentiments, merci pour chaque jour et chaque moment, merci pour ton encouragement et soutien pendant ces deux années, et merci pour la fabuleuse cuisine, tu es une femme merveilleuse.

Chapter 1

Introduction

1.1. Background

Can computers really read our minds? Can we ever truly forget our past? Can we control anything in the real world with only our thoughts? Brain-computer interaction has been a hot research concept since the beginning of the computer era. Since the first experiments of Electroencephalography (EEG), i.e. Brain waves recording on humans by Hans Berger in 1929, the idea that brain activity could be used as a communication channel has rapidly gained popularity [24].

However, it is only in 1964 that the first prototype of a Brain-Computer Interface (BCI) came out, in the laboratory of Dr.Grey Walter when he connected the EEG system of a patient to a slide projector so that the slide projector advanced whenever the patient's brain activity indicated that he wanted to do so [8].

A BCI is a communication system that bypasses the body's neuromuscular pathways, measures brain activity associated with the user's intent and translates it into corresponding control signals to an electronic device, only by means of voluntary variations of his brain activity. Such a system appears as a particularly promising communication channel for persons suffering from severe paralysis, like those with the "locked-in" syndrome and, as such, is locked into their own body without any residual muscle control [24]. Therefore, a BCI appears as their only way of communication, where their speech brain activity has been translated to a computer speller [100], [24], as well as their intention of moving their wheelchairs has been translated into real movements of those wheelchairs [24].

Studies to date show that humans can learn to use electroencephalographic activity (EEG) to control the movements of a cursor or other device in one or two dimensions[27],[52],[96],[101],[30]. Both actual movement and activity movement imagery are accompanied by changes in the amplitudes of certain EEG rhythms, specifically 8–12 Hz mu rhythms and 18–30 Hz beta rhythms [35]. These changes are focused over sensorimotor cortex in a manner consistent with the homuncular organization of this cortical region [24].

It was also found that while observing movements performed by others, the observers' cortical motor areas and spinal circuits were activated, reflecting the specific temporal and muscular pattern of the actual movement [10]. The BCIs of Wolpaw's group in Albany and the Graz group are both based on motor imagery and classification of sensorimotor EEG rhythms , where they discovered that motor imagery (imagining a movement) can modify the neuronal activity in the primary sensory-motor areas in a very similar way as observable with a real executed movement [18],[59].

In the 1980s, Wolpaw et al. started on EEG-based cursor control in normal adults using band power centered at 9 Hz. They used an Auto-regressive model to compute power in a specific frequency band, where the sum power was used in a linear function to control the cursor's direction of movement [24]. However, and for the same goal, Yuanqing Li et al. in 2010 have controlled a 2-D cursor using a hybrid BCI, where they used both beta rhythm and P300 signals [101](The P300 is the positive component of the evoked potential that may develop about 300 ms after an item is flashed [5]).

Nowadays, the world of BCI is expanding very rapidly. One new field involves BCIs to control virtual reality (VR), including BCIs for games [37],[51],[84],[23],[29]. Virtual environments (VE) can provide an excellent testing ground for procedures that could be adapted to real world scenarios, especially for patients with disabilities. If people can learn to control their movements or perform specific tasks in a VE, this could justify the much greater expense of building physical devices such as a wheelchair or robot arm that is controlled by a BCI. One of the main goals of implementing BCI in VR is to understand how humans process dynamic visual scenes and how well they can interact with these natural environments. A better understanding of the normal brain will help us decipher the important mechanisms for certain activities such as way finding and reaching gestures that are critical in real life situations. Such basic understanding will also lead to a better understand of how neurodegenerative disorders such as how Alzheimer can influence daily living activities and help us find the right interventions to alleviate the impact of such disorders on quality of life of the patients.

The first efforts to combine VR and BCI technologies were In year 2000 and 2003 by Bayliss and Ballard who introduced a VR smart home in which users could control different things using a P300 BCI [6],[7].

Then in 2003, researchers showed that immersive feedback based on a computer game can help people learn to control a BCI based on imaginary movement more quickly than mundane feedback [42]. In year 2010, researchers used a steady-state visual evoked potential (SSVEP)-based BCI to navigate an avatar in virtual reality to two waypoints along a given path in two runs, by alternately focusing attention on one of three visual stimuli that were flickering at 12, 15 and 20 Hz [40]. Successful classifications of the following classes triggered the associated commands: turn 45° left, turn 45° right and walk one step ahead (Steady-state evoked potentials occur when sensory stimuli are delivered in frequencies high enough that the relevant neuronal structures do not return to their resting states). In [41] the same technique was used to control a character in an immersive 3-D gaming environment

In 2005 researchers in [54] used BCI for walking in a virtual street, in 2007 to visit and navigate in a virtual reality representation of the Austrian National library [76], and exploring a smart virtual apartment using a motor imagery-based BCI in 2009.

In [53] Researchers used the BCI to navigate in virtual reality with only beta waves, where a 35 year old tetraplegic male subject learned to control a BCI, where the mid-central focused beta oscillations with a dominant frequency of approximately 17 Hz allowed the BCI to control VE . Only one single EEG channel was recorded bipolarly at Cz (foot representation area). One single logarithmic band power feature was estimated from the ongoing EEG. A simple threshold (TH) was used to distinguish between foot movement imagination (IC) and rest (INC). This study, which was based only on beta waves, has classified two different mental states: one directional movement (forward) and a rest state but not for backward movement.

Brosseau-Lachine et al in [11] and [12] psychophysically studied Infants and made electrophysiological recordings of brain cells in cats' response to radial optic flow fields, and found superior sensitivity for expansion versus contraction direction of motion in both studies. This is further supported by an imaging study with adults where the researchers have found a bias for expanding motion stimuli [77]. This dissociation may suggest that sensitivity to direction corresponding with forward

locomotion (expansion) develops at a faster rate than the opposite direction encountered when moving backwards (contraction).

Researchers in [77] found with PET scan that several loci of activation were observed for contraction and expansion condition in the same areas of the human brain, but the increase in rCBF in contraction was much lower than in the expansion condition in the right brain. So, we wanted to see in the present study if we could classify those two-directional movements in virtual reality from only 1, 2 or 3 EEG channels. Therefore, the main goal of the present project was to enhance navigation in virtual reality with the brainwaves by using beta ERS obtained from a small number of channels. Further, we wanted to see if we could classify two-directional movements (forward or backwards) in virtual reality from these channels so in the future a subject could efficiently navigate by altering the brain waves, freeing the limbs for other activities.

1.2. Hypothesis and originality

1) It is possible to distinguish and predict single-trial forward and backward movement commands with the methods proposed.
2) Backward commands will require more signal-training to achieve the same strength.
3) Motor imagery of forward-backward movement can activate the motor cortex similarly to real optic flow.

1.3. Objectives

1.3.1. General objective

The aim of the research is to navigate backward and forward in a virtual reality tunnel using biofeedback from the brainwaves.

1.3.2. Specific objectives

1. Design and investigate a short-training motor imagery BCI for navigation in virtual reality with:

- ✓ 3 EEG channels (the later investigation and analysis would reveal if we can rely on 1 or 2 electrodes to use in the BCI).

2. Session1: Acquire EEG during an optic flow moving both forward and backward within a tunnel, and during imaging navigation in the virtual reality
   - ✓ Use features extracted with different feature extraction methods and classification methods using MATLAB on session 1 data
3. Session 2: perform a short band-power training for navigation direction in the tunnel with Biograph (the EEG acquisition and biofeedback software)
   - ✓ Perform offline classification of session 2 data in MATLAB using the session 1 data as training data
4. Compare MATLAB and Biograph efficiencies

After EEG acquisition, pre-processing and processing methods (IIR filtering ,Time-Frequency Representation and Band Power feature extractions) will be conducted via Biograph, then we want to import EEG data to MATLAB, where we will apply signal processing methods (Auto-regression analysis , Band-Power, and power spectral density asymmetrical ratio), and then feed all these features to LDA classifier (Linear Discriminant Analysis) and SVM (Support Vector Machine) in order to classify these signals in an attempt to identify both movements; where we can later threshold the signals to control navigation direction in virtual reality.

1.4. Thesis Outline

Chapter 2 of this thesis will go through the main principals and methods of recording brain waves, as well as locations of recordings on the scalp in relation with the brain anatomy and physiological functions. Chapter 3 will introduce Brain computer Interfaces (BCI) and explain the fundamental approaches of BCI design and control, then the fourth chapter will go through some of the main signal processing techniques used in pre-processing, feature extraction and selection, and classification of signals [5], where these techniques are implemented in some BCI applications illustrated in the fifth chapter of the thesis, followed by chapter 6 which presents some BCI applications in Virtual Reality. Finally, chapter 7 presents the

experiments conducted for this research as well as the results, where the discussions and conclusion will be presented in chapter 8 of the thesis.

Chapter 2

Electroencephalography (EEG)

2.1. History

Richard Caton, In 1887, had recorded the first brain very-low-Amplitude electrical activity from the cerebral cortex of an experimental animal. In 1924 in Austria, the first human EEG recordings using metal strips pasted to the scalps of the subjects as electrodes were carried out by Hans Berger. He used a sensitive galvanometer as the recording instrument to record the μV brain signals, and was able to study the different waves of this electrical activity, which he gave the name "electroencephalogram"[43].

Berger also reported that these brain waves were sort of periodic. He compared the slow brain waves during sleep to the brain waves during a mental activity or during a walk, and suggested, quite correctly, that EEG changed in a consistent and recognizable fashion when the general status and health conditions of the subject changed. However, despite the insights provided by these studies, Berger's original paper, published in 1929, did not generate much attention. It was not until 1934 that Adrian and Matthews confirmed Berger's discoveries. They studied the "alpha rhythm", 8-12 Hz from the occipital lobe and discovered that this rhythm disappeared when a subject displayed any type of attention or alertness or focused on objects in the visual field. Moruzzi and Magoun in 1949, demonstrated the existence of pathways widely distributed through the central reticular core of the brainstem that were capable of exerting a diffuse activating influence on the cerebral cortex. This "reticular activating system" has been called the brain's response selector because it alerts the cortex to focus on certain pieces of incoming information while ignoring others. It is for this reason that a sleeping mother will immediately be awakened by her crying baby or the smell of smoke and yet ignores the traffic outside her window or the television playing in the next room [43].

2.2. Brain anatomy and function

The average adult human brain weighs around 1.4 kg. The brain is surrounded by cerebrospinal fluid that suspends it within the skull and protects it by acting as a motion dampener [79]. In relation to the stages of brain development, Carlson categorizes its components into three groups; the Forebrain, Midbrain and Hindbrain. Anatomically the brain can be divided into the three largest structures: The brain stem (hindbrain), the cerebrum and the cerebellum (forebrain). The functions of these structures are summarized as follows[79]:

• The **brainstem** controls the reflexes and autonomic nerve functions (respiration, heart rate, blood pressure).

• The **cerebrum** consists of the cortex, large fiber tracts (corpus callosum) and some deeper structures (basal ganglia, amygdala, hippocampus). It integrates information from all of the sense organs, initiates motor functions, controls emotions and holds memory and higher thought processes.

• The **cerebellum** integrates information from the vestibular system that indicates position and movement and uses this information to coordinate limb movements and maintain balance.

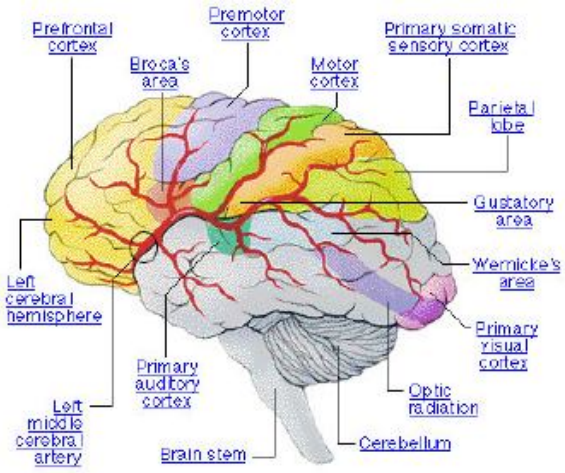

Figure 2-1 Human brain Lobes [79]

• The **hypothalamus** and pituitary gland control visceral functions, body temperature and behavioral responses such as feeding, drinking, sexual response, aggression and pleasure.

• The **thalamus** or specifically the thalamic sensory nuclei input is crucial to the generation and modulation of rhythmic cortical activity.

The cerebrum can be spatially sub-divided. Firstly into two hemispheres, left and right, connected to each other via the corpus callosum. The right one senses

information from the left side of the body and controls movement on the left side. Similarly the left hemisphere is connected to the right side of the body. Each hemisphere can be divided into four lobes. They are [79]:

1. Frontal Lobes -involved with decision-making, problem solving, and planning
2. Occipital Lobes-involved with vision and color recognition
3. Parietal Lobes - receives and processes sensory information
4. Temporal Lobes - involved with emotional responses, memory, and speech

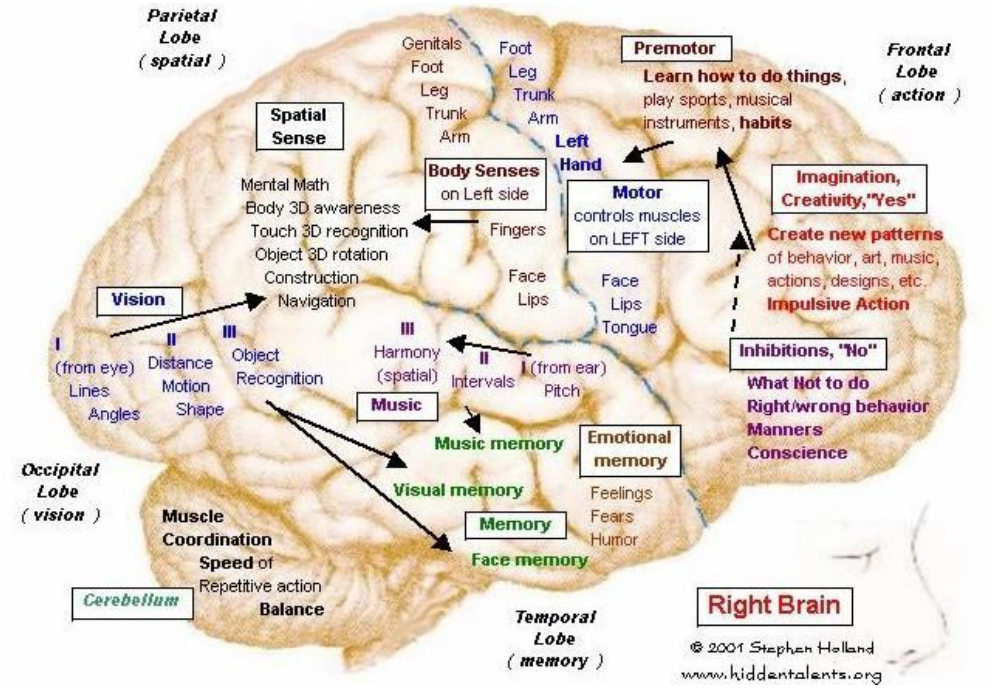

Figure 2-2: Human Brain functions

The cerebral cortex is the most relevant structure in relation to EEG measurement. It is responsible for higher order cognitive tasks such as problem solving, language comprehension and processing of complex visual information. Due to its surface position, the electrical activity of the cerebral cortex has the greatest influence on EEG recordings [79].

The functional activity of the brain is highly localized. This facilitates the cerebral cortex to be divided into several areas responsible for different brain functions.

Table 2-1: main cortical areas functions [79]

Cortex area	Function
Auditory	complex processing of auditory information, detection of sound, Speech production and articulation
Prefrontal	Problem solving, emotion, complex thought
Pre-motor	Planning and Coordination of complex movement
Motor	Initiation of voluntary movement
somatosensory	Receives tactile information from the body
Gustatory area	Processing of taste information
Wernicke's	Language comprehension
Visual	Complex processing of visual information

Since the architecture of the brain is non-uniform and the cortex is functionally organized, the EEG can vary depending on the location of the recording electrodes. Most of the cortical cells are arranged in the form of columns, in which the neurons are distributed with the main axes of the dendrite trees parallel to each other and perpendicular to the cortical surface. This radial orientation is an important condition for the appearance of powerful dipoles.

It can be observed that the cortex, and within any given column, consist of different layers. These layers are places of specialized cell structures and within places of different functions and different behaviors in electrical response. An area of very high activity is, for example, layer IV, which neurons function to distribute information locally to neurons located in the more superficial (or deeper) layers. Neurons in the superficial layers receive information from other regions of the cortex. Neurons in layers II, III, V, and VI serve to output the information from the cortex to deeper structures of the brain**.** The anatomy of the brain is complex due its intricate structure and function. This amazing organ acts as a control center by receiving, interpreting, and directing sensory information throughout the body [43].

2.3. Neurons and brainwaves

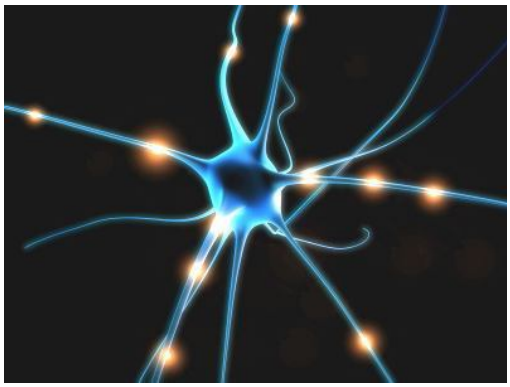

Figure 2-3: the Neuron [4]

The brain's electrical charge is maintained by 10^{14} pyramidal neurons and 10^{20} synapses. Neurons are electrically charged (or "polarized") by membrane transport proteins that pump ions across their membranes. Neurons are constantly exchanging ions with the extracellular milieu, for example to maintain resting potential and to propagate action potentials. Ions of similar charge repel each other, and when many ions are pushed out of many neurons at the same time, they can push their neighbours, who push their neighbours, and so on, in a wave. This process is known as volume conduction. When the wave of ions reaches the electrodes on the scalp, they can push or pull electrons on the metal on the electrodes. Since metal conducts the push and pull of electrons easily, the difference in push or pull voltages between any two electrodes can be measured by a voltmeter. Recording these voltages over time gives us the EEG [89]. Pyramidal neurons have a pyramid-like soma and large apical dendrites, oriented perpendicular to the surface of the cortex. Activation of an excitatory synapse at a pyramidal cell leads to an excitatory Postsynaptic potential, i.e. a net inflow of positively charged ions [82]. Consequently, increased extracellular negativity can be observed in the region of the synapse. The extracellular negativity leads to extracellular positivity at sites distant from the synapse and causes extracellular currents flowing towards the region of the synapse. The temporal and spatial summation of such extracellular currents, at hundreds of thousands of neurons with parallel oriented dendrites, leads to the changes in potential that are visible in the EEG. The polarity of the EEG signals depends on the type of synapses being activated and on the position of the synapses. However, due to volume conduction in the cerebrospinal fluid, skull, and scalp, signals from a local ensemble of neurons also spread to distant electrodes. EEG activity shows oscillations at a variety of frequencies. Several of these oscillations have characteristic frequency ranges, spatial distributions and are

associated with different states of brain [82]. Most of the patterns observed in human EEG could be classified into one of the following bands:

Table 2-2: EEG frequency bands [79], [43], [89], [75], [35], [24]

Band	Range (Hz)	Normal amplitude (μV)	Appearance
Delta	0.1-4	< 100	infants and during sleep in adults
Theta	4 -7	< 100	Drowsiness
Alpha	8-12	20-60	Physical relaxation at occipital and parietal area, can be temporarily blocked by mental activities or light influx
μ	8-13	<50	Movement or intent to move, mirror neurons: central area
SMR	12-15	20-60	synchronized brain activity, Immobility, decreases in motor task: central area
Low Beta	16-20	< 20	Muscle contractions in isotonic movements , bursts when strengthening of sensory feedback in static motor control: central regions, mental activity: frontal region
Mid Beta	20-24	< 20	Intense mental activity and tension: frontal and central area
High Beta	25-30	< 20	anxious thinking and active concentration: frontal and central area
Gamma	> 30	< 2	Conscious Perception

2.4. EEG recordings and techniques

EEG is the measurement of potential changes over time between a signal electrode and a reference electrode, where electrodes measures a field averaged over a volume large enough to contain perhaps 10^7–10^9 neurons [43].

Any EEG system consists of electrodes, amplifiers (with appropriate filters), and a recording system. Commonly used scale electrodes consist of Ag-AgCl disks, 1 to 3 mm in diameter, with long flexible leads that can be plugged into an amplifier. Although a low-impedance contact is desirable at the electrode-skin interface (<10 kΩ), this objective is confounded by hair and the difficulty of mechanically stabilizing the electrode [43]. Conductive electrode paste helps obtain low impedance and keeps the electrodes in place. Often contact cement is used to fix small patches of gauze over the electrodes for mechanical stability, and leads are usually taped to the subject to provide some strain relief.

Considerable amplification (gain = 10^6) is required to bring signal strength up to an acceptable level for input to recording devices [43]. Because of the length of electrode leads and the electrically noisy environment where recordings commonly take place, differential amplifiers with inherently high input impedance and high common-mode rejection ratios are essential for high-quality EEG recordings.

EEG is converted into a digital representation by an analog-to-digital (A/D) converter. The A/D converter is interfaced to a computer system so that each sample can be saved in the computer's memory. The resolution of the A/D converter is determined by the smallest amplitude that can be sampled. This is determined by dividing the voltage range of the A/D converter by 2 raised to the power of the number of bits of the A/D converter. For example, an A/D converter with a range of ±5 V and 12-bit resolution can resolve sample amplitudes as small as ±2.4 mV. Appropriate matching of amplification and A/D converter sensitivity permits resolution of the smallest signal while preventing clipping of the largest signal amplitudes [43].

A set of such samples, acquired at a sufficient sampling rate (at least 2 × the highest frequency component of interest in the sampled signal), is sufficient to represent all the information in the waveform. To ensure that the signal is band-limited, a low-pass filter with a cutoff frequency equal to the highest frequency of interest is used. Since physically realizable filters do not have ideal characteristics, the sampling rate is usually set to 2×the cutoff frequency of the filter or more. Furthermore, once converted to digital format, digital filtering techniques can be used [43].

2.4.1. Electrodes & electrode placement

An electrode is a small conductive plate that picks up the electrical activity of the medium that it is in contact with. In the case of EEG, electrodes provide the interface between the skin and the recording apparatus by transforming the ionic current on the skin to the electrical current in the electrode. Conductive electrolyte media ensures a good electrical contact by lowering the contact impedance at the electrode-skin interface [79].

The following types of electrodes are available:

• Reusable Cup electrodes (gold, silver, stainless steel or tin)

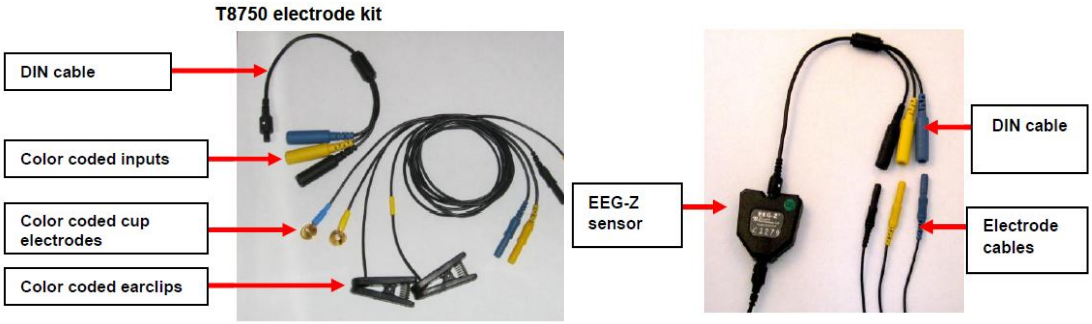

Figure 2-4: EEG electrodes and sensor [104]

• Electrodes Cap

• Needle electrodes

Figure 2-5: Cup electrodes [104]

Figure 2-6: Electrodes Cap [79]

For large multi-channel montages comprising of up to 256 or 512 active electrodes, electrode caps are preferred to facilitate quicker set-up of high density recordings. Commonly, Ag-AgCl cup or disc electrodes of approximately 1cm diameter are used for low density or variable placement recordings [79].

Electrodes are placed on the scalp in specific positions, known as the 10-20 electrode positioning system.

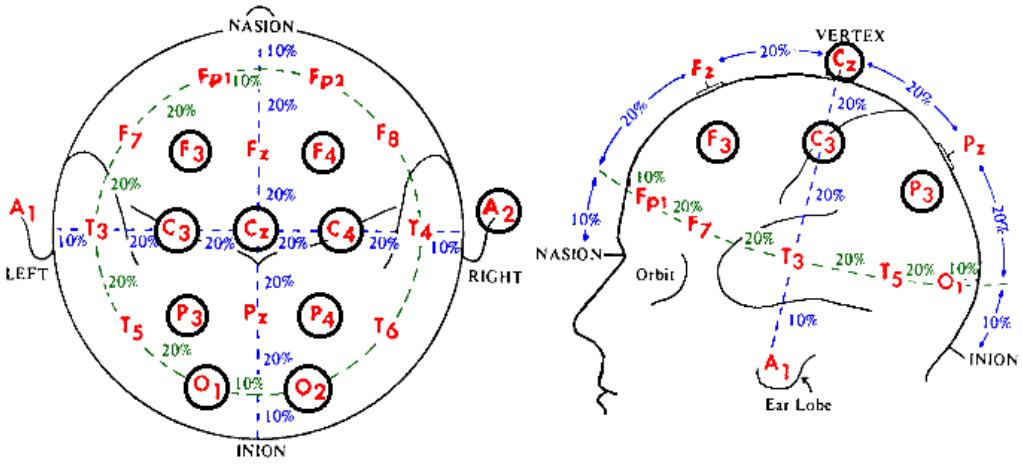

Figure 2-7(a): 10-20 International System [79]

In 1949, the International Federation of Societies for Electroencephalography and Clinical Neurophysiology (IFSECN) adopted a system proposed by Jasper which has now been adopted worldwide and is referred to as the 10-20 electrode placement International standard. This system, consisting of 21 electrodes, standardized physical placement and nomenclature of electrodes on the scalp. This allowed researchers to compare their findings in a more consistent manner. In the system, the head is divided into proportional distances from prominent skull landmarks (nasion, inion, mastoid and preauricular points). The '10-20' label in the system title designates the proportional distances in percents between the nasion and inion in the anterior-posterior plane and between the mastoids in the dorsal-ventral plane. Electrode placements are labeled according to adjacent brain regions: F (frontal), C (central), P(parietal), T (temporal), O (occipital). The letters are accompanied by odd numbers for electrodes on the ventral (left) side and even numbers for those on the dorsal (right) side. The letter 'z' instead of a number denotes the midline electrodes. Left and right side is considered by convention from the point of view of the subject. For example, if a researcher wants to study the brain signals related to visual perception, he will have to use electrodes O1, O2 and Oz. O1 is the electrode over the occipital area and on the right hemisphere, right next to the Inion. Electrode O2

is located over the occipital area but on the left hemisphere, left to inion, However electrode Oz is over occipital area but in the middle, right above the inion. Based on the principles of the 10–20 system, a 10–10 system and a 10-5 system have been introduced as extensions to further promote standardization in high resolution EEG studies. This high density EEG electrode placement can help pinpoint more accurately the brain region contributing to the recording at a given electrode. This is known as source localization [79].

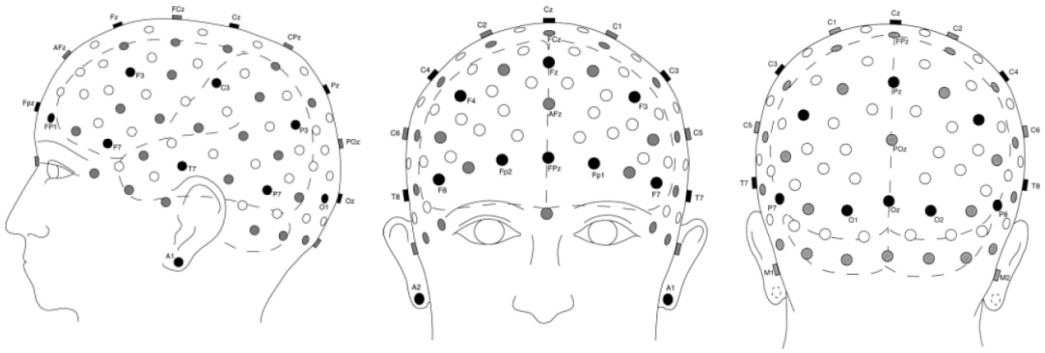

Figure 2-7(b): Selection of 10–10 electrode positions in a realistic display, lateral, frontal and posterior views. The head and brain contours based on typical models. Black circles indicate positions of the original 10–20 system, grey circles indicate additional positions in the 10–10 extension [79]

2.4.2. Mono-polar and bipolar recordings

EEG is a measurement of potential changes over time in a basic electric circuit conducting between signal (active) electrode and reference electrode. For getting a differential voltage, an extra third electrode called the ground electrode, is needed by the amplifiers to subtract the active and reference channels from it.
Reference electrode(s) must be placed on the parts of the body where the electrical potential remains fairly constant, so the most preferred reference is linked ears due to the relative electrical inactivity, ease of use and symmetry which prevents a hemispheric bias being introduced. This way of montage is called mono-polar.
Another type of electrodes montage is bipolar recording. They are differential measurements that are made between successive pairs of electrodes. Closely linked bipolar recordings are superior to mono-polar recordings because they are less affected by some artifacts, particularly ECG, due to the differential cancelling out of signals similarly picked up at the pair of electrodes, so each electrode is referenced

to a neighbor electrode or to common reference electrode. However, in terms of placement and spatial resolution, the mono-polar is more favorable [79],[89].

2.6. EEG signals used to drive BCIs

The EEG recorded brain waves originate from a multitude of different neural communities from various regions of the brain. These neural communities produce electrical contributions or components that can differ by a number of characteristics such as topographic location, firing rate (frequency), amplitude, latency etc.
Here are the main EEG patterns used to drive BCIs:

Table 2-3: EEG signals to drive BCIs [5], [35]

Signal	Short Description
ERD/ERS	A voluntary movement results in a circumscribed Event Related De-synchronization (ERD) in the μ and lower beta bands. It begins in the contra-lateral rolandic region about 2 s prior to the onset of a movement and becomes bilaterally symmetrical immediately before execution of movement. The power in the brain rhythms increases with an Event-Related Synchronization (ERS). It is dominant ipsilaterally during and contra-laterally after the movement over sensorimotor area and reaches a maximum around 600 ms after movement offset.
MRP	MRPs are low-frequency potentials that start about 1–1.5 s before a movement. They have bilateral distribution and present maximum amplitude at the vertex. Close to the movement, they become contra-laterally preponderant
SCPs	Slow Cortical Potentials are slow, non-movement potential changes generated by the subject. They reflect changes in cortical polarization of the EEG lasting from 300 ms up to several seconds. Functionally, SCP reflects a threshold regularization mechanism for local excitatory mobilization
VEP	Visual Evoked Potentials (VEP) are generated in response to a flashing

	visual stimulus. These potentials are more prominent in the occipital area.
SSVEP	Steady State Visual Evoked Potentials (SSVEP) are generated in response to a flashing visual stimulus with a repetition frequency greater than 6 Hz. These potentials are at the same frequency of the stimulus and they are more prominent in the occipital area.
SSAEP	Steady State Auditory Event Potentials (SSAEP) are sustained responses to continuous trains of click stimuli, tone pulses or amplitude-modulated tones, with a repetition or modulation rate between 20 and 100 Hz. The resulting brain response can be localized in the primary auditory cortex and are frequency-matched and phase-locked to the modulation.
P300	Infrequent or particularly significant auditory, visual, or somatosensory stimuli, when interspersed with frequent or routine stimuli, typically evoke in the EEG over the parietal cortex a positive peak at about 300 ms after the stimulus is received. This peak is called P300
Response to mental tasks	BCI systems based on non-movement mental tasks assume that different mental tasks (e.g., solving a multiplication problem, imagining a 3D object, and mental counting) lead to distinct, task-specific distributions of EEG frequency patterns over the scalp

Chapter 3

Brain Computer Interfaces (BCIs)

3.1. Introduction

A brain-computer interface (BCI) is an artificial communication system that passes the brain's normal output pathways of peripheral nerves and muscles, measures brain activity associated with the user's voluntary intend and desire, and characterizes these intentions with signal Digital Signal Processing (DSP) algorithms, in order to translate those intentions into a control signal that commands a device to act accordingly with those intentions only and without presence of any muscle activity[8].

BCIs use EEG system where the computer processes the EEG signals and use them to accomplish tasks such as communication and environmental control. Due to EEG complexity and noisiness, which in turn complicates processing those signals, these factors make using those signals for performing a simple task, such as moving a cursor left or right a very hard and challenging work, which makes BCIs slow in comparison with normal human actions.

EEG signals are too complex to be analyzed in terms of underlying neural events. EEG signals are in micro-volts and may be affected by muscular artifacts as eye and jaw movements. Also, a potential change at the scalp could be caused by the same polarity produced near the surface of the cortex, but it may also be caused by a potential change of the opposite polarity occurring at cell bodies deeper in the cortex. Excitation in one place cannot be distinguished from inhibition in another place and thus individual thoughts cannot be divined [6].

Individual thoughts cannot be picked up and are probably not even correlated with the ongoing EEG activity. It is possible for an individual to be trained to produce a reliable signal or an individual may have a reliable response to a specific stimulus in a specific context. BCIs make use of such signals and if reactions to computer generated stimuli may be detected, then they can be used in order to control a light

switch or a television set. If individuals may be trained to produce reliable signals that may be separated from ongoing EEG activity, then these signals may be used.[6] On the other hand, recent advances in computers and signal processing have opened up a new generation of research on real-time EEG signal analysis and BCIs. With a small comparison between the first BCI presented by Dr. Grey Walter in 1964, and the new state-of-the-art BCIs presented by Wolpaw in 2010, we can see how computers have become fast enough to handle the real-time old constraints of BCI signal processing.

3.2. BCI design approaches: Pattern Recognition Vs Operant conditioning

In *Pattern recognition approach (PR),* the BCI recognizes the characteristic EEG in response to performing a cognitive mental task like motor imagery, visual, arithmetic and baseline tasks [79]. It is mainly used in SSEVP-BCI.
However*, Operant conditioning approach (OC)* requires the user to perform lengthy training sessions in a biofeedback environment to master the skill of being able to *self-regulate* one's EEG, and is mainly used for ERD-BCI [79],[86].

3.3. BCI control approaches: Synchronous Vs Asynchronous

Synchronous BCI approach implies that the user can interact with the targeted application only during specific time periods triggered by external audio/visual stimuli and imposed by the computer system, whereas in Asynchronous BCI, the user willingly decides when to perform a mental task and at any time [24].
However, designing an asynchronous BCI is much harder than designing a synchronous BCI. In the latter, the system is programmed to know when the mental states should be recognized and analyzes EEG only in predefined time windows, however, with a self-paced BCI; the system has to analyze EEG continuously in order to determine whether the user is trying to interact with the system by performing a

mental task. So it requires computations much more than synchronous BCI does which leads to less accuracy due to the high amount of data being processed. This in turn limits the speed of command generation for such an approach [24].

3.4. BCI framework

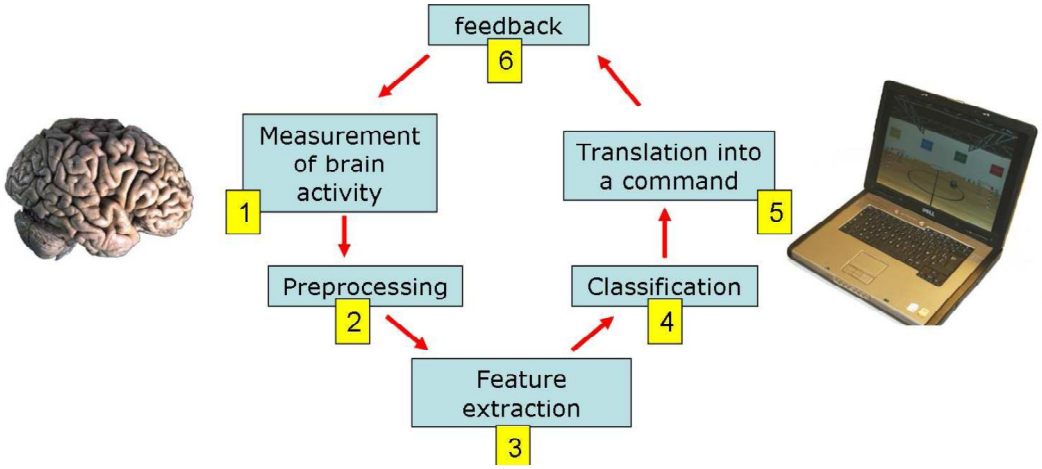

Figure 3-1: BCI framework [24]

The design of a BCI system consists of six main stages: the acquisition of EEG signals, pre-processing the signals, feature extraction and selection, classification and translation into a command or a control signal, and finally to feedback the subject with a desired action [5],[24].

A BCI system commences with acquisition of brain signals, which is done via an EEG system with one up-to 256 electrodes. Each mental activity generates specific EEG signals related to this task topographically and rhythmically, so numbers and locations of electrodes (according to the 10-20 system) are related to the task the designer wants to achieve with a BCI.

The signals are then amplified, filtered, epoched (in order to center and maximize the information of the data in the specific related rhythm), A/D converted and passed through an artifact removal algorithms (de-noised) in what is known as pre-processing stage [79]. The main goal of this stage is to improve the signal-to-noise ratio (SNR) by cleaning the EEG signals and removing all irrelevant information, such as the electrical activity of the eyes (EOG: ElectroOcculoGram), the muscles (EMG: Electromyogram) and the power line network, which have an amplitude much larger

than the one of EEG signals. Thus the pre-processing stage reduces the amount of data for the next stages. This reduction is essential, because EEG signals ports a large amount of data which make it harder to work with, so focusing on a smaller amount of data that has the relevant information, would facilitate the design [79].

After cleaning the signals from irrelevant information, the relevant information, which is known in the world of BCI as features, needs to be extracted [5]. The feature extraction represents the resultant signals as feature values that are related to the underlying neurological mechanism generated by the user's brain for control. These features can be for example the magnitude at a specific frequency range. Features are extracted with DSP algorithms and assembled into a feature vector. Hence, feature extraction is the stage where DSP algorithms are applied in order to convert one or several signals into a feature vector [5],[24].

This stage may results in too many irrelevant overlapping feature vectors which increase the computational complexity, so feature selection with DSP algorithms may be applied for optimization [32].

In the next stage, the classification stage, classification algorithms are applied to categorize different brain patterns and features from the feature vectors [5],[24], where each classified features will be translated into a distinct control signal related to the underlying brain pattern. In this final stage, control signals instruct the device to act and feedback the user. Each control signal represents a specific brain pattern related to the user's intention, so the device will act accordingly with the identified user’s intention. The BCI performance is determined in terms of classification accuracy [8], computational efficiency and complexity [79].

Consequently, designing a BCI is a complex and challenging task which requires multidisciplinary expertise such as programming, signal processing, neurosciences and psychology [8]. To complete a BCI design, two phases are essential: 1) an offline training phase which calibrates the system. An experimental paradigm [14] is implemented to guide the user on how to generate the characteristics EEGs. It is mainly characterized by its duration, repetitiveness, pause between trials and complexity of the mental task. The training paradigm is generally done without the feedback stage, even thought that there is some evidence that a continuous or

discrete visual representation of the feedback signal, such as a 3D video game or virtual reality environment, may facilitate learning to use a BCI [42].

2) an online phase which uses parameters from phase 1 in the BCI to distinguish mental states and feedback the user accordingly.

Chapter 4

BCI signal processing

4.1. Pre-processing Methods

4.1.1. Temporal filters

Low-pass or band-pass filters are generally used in order to restrict the analysis to frequency bands known as representing neurophysiological signals [24]. For Instance, BCI based on sensorimotor rhythms generally band-pass filter the data in the 8-30Hz frequency band, as this band contains both the μ and ß rhythms. This temporal filter can also remove various undesired effects such as slow variations of the EEG signal (which can be due, for instance, to electrode polarization) or power-line interference (60 Hz in Quebec). Hence, such a filtering is generally achieved using Discrete Fourier Transform (DFT) or using Finite Impulse Response (FIR) or Infinite Impulse Response (IIR) filters (Butterworth, Tchebychev or elliptic IIR filters) [24].

4.1.2. Spatial filters

Spatial filters are used to isolate the relevant spatial information embedded in the signals. This is achieved by selecting the electrodes for which we know they are measuring the relevant brain signals, and ignoring other electrodes [24]. The most popular spatial filter is the Common Average Reference (CAR) which is obtained as follows:

$$\widehat{\mathbf{Vi}} = \mathbf{Vi} - \frac{\mathbf{1}}{\mathbf{Ne}} \sum_{\boldsymbol{j=0}}^{\mathbf{Ne}} \mathbf{Vj} \qquad (\mathbf{1})$$

Where $\widehat{\mathbf{Vi}}$ and $\boldsymbol{V_i}$ are the *ith* electrode potential, after and before filtering respectively, and $\boldsymbol{N_e}$ is the number of electrodes used [24]. Thus, with the CAR filter, each electrode is re-referenced according the average potential over all electrodes.

4.1.3. Independent Component Analysis (ICA)

ICA is a method for separating a multivariate signal into additive subcomponents supposing the mutual statistical independence of the non-Gaussian source signals [24]. It is a special case of blind source separation.

When the independence assumption is correct, blind ICA separation of a mixed signal gives very good results. It is also used for signals that are not supposed to be generated by a mixing for analysis purposes. A simple application of ICA is the "cocktail party problem", where the underlying speech signals are separated from a sample data consisting of people talking simultaneously in a room.

Blind signal separation, also known as blind source separation, is the separation of a set of signals from a set of mixed signals, without the aid of information (or with very little information) about the source signals or the mixing process [20], [55].

Blind signal separation relies on the assumption that the source signals do not correlate with each other. For example, the signals may be mutually statistically independent or de-correlated. Blind signal separation thus separates a set of signals into a set of other signals, such that the regularity of each resulting signal is maximized, and the regularity between the signals is minimized (i.e. statistical independence is maximized).

4.1.4. Common Spatial Patterns (CSP)

This method is based on the decomposition of the EEG signals into spatial patterns selected in order to maximize the differences between the classes involved once the data have been projected onto these patterns [91],[24],[55]. Determining these patterns is performed using a joint diagonalization of the covariance matrices of the EEG signals from each class. With the projection matrix $\mathbf{W}$, the original EEG can be transformed into uncorrelated components:

$$Z=WX \qquad (2)$$

$\mathbf{Z}$ can be seen as EEG source components, and the original EEG X can be reconstructed by

$$X=W^{-1}Z \qquad (3)$$

Where $\mathbf{W}^{-1}$is the inverse matrix of $\mathbb{W}$. the columns of $\mathbf{W}^{-1}$are spatial patterns, which can be considered as EEG source distribution vectors. The first and last columns are the most important patterns that explain the largest variance of one task and the smallest variance of the other [91].

4.2. Feature extraction

4.2.1. Temporal Methods

4.2.1.1. Signal amplitude [24]

The simplest (but still efficient) temporal information that could be extracted is the time course of the EEG signal amplitude. Thus, the raw amplitudes of the signals from the different electrodes, possibly preprocessed, are simply concatenated into a feature vector before being passed as input to a classification algorithm. In such a case, the amount of data used is generally reduced by preprocessing methods such as spatial filtering or sub sampling. This kind of feature extraction is one of the most used for the classification of P300.

4.2.1.2. Band power features [35],[41]

For EEG data, Band-pass filtering of each trial, squaring of samples and averaging of N trials results in a time course of instantaneous band power [41]. It is also possible to log-transform this value in order to have features with a distribution close to the normal distribution. The power is calculated as:

$$\widehat{\mathbf{P}}_{\mathbf{J}} = \frac{\mathbf{1}}{\mathbf{N}} \sum_{i=1}^{\mathbf{N}} x^{2}{}_{\mathbf{f(i,j)}} \qquad (\mathbf{4})$$

where P(j) = averaged power estimation of band-pass filtered data (averaged over all trials), xf(i,j)=j-th sample of the i-th trial of the band-pass filtered data[25].
Then, The ERD is quantified as the percentage change of the power (A(j)) at each sample point or an average of some samples relative to the average power in a reference interval:

$$\boldsymbol{ERD\%_{(j)} = \frac{A_{(j)} - R}{R} X\ 100\%} \qquad (5)$$

$$\mathbf{R = \frac{1}{K} \sum_{j=n_0}^{n_{0+K}} A_j} \qquad (6)$$

where R = average power in reference interval, averaged over k samples,

and A(j) = power at the j-th sample [25].

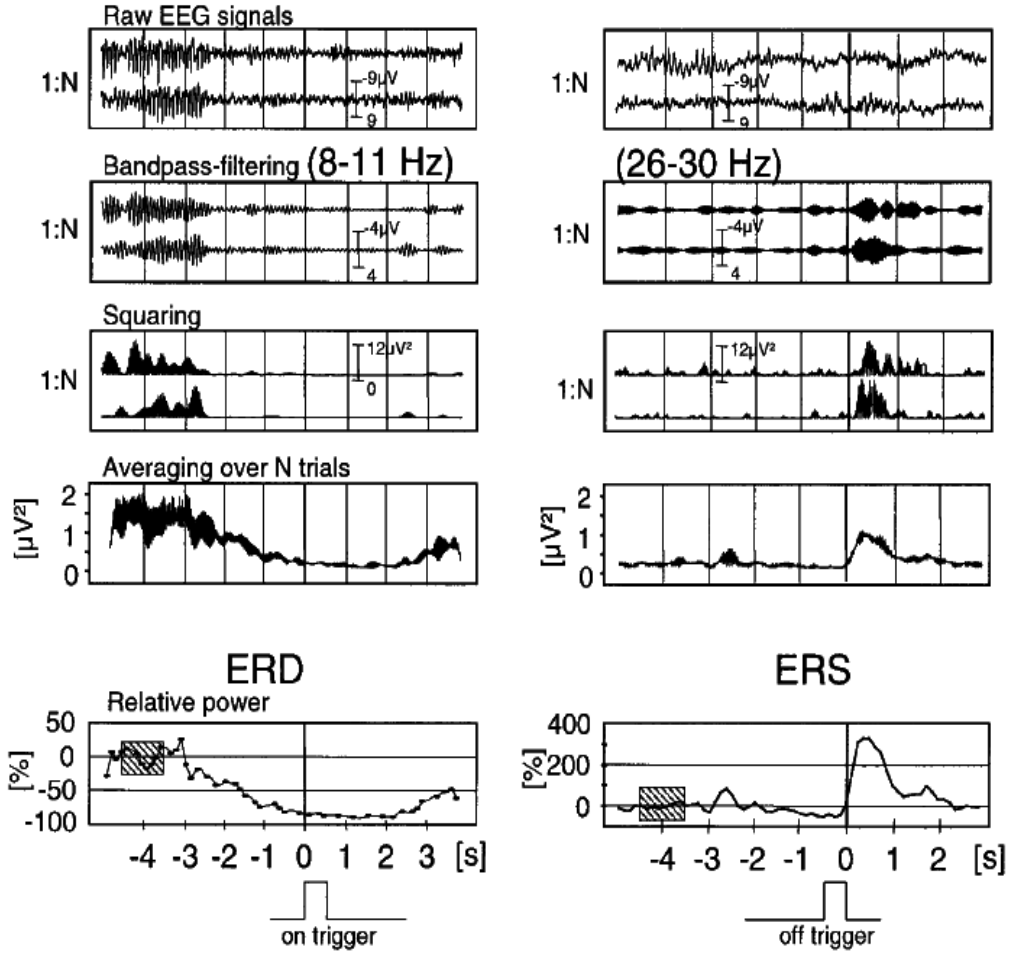

Figure 4-1: ERD calculation method [35]

4.2.1.3. Autoregressive (AR) Parametric model

Autoregressive (AR) methods assume that EEG signal $y(t)$, measured at time t, can be modeled as a formula, or a polynomial model that is optimally fitted into a time series, and that attempt to predict an output of a system based on the previous outputs, to which we can add a noise term e_t (generally a Gaussian white noise):

$$y(t) = -a_1 y(t-1) - \ldots - a_n (t-n_a) + e(t) \qquad (7)$$

Where $a_1, a_2 \ldots . a_n$ are the autoregressive parameters which are generally used as features for BCI to distinguish one time-series from another, and n is the model order [79], $e(t)$ is a purely random (white noise) process with zero mean and variance σ^2_n. n(t) is uncorrelated with the signal, and the cross-covariance $E\{X_t * N_{t-k}\}$ is zero for every k. In [79] the author mentioned that Mc Ewen et al. showed that 80-90% of EEG segments of duration 4-5 seconds can be modeled as being Gaussian. The AR model can be rephrased in the frequency domain as a white noise source driving a spectral shaping network $A^{-1}(z)$[79].

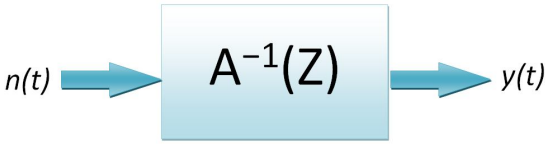

Figure 4-2 AR Model [79]

Several extensions to the AR have been proposed [24]:

1. AAR (Adaptive Auto-Regression)
2. ARX (Auto-Regression with exogenous input)
3. ARMA (Auto-Regression with Moving Average)
4. ARMAX (Auto-Regression with Moving Average and exogenous input)

Using an AR Moving Average (ARMA) as the Exogenous input has proved to better model the underlying event-related potential amidst the background EEG offering improved classification rates [79]. It makes the distinction between the ERP and background neuronal activity contributing to the single trial EEG recording, but requires more computational time and processing capabilities due to its iteration functionality. ARX, an extension of AR modeling, involves the introduction of an

exogenous input assumed to be a contributory signal to the overall signal being modeled. Its pole-zero filtered contribution and the AR noise estimate combine to form the forward prediction estimate of the overall recorded EEG signal. The ARX filter coefficients are used as input features to characterize the single-trial EEG. The ARX method of modeling both the signal ERP and the noise (background EEG) is more physiologically reasonable than modeling the noise alone as ongoing EEG contributions from neighboring neural populations contribute mostly to the background noise [19]. Ensemble averaging over a large number of trials exposes the underlying ERP that is hidden amidst background EEG by averaging out this random neuronal noise.

The EEG can be expressed by means of the following equation (assuming a linear relationship):

$$\boldsymbol{y(t)} = \boldsymbol{s(t)} + \boldsymbol{n(t)} + \boldsymbol{a(t)} \quad 0 \leq \ t \leq T \qquad (8)$$

where: $\boldsymbol{y(t)}$is the scalp recorded EEG response prior to the onset of movement, $\boldsymbol{s(t)}$ is the useful signal corresponding to the ERP attained by ensemble averaging across preceding trials [19], $\boldsymbol{n(t)}$ is the background EEG and $\boldsymbol{a(t)}$ is the component generated by a combination of all possible artifacts. *T* is the duration of each fixed length trial epoch. Alternatively, the ARX model can be extended for artifact filtering by introducing additional noise modeling stages to filter the acquired signal *y*(*t*) , resulting in increased exogenous inputs.

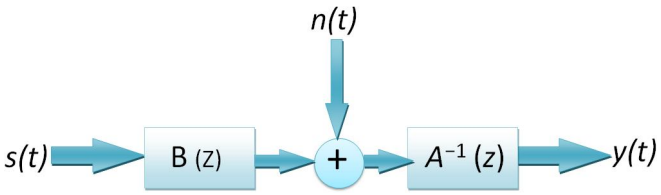

Figure 4-3 ARX Model [79]

The basic ARX model, in terms of the shift operator *q*, and assuming a sampling interval of one unit, is as follows

$$\boldsymbol{A(q)y(t)} = \boldsymbol{B(q)s(t)} + \boldsymbol{n(t)} \qquad (9)$$

The prediction is written as

$$\boldsymbol{y(t) = -a_1 y(t-1) - \cdots - a_n(t-n_a) + b_1 s(t-k) + \cdots + b_{1nb}\, s(t-k-n_b) + e(t)} \quad (\mathbf{10})$$

Where $\boldsymbol{n_a}$ and $\boldsymbol{n_b}$ are the model orders and *k* is the delay. Coefficients of the AR and ARX models are usually used as features in the classification. This feature extraction technique is impractical for a large number of electrodes due to the resultant large feature vector dimensionality and resulting computational demands. Different model orders are tested to select the optimum model order that represents the input data. This selection is based on the standard prediction error method over the state-space model. State-space models are common representations of dynamical models, and they describe the same type of linear difference relationship between the inputs and the outputs as in the AR and ARX model [50].These models use state variables to describe the system by a set of first-order differential or difference equations, rather than by one or more nth-order differential or difference equations. They can be reconstructed from the measured input-output data, but are not themselves measured during an experiment [50]

$$\boldsymbol{x(t) = Ax(t) + Bu(t) + Ke(t)}$$

$$\boldsymbol{y(t) = Cx(t) + Du(t) + e\,(t)} \quad (11)$$

A, *B*, *C*, *D*, and *K* are state-space matrices. *u*(*t*) is the input, *y*(*t*) is the output, *e*(*t*) is the disturbance and *x*(*t*) is the vector of orders states. All the entries of *A*, *B*, *C*, and *K* are free estimation parameters. The elements of the *D* matrix, however, are fixed to zero. That is, there is no feed-through. For ARX model order selection, the Akaike Information Criterion (AIC) was applied for this study [50]. In this method, the input was assumed to have Gaussian statistics, thus the AIC for an AR process is as follows

$$\boldsymbol{v = log(e) + \frac{2p}{n}} \quad (\mathbf{12})$$

Where $\boldsymbol{v}$ is the loss function, $\boldsymbol{e}$ is the modeling error, $\boldsymbol{p}$ is the AR model order, and $\boldsymbol{n}$ is the number of data samples.

4.2.2. Time-Frequency Representations (TFR) with Short-time Fourier transform (STFT)

Short-Time Fourier Transform simply consists in first multiplying the input signal by a given windowing function *w* which is non-zero only over a short time period, and then in computing the Fourier transform of this windowed signal [24]. In discrete time, the STFT $X(n,w)$ of a signal $x(n)$ is as follows:

$$\boldsymbol{X_{(n,w)} = \sum_{n=-\infty}^{+\infty} x(n)w(n)e^{-jwn}} \qquad \boldsymbol{(13)}$$

The Time-Frequency (TF) representation is obtained by computing this Fourier transform along a sliding window, i.e., for different segments with a given level of overlapping. This results in a 2D colored Spectrogram map of μV^2 amplitudes within frequency bands and in respect to the time [24].

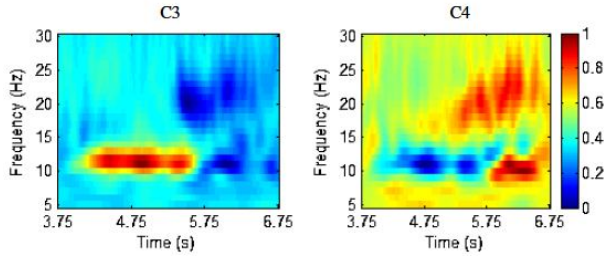

Figure 4-4 TFR spectrogram at channels C3 and C4 with motor imagery of right hand movement [12]

It should be noted that a shorter time window improves time resolution, a longer one resolves frequency better but diminishes time resolution.

On the other hand**,** determination of the number of points on frequency axis (Frequency bins) determines the resolution. A larger number of frequency bins increases spectrogram detail but also increases computation time.

The STFT method has been successfully used in several BCI studies, and its main advantage is the use of an analysis window with a variant size, which leads to a different frequency-temporal resolution in all frequency bands. For instance, it would be more interesting to have a high temporal resolution for high frequencies which describe a fine scale [24].

4.2.3. Frequential methods

4.2.3.1. Power Spectral Density features

Power Spectral Density (PSD) features, sometimes simply called spectrum, inform on the distribution of the power of a signal between the different frequencies [24]. PSD features can be computed by either non-parametric or parametric methods. Non-parametric methods compute PSD directly from the signal itself. Examples are Welch method and Periodogram. For instance Periodogram computes PSD by squaring the Fourier transform $X[K]$ of a signal.

Fast Fourier transform (FFT) is an extremely fast computing algorithm for discrete Fourier transform (DFT). Let x[n] be our trial. The N-point DFT of x[n] is given by

$$\mathbf{X[k]} = \sum_{\boldsymbol{n=0}}^{\boldsymbol{N}} \mathbf{x[n]w_N^{nk}}, \mathbf{k} = \mathbf{0}, \mathbf{1}, \ldots\ldots, \mathbf{N} \qquad (\mathbf{14})$$

Where $\omega_N = e^{-2\pi i/N}$ is an Nth root of unity. Since the PSD is the FFT squared, so, for example, the PSD for delta band (0-3 Hz) is defined as:

$$\mathbf{PSD} = \sum_{\boldsymbol{k=0}}^{\boldsymbol{4}} \boldsymbol{X[K]^2/N} \qquad \mathbf{(15)}$$

Where N is the frequency resolution. PSD features can be also obtained by computing the Fourier transform of the autocorrelation function of the signal. On the other hand, parametric methods *model* the data as the output of a linear system that hypothetically generates the data, driven by white noise, and then attempt to estimate the parameters of that linear system. AR models are a very common method for the evaluation of the spectra of short data segments due to the improved resolution, and they represent sharp peaks in the frequency domain.

The most commonly used linear system model is the *all-pole model*, a filter with all of its zeroes at the origin in the *z*-plane, thus it can represent sharp peaks in the frequency domain. The output of such a filter for white noise input is an autoregressive (AR) process. For this reason, these methods are sometimes referred to as *AR methods* of spectral estimation. For the model identification, the parametric modelling parameters have to be identified.

Parametric methods can yield higher resolutions than nonparametric methods in cases when the signal length is short, where all AR methods yield a PSD estimate given by:

$$\boldsymbol{PSD} = \frac{\mathbf{1}}{\mathbf{Fs}} \frac{\mathbf{P}}{\mathbf{1} - \sum_{\boldsymbol{k}=\mathbf{1}}^{\boldsymbol{p}} \left(\hat{\boldsymbol{a}}_{\boldsymbol{p}}(\mathbf{k}) \mathbf{e}^{-\mathbf{j}2\boldsymbol{\pi}\mathbf{k}\mathbf{f}/\mathbf{Fs}}\right)^{\mathbf{2}}} \qquad \textbf{(16)}$$

The most used methods to model the data or estimate the power spectrum are Yule-Walker and Burg method. In this thesis we used Burg method to only model the input data. By minimizing (least squares) the forward and backward prediction errors while constraining the AR parameters to satisfy the Levinson-Durbin recursion, it estimates the reflection coefficients. The primary advantages of the Burg method are two:

[1]. High frequency resolution, [2]. Stable AR model

However, the accuracy of the Burg method is lower for high-order models, long data records, and high signal-to-noise ratios (which can cause line splitting, or the generation of extraneous peaks in the spectrum estimate). It is superior to the YW method for short data records, and also removes the tradeoff between utilizing the biased and unbiased autocorrelation estimates, as the weighting factors divide out. PSD features are probably the most used features for BCI, and have proved to be efficient for recognizing a large number of neuro-physiological signals [24].

4.2.3.2. Power Asymmetrical ratio

This method is especially useful in tasks that involve inter-hemispheric difference. EEG traces are recorded simultaneously from two or more inter-hemispheric electrodes (ex. C3-C4). The power asymmetrical ratio is defined as:

$$Ra = \frac{\mathrm{R}-\mathrm{L}}{\mathrm{R}+\mathrm{L}} \qquad (17)$$

Where R is the PSD or power of a specific band in the right electrode and L is the PSD or power of a specific band in the left electrode. Asymmetry ratios are formed for all the frequency bands and all of the possible right to left combinations of electrodes.

4.3. Feature selection and dimension reduction

Genetic algorithms (GA) approach is used. A GA can be described as a stochastic search and optimization technique based on evolutionary computation [5], [24]. They can be divided into three main groups: Embedded algorithms, where the selection is embedded within the induction algorithm; Filter algorithms, where features are selected before passing them to the classification stage; and wrapper algorithms, which perform feature selection in unison with the classification algorithm. PCA can be used for dimensionality reduction in a dataset while retaining those characteristics of the dataset that contribute most to its variance, by keeping lower-order principal components which contain the 'most important' aspects of the data and ignoring higher-order ones [24].

4.4. Feature Classification Methods

4.4.1. Linear Discriminant Analysis (LDA)

The aim of LDA is to find a linear combination of features which characterizes or separates two or more classes with k, n-space hyperplanes [24], [5]. For a two-class problem, the class of a feature vector depends on which side of the hyperplane the vector is.

LDA assumes a normal distribution of the data, with equal covariance matrices for both classes. The separating hyperplane is obtained by seeking the projection that maximizes the distance between the two classes' means and minimizes the interclass variance [24]. LDA finds a linear transformation of two weights, X and Y, that yields a new set of transformed values that provides accurate discrimination:

$$\mathbf{Transformed\ Target = X*X_1 + Y*X_2} \qquad (18)$$

Finding the weights implies calculating the scatter matrices and means of the each dataset, finding the transpose of the addition of the two scatter matrices and multiplying the result by the difference of the means. The scatter matrix is

$$S = \sum_{j=1}^{n} (x_j - \bar{x})(x_j - \bar{x})^T \qquad (19)$$

Where T denotes matrix transpose, x_j is the *j*th column of *X*. For validation, usually a 10-k-fold cross-validation is used. This algorithm breaks data into 10 sets of size n/10, trains on 9 datasets and tests on 1, repeats 10 times and finally takes a mean accuracy. The advantage of this method over repeated random sub-sampling is that all observations are used for both training and validation, and each observation is used for validation exactly once. LDA requires less training and computation compared with neural network based classifiers but as a trade-off requires more discriminatory feature vectors to distinguish successfully between the classes.

4.4.2. Support Vector Machines (SVM)

SVM are supervised learning methods that analyze data and recognize patterns by constructing a hyperplane or set of hyperplanes in a high- or infinite-dimensional space, where a good separation is achieved by the hyperplane that has the largest distance to the nearest training data point of any class (so-called functional margin), since in general the larger the margin the lower the generalization error of the classifier [20],[100],[24]. SVM are known to have good generalization properties, to be insensitive to overtraining and to the curse-of-dimensionality but with a low speed of execution [24].

If the problem is not originally linearly separable, the kernel trick is used to turn it into a linearly separable one, by increasing the number of dimensions. Thus a general hypersurface in a small dimension space is turned into a hyperplane in a space with much larger dimensions. When training an SVM the practitioner needs to define what kernel to use, and setting the parameters of the SVM and the kernel.

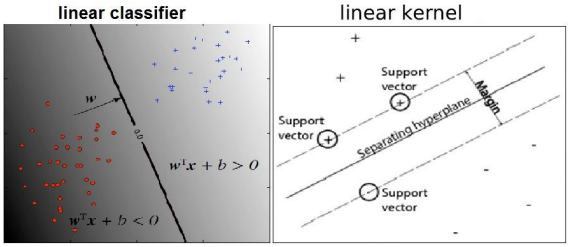

Figure 4-5 classification basics [102]

The *support vectors* are the data points that are closest to the separating hyperplane; these points are on the boundary of the slab. The above figure

illustrates these definitions, with + indicating data points of type 1, and – indicating data points of type –1.

The data for training is a set of points (vectors) x_i along with their categories y_i. For some dimension d, the $x_i \in R^d$, and the $y_i = \pm 1$. The equation of a hyperplane is $w^T.x + b = 0$, where $w \in R^d$, $w^T.x$ is the inner (dot) product of w and x, and b is real [102]. The support vectors are the x_i on the boundary, those for which $y_i(w^T,.x_i + b) = 1$. The data might not allow for a separating hyperplane. So, SVM can use a *soft margin* that separates many, but not all data points. There are two standard formulations of soft margins. Both involve adding slack variables s_i and a penalty parameter *C (box constraint)*. The norm problem is:

$$\min_{w,b,s}\left(\frac{1}{2}\langle w,w\rangle + C\sum_i s_i^2\right) \qquad (20)$$

To solve this problem, the Lagrange multipliers are used in a function, where the C factor keeps the allowable values of the Lagrange multipliers in a bounded region (Box). To achieve better classification performance, one strategy is to try a geometric sequence of the box constraint parameter [102].

4.4.3. MultiLayer Perceptron Neural Networks

MLP is a feed-forward artificial neural network that maps sets of input data onto a set of appropriate output [24]. It consists of multiple layers of nodes in a directed graph, with each layer fully connected to the next one whereas the neurons of the output layer determine the class of the input feature vector. Except for the input nodes, each node is a neuron. Careful architecture selection and regularization is required because MLP are approximators, so are highly sensitive to non-stationary data such as EEG [24]. Neural networks try to learn the decision boundary which minimizes the empirical error, while SVMs try to learn the decision boundary which gives the best generalization.

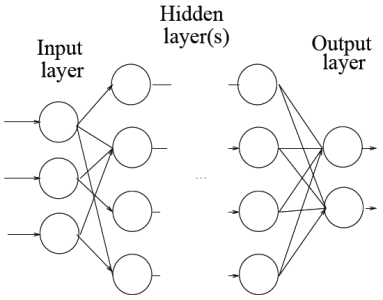

Figure 4-6: Multi Perceptron Neuron Network[24]

Chapter 5

BCI applications

5.1. The Brain Response Interface

After giving visual or audio stimuli to a subject, we can see a response to this stimulus in is different classes of his brain signals. Once the class of the stimuli signals have been identified, the system can associate a specific command to this identified mental state and send this command to a given application or device.
It is also particularly essential to provide a visual/audio feedback to the subject, concerning the mental state that has been recognized by the system. Indeed, this feedback enables the user to know whether he has correctly performed the mental task which enables him to learn how to control his brain activity [24].

5.2. P300 Speller and Character Recognition

The P300 potential is a response to an infrequent stimulus. Each stimulus event corresponds to a symbol/picture with a particular meaning for the interface (e.g. letters, high level commands). The stimulus must be perceptible on the user field of view without gazing the specific stimulus. It usually appears in EEG signals around 300 ms after the in frequent stimulus occurs [5].TheP300 speller BCI system is able to detect which character in the spelling matrix is

Figure 5-2(a): P300 Speller Paradigm [100]

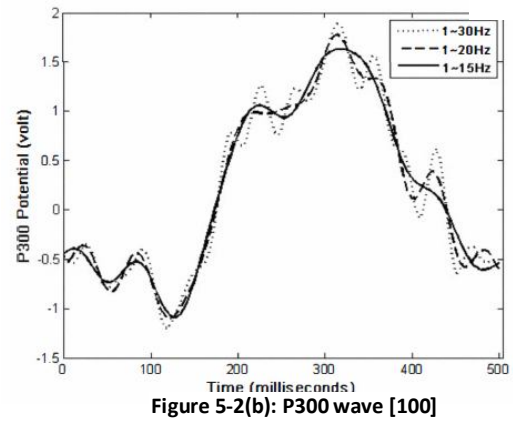

Figure 5-2(b): P300 wave [100]

the target that the user is focusing on, and then show the detection result (target character) on the screen, thereby enabling locked-in people to communicate with others [100]. The task of target character detection in a P300 speller BCI was generally treated as a two-class classification problem: P300 and non-P300 classification. For this BCI with six electrodes placed on Fz, Fcz, Cz, Pz, P7 and P8, the data collection task is done by a software written in C#. In P300-BCI, characters are based on their individual P300 EEG responses.

Figure 5-2 (c): Setup of EEG operated spelling device and a skull cap
Source: www.intendix.com

Therefore, the characters of the English alphabet (A, B,… , Z) were arranged in a 6 x 6 matrix on a computer screen. Then each character was highlighted for 4 seconds in a random order and the subject had the task to concentrate on the specific character he/she wanted to spell. After the attention-catching intensification, a 2.5 s preparation gap is given before a data collection procedure. During this procedure, the subject is asked to focus on the target character, and then the system will initiate a 10-round intensification process, where within each round, 12 randomly-ordered visual stimuli will be presented.Each stimulus is the intensification of either one row or one column, and will be presented for 100 ms, and after a 75 ms inter-stimuli interval, the next stimulus will be presented. After presentation of 12 stimuli, a

round is ended, and after a pause of 0.5 s, the next round begins. Therefore, a 10-round intensification process will take 27.75 s. The highlight of the desired letter being a rare and expected event, this triggers a P300 in the user's EEG signals. Detecting the absence or presence of the P300 makes it possible to find which are the line and column that contain the desired letter, and as such to find this letter. This way, several user intentions correspond to a unique brain pattern (P300 peak signal), representing a high volume of information, where DFT is used as processing tool and then the SVM classifier is used to classify different character recognitions [100].

5.3. μ and Beta ERS/ERD Cursor Control

ERD is the event-related, short-lasting and localized amplitude attenuation of EEG rhythms within the alpha or beta band, while event-related synchronization (ERS) describes the event-related, short-lasting and localized enhancement of these rhythms [35],[5],[24]. Sensory stimulation, motor behavior, and mental imagery can change the functional connectivity within the cortex and results in ERS/ERD due to modulating influences of neurochemical brain systems, changes in the strength of synaptic interactions, changes of intrinsic membrane properties of the local neurons, or the dynamics of brain oscillations associated with sensory and cognitive processing and motor behavior [35], [41].

Event Related Potentials are series of transient post-synaptic responses of main pyramidal neurons triggered by a specific stimulus, ERD/ ERS reflect changes in one or more parameters that control oscillations in neuronal networks like the strength, modulations, synaptic processes dynamics and extent of the interconnections between the network elements, most often formed by feedback loops.

Neuronal networks can display different states of synchrony, with oscillations at different frequencies. The frequency of brain oscillations is negatively correlated with their amplitude. The mu rhythm (8 and 13 Hz) has larger amplitude than the central beta rhythm (around 20 Hz). Because the amplitude of oscillations is proportional to the number of synchronously active neural elements, slowly oscillating cell assemblies comprise more neurons than fast oscillating cells. When

the neuronal populations display oscillations, and in a rest state for example, this recruits neurons in larger cortical areas in the case of low frequencies, and to be more spatially restricted in the case of higher frequencies, as for beta/gamma rhythms. However, in more complex states such as attention, the cortex appears to be functionally organized as a mosaic of neuronal assemblies characterized by relatively high frequency synchronous oscillations that may display a large variability in dominant frequencies. Thus, ERD/ ERS reflect changes in the activity of local interactions between main neurons and inter-neurons that control the frequency components of the ongoing EEG.

The degree of desynchronization is closely linked to semantic memory processes. For example, during semantic encoding of words, good memory performers showed a significantly larger ERD in the lower alpha band as compared to bad performers Voluntary movement results in a circumscribed desynchronization in the upper alpha and lower beta bands, localized close to sensorimotor areas. This desynchronization starts about 2 s prior to movement-onset over the contralateral Rolandic region and becomes bilaterally symmetrical immediately before execution of movement.

One interesting oscillating brain signal, with a relatively good signal-to-noise ratio in the human scalp EEG, is the post-movement beta ERS. These induced beta oscillations are found in the first second after termination of a voluntary movement. This low amplitude activity, with a focus around the corresponding sensorimotor representation area, results in embedded beta oscillations with a good signal-to-noise ratio.

Therefore, ERD can be interpreted as an electrophysiological correlate of activated cortical areas involved in processing of sensory or cognitive information or production of motor behavior [41]. An increased and/or more widespread ERD could be the result of the involvement of a larger neural network or more cell assemblies in information processing. Factors contributing to such an enhancement of the ERD are increased task complexity and/or more effort and attention.

In all types of ERD-BCI, motor imagery of a movement is used rather than a movement itself. Motor imagery can modify the neuronal activity in the primary sensorimotor areas in a very similar way as observable with a real executed movement, and may be seen as mental rehearsal of a motor act without any overt

motor output. It is broadly accepted that mental imagination of movements involves similar brain regions/functions which are involved in programming and preparing such movements. According to this view, the main difference between performance and imagery is that in the latter case execution would be blocked at some cortico-spinal level [130],[68].

During movement preparation and execution, μ and beta ERD at a specific cortical location may be accompanied by a 10-Hz ERS over areas not engaged in the task and represent idling or inhibitory cortical activity movement task. For example a central ERD is accompanied by an occipital ERS and an occipital ERD is found in parallel with a central ERS central beta, which reflects the concept termed ‘‘focal ERD/ surround ERS’’, that emphasizes the idea of deactivation or inhibition of surrounding cortical areas, which are outside the focus of attention (‘‘surround ERS’’). This inhibition results in a divergent behavior of μ and beta activities, i.e., in an enhanced synchronization of the hand area mu rhythm.

This effect of selective attention to one motor subnetwork (e.g., foot area) may be accentuated when other motor subnetworks (e.g., hand area) are ‘‘inhibited.’’ This is in agreement with more recent studies showing that especially the frequency band 11–13 Hz displays ERS in the hand area, when the subject is engaged in another motor task ERD followed by a rebound in the form of an ERS.

One part of ERD-BCI is based on the recording and classification of transient EEG changes during different types of motor imagery such as, e.g., imagination of left-hand, right-hand, or foot movement, where a discrimination of two brain states (e.g., left- versus right-hand movement imagination) can be reached within only a few days of training [20].

- ✓ The most significant ERD/ERS for left and right hand motor imageries appears at the contra-lateral channels, C4 for left hand and C3 for right hand [20].
- ✓ Represent as ERD, the most modulated channel for foot imagery, is Cz, and is weaker than that of hands [20],[128].
- ✓ 10-Hz ERS during foot motor imagery was only significant on C3.
- ✓ Tongue imagery expresses strong Cz-ERS.

Researchers in [14] have built their ERD-BCI with its two channels over Cz (foot representation area) and C3 (right hand representation area), to control a cursor on

a computer screen. Subjects were instructed to imagine a right-hand movement or a foot movement after a cue stimulus depending on the direction of an arrow.

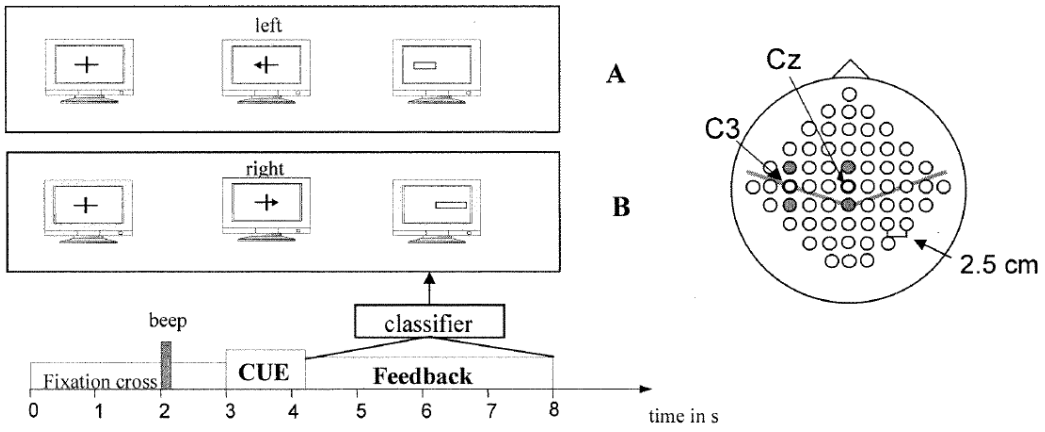

Figure 5-3: ERD-BCI paradigm [14]

Each subject spent 20–30 min on a two-session BCI investigation. The first session consisted of 40 trials conducted without feedback. One trial lasted 8 s and the time between two trials was randomized in a range of 0.5–2.5 s to avoid adaptation, and started with the display of a fixation cross in the center of a screen. After 2 s, a warning stimulus was given in the form of a "beep." After 3 s, an arrow (cue stimulus) pointing to the left or right was shown for 1.25 s. The subjects were instructed to imagine a right-hand movement or both-feet movement until the end of the trial, depending on the direction of the arrow. Signals were then analyzed using two methods: Auto-regression analysis and Band Power estimation. An LDA classifier was then used for the classification of the subject specific parameters. The classification result was used to give a continuously updated feedback stimulus in form of a horizontal bar that appeared in the center of the screen. If the person imagined both-feet movement, the bar—varying in length—extended to the left
If the subject imagined a right-hand movement, the bar extended to the right.
During this 40 trials- second session, the subjects' task was to extend the bar toward the left or right edge of the screen.
It is interesting that in about 20% of the sessions, the two brain states were distinguished with an accuracy of greater than 80% after only 20–30 min of training, and, 70% of the sessions were classified with an accuracy of 60%–80%.

5.4. Multi command Steady State Visual Evoked Potential BCIs

SSVEP is a natural periodic response of the visual cortex to a periodic visual stimulus pattern generated when the gaze of the subject is focused on a two-color flickering visual pattern at frequencies higher than 6 Hz [5]. The BCI presented allows a BCI user to navigate a small car (or any other object) on the computer screen in real time, in any of the four directions and to stop it if necessary.

This BCI uses 6 channels (CPZ, PZ, POZ, P1, P2 and FZ) to detect SSVEPs of four small checkerboards flickering at different but fixed frequencies move along with a navigated car, where two sets of flickering frequencies were used: (i) Low-frequency range {UP: 5 Hz, LEFT: 6 Hz, DOWN: 7 Hz, RIGHT: 8 Hz} and (ii) Medium-frequency range {UP: 12 Hz, LEFT: 13.3Hz, DOWN:15Hz, RIGHT: 17Hz}.

Figure 5-4: Multi-Command SSVEP-BCI [5]

The subject was able to control the direction of movement of the car by focusing her/his attention on a specific checkerboard, where EEG frequencies identical to the frequencies of the desired direction were detected, and classified with an Adaptive Network Based Fuzzy Inference System.

The performance for the medium-frequency range flicker (100% success) was slightly higher when compared to the low frequency range (92.3% success) flicker responses, in terms of controllability of the car and execution time delay.

5.5. Functional Electric Stimulation controlled by thoughts

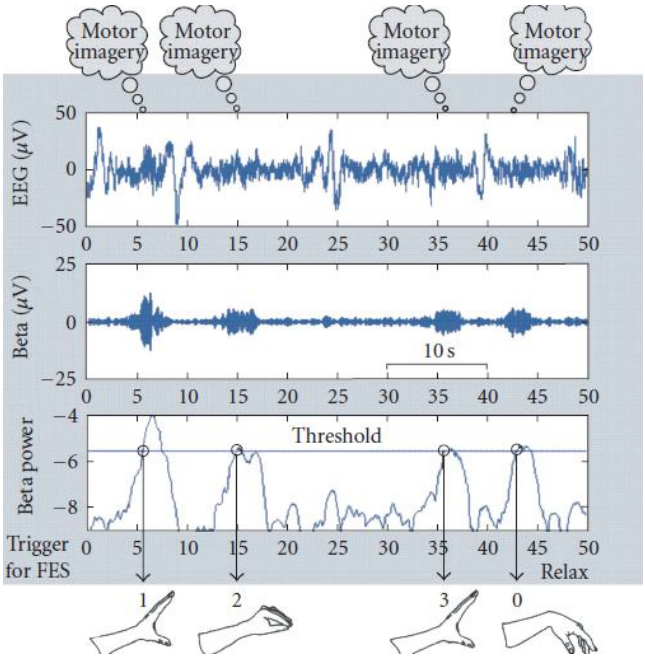

Figure 5-5: FES controlled by thoughts [74]

The BCI used in [74] is an ERD-BCI based on motor imagery, where an imagined movement of the left hand, right hand, feet or tongue is associated to specific commands, same concept illustrated in 5.2. but the control signal here is extracted to control the Functional Electric Stimulation (FES). In this application, a subject, with a complete paralysis of his left hand, is equipped with an FES system. Such a system uses electrodes, placed on the forearm of the subject, in order to send him an electrical current which forces his muscles to tense, a task that the subject is not able to perform voluntarily. So, with a self-paced ERD-BCI, the subject had to use foot motor imagery in order to activate the FES system for tensing or relaxing his muscles, i.e., for closing or opening his hand, thus , the BCI has to output four signals to be used as trigger signals for switching between the different grasp phases (phase 0 – no stimulation phase
phase 1 - opening hand, phase 2 - grasping, phase 3 - releasing, phase 4 = phase 0). This two-channel BCI uses Band Power (BP) Method in the lower beta frequency band 15-19 Hz of the signals from location Cz and C3. At the end of the training, the patient had learned to voluntarily induce beta bursts and was able to control the opening and closing of an electromechanical hand orthotics, and was able, for the first time after the accident, to drink from a glass without any help and without the use of a straw.

Chapter 6

Virtual reality applications based on BCI

6.1. The Virtual Reality application: “Use the force!”

This application performed by researchers in [29] was inspired by *Star Wars*. Participants were asked to control the takeoff of a virtual spaceship by using real or imagined foot movements. This one-channel asynchronous BCI uses Band Power (BP) method in the beta frequency band 16-24 Hz of the signals from location Cz. The threshold was computed according to a baseline (rest) reference, and the Control Signal (CS) was computed as in the formula:

$$Th = m + 3.stdev \qquad (21)$$

Where Th is the threshold, m is the baseline mean of power and $stdev$ is the Standard Deviation.

Whenever a beta ERS occurs, which means imaginary foot movement and CS is higher than Th, the virtual spaceship is lifted up [29].

Figure 6-1: The application "use the force" [29]

6.2. Walking through a Virtual City by Thought

The goal of the study in [54] was to move forward/backward within a virtual street by imaging right hand/ foot movement, recorded with a 3 bipolar channels BCI at C3, Cz and C4, where the logarithmic band power in the alpha and beta bands of the ongoing EEG were computed and classified by a linear discriminant analysis (LDA). So if the categorization was “right hand movement” the subject stopped and if it was “foot movement” the subject began walking with constant speed. The given task of the subject was to walk to the end of the street inside this virtual city, but walking was only allowed if the cue was indicating the “foot” class (arrow pointing downwards and double beep, respectively). Any time the computer identified the subject’s brain pattern as a foot movement a forward motion happened, but if the subjects were thinking on a “foot” movement during the wrong cue class (“right hand”) a backward movement happened as a consequence.
These results suggest that improving the visual display in a BCI could improve a person’s control over his/her brain activity.

Figure 6-2: Walking through a virtual city by thoughts [54]

6.3. Self-paced exploration of the Austrian National Library through thought

This application [76] was also a 3 bipolar channels BCI at C3, Cz and C4, where the logarithmic band power in the alpha and beta bands of the ongoing EEG were computed and classified by a linear discriminant analysis (LDA). It is quite similar to the application discussed in 6.2. with the same imaginary patterns, but with two differences. The first one was that the virtual environment here was a model of the Austrian National Library that was modeled in Maya and 3D Studio with 120.000 faces and 60.000 vertices together with 30MB of texture to create such a photo-realistic model of the 80 meter long and 14 meter wide main hall .

Figure 6-3: Exploration of the national Austrian Library through Thoughts [24]

In all experiments, the subjects were sitting in a comfortable chair in the middle of the virtual environment system DAVE, and were asked to move through motor imagery towards the end of the main hall of the Austrian National Library along a predefined pathway where the starting point was at the entrance door and the subject had to stop at five specific points

The second difference was that at each time the LDA output was exceeding a selected threshold ,the BCI replied the DAVE request with a move command (speed = 1.5 m/s and rotation = 0.9°/s).

The initiation to move forwards was given by the experimenter (verbal cue, synchronous event), but the time necessary to move to the next specific stopping point depended only on the performance of the subject (asynchronous task). The duration of the pause time was given by the experimenter, but the activity within the pause was controlled by the subject.

One disadvantage of the experimental strategy applied was that the subjects had to perform the motor imagery over 10.5 and 25.6 seconds, which is a very long period.

6.4. Virtual Smart Home Controlled By Thoughts

In [39], a P300-BCI with 8 channels located over the parietal and occipital areas was presented. This BCI was connected to a virtual reality (VR) system in order to control a smart home application. During the experiment the subjects have to do different tasks, like to switch on and off the light, to open and close the doors and windows, to control the TV set, to use the phone, to play music, to operate a video camera at the entrance, to walk around in the house and to move him/herself to a specific location in the smart home. Therefore 7 control masks for the BCI system were created: alight mask, a music mask, a phone mask, a temperature mask, a TV mask, a move mask and a go to mask.

12 subjects were trained firstly on selecting specific commands from the P300 matrices. Each person had to select 7icons of each of the 7 control masks for training the computer system on its individual EEG data. Therefore the icons were highlighted in a random order and the subject had the task to concentrate on the specific icon he/she wanted to choose. All experiments were undertaken in a so called “single character speller” mode where only one icon is highlighted at one specific time point. In order to increase the recognition accuracy it is necessary to highlight each icon several times. For the training every icon flashes 15 times.

The best result was achieved for subject 6 with 100 %accuracy for 8 and 4 flashes.

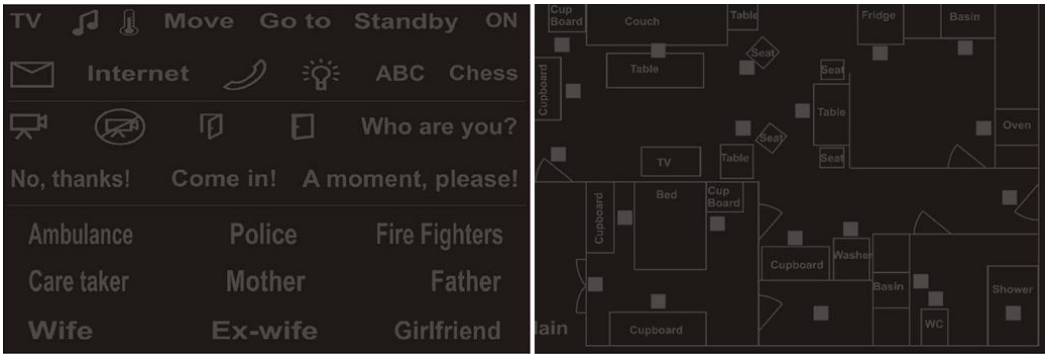

Figure 6-4: Virtual Smart Home Controlled By Thoughts [39]

Figure 6-5: Virtual Smart Home Controlled By Thoughts [21]

6.5. Controlling an avatar to explore a virtual apartment using an SSVEP-BCI

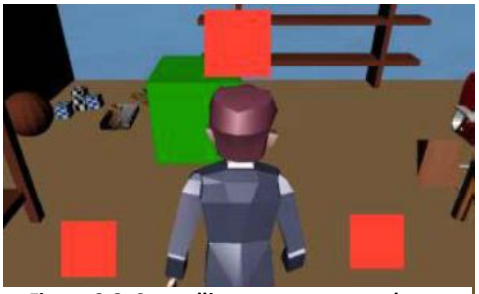

Figure 6-6: Controlling an avatar to explore a virtual apartment using an SSVEP-BCI [40]

In this SSEVP-BCI presented in [40] with 2 channels over O1 and O2.The participants were instructed to navigate an avatar to two waypoints along a given path in two runs, by alternately focusing attention on one of three visual stimuli that were flickering at the different frequencies 12, 15 and 20 Hz, where control signals were produced proportional to power increase in these frequencies. Successful classifications of the according classes produced those control signals which to achieve the associated commands (i) turn 45° left (ii) turn 45° right and (iii) walk one step ahead.

The main performance measure was the time to finish. All subjects were able to control the self paced VR scenarios using an SSVEP-BCI [40],[37].

6.6. BCI-based VR applications for disabled subjects

This application presented in [53] was similar to what has been presented in 6.1. but also with differences. The differences were that the subject was a tetraplegic patient who mastered control of his wheelchair's simulated movements along a virtual

street populated with 15 virtual character avatars, with the ERD-BCI at the mid-central area with a dominant frequency of 17 Hz.

Earlier, during an intensive training period of approximately four months, the participant learned to control the ERD-BCI. The tetraplegic participant was placed with his wheelchair in the middle of a multi-projection based stereo VR system ("CAVE"), During the wheelchair simulation, the subject moved from avatar to avatar while progressing toward the end of the virtual street(65 length units with shops on both sides), using only imagined movements of his feet. He could move forward along the virtual street with a speed of 1.25 unit/second, only when the system detected foot motor imagery (MI). Experimenters requested that the subject stop as close to an avatar as possible. Each avatar was surrounded by an invisible communication sphere (0.5 – 2.5 units) and the subject had to stop within this sphere. The size of the sphere approximated the distance for a conversation in the real world. The avatar started talking to the subject if he was standing still for one second within this sphere. After finishing a randomly chosen short statement (like: "Hi", "My name is Maggie", "It was good to meet you"…), the avatar walked away. Communication was only possible within the sphere; if the subject stopped too early or stopped too close to the avatar, nothing happened [37].

After a while, of his own free will, the participant could imagine another foot movement and start to move again toward the next avatar, until he finally reached the end of the street. Over two days, the tetraplegic participant performed 10 runs of this experiment and could stop by 90 percent of the 15 avatars.

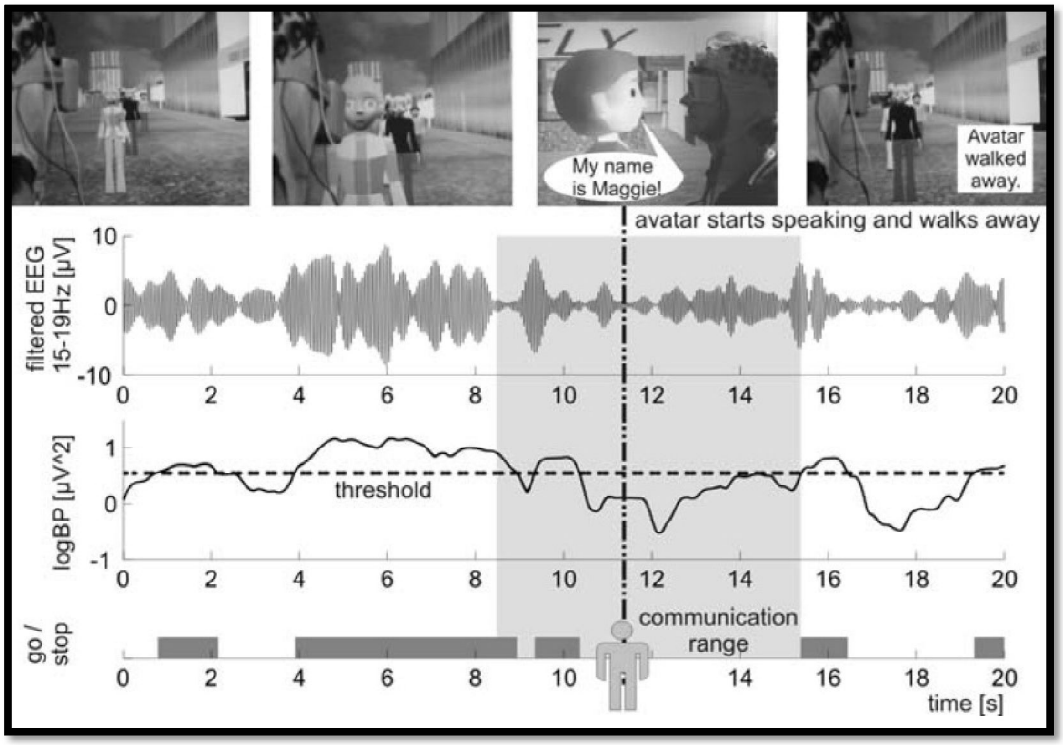

Figure 6-7: BCI-based VR applications for disabled subjects [37]

The subject mentioned that "*It has never happened before, in the sense of success and interaction. I thought that I was on the street and I had the chance to walk up to the people. I just imagined the movement and walked up to them"[37].*

The subject stated that he felt surprised as one avatar walked through him; he wanted to get out of the way, to go backwards. This suggests that the subject felt very absorbed in the virtual reality environment [37].

Using a VE can give such persons access to experiences that may be long forgotten (or which they have never had). The fact that the subject could still perform feet motor imagery, years after an injury that rendered him unable to use his feet, is a testament to the plasticity of the human brain [24]. Another advantage here is that VEs can be used to create virtual prototypes of new navigation or control methods, and give potential users experience of them in a safe environment before they are ever physically built [51],[24].

Chapter 7

The Experiment

7.1. Introduction

Virtual Reality has become an essential tool in daily life. It has been integrated to medicine, education, manufacturing technology, psychophysics, psychology, engineering and research. This integration had induced a very high interest of BCI interaction with virtual environments. Using immersing Virtual Environments has become a much demanded solution for many problems in the field of visual Psychophysics. For example, to analyze the visual and motor response resulting from an optic flow, to analyze these responses with EEG recordings in the lab is a hard challenge, because large artifacts resulting from walking and moving would noise the EEG and make the analysis a very hard process to achieve. However, using an immersive VE by creating realistic visual scenes is a very powerful alternative platform. This is the main reason to use a BCI in VE. Brain-computer interaction with virtual worlds Interactions can be decomposed into elementary tasks such as navigation using ERD-BCI, selection and manipulation of virtual objects using SSVEP-BCI or P300-BCI and performing other visual tasks while using a hybrid ERD&SSVEP-BCI [2],[3],[139],[157],[80]. The feedback was found to be very important in a BCI design as it provides the user with information about the efficiency of his/her strategy and enables learning**.** The following sections will explain the system we have designed for our study, the equipment used, as well as the methodology and paradigm used in the present experiments.

7.2. Overall system flowchart

We can see in the figure below our system flowchart where everything in blue was performed online starting with presenting the stimuli to the subject, send it wirelessly to the PC and process it with Biograph and then feedback the subject via

connection.dll, the interface code between Biograph and the virtual reality application , and everything in red was performed offline.

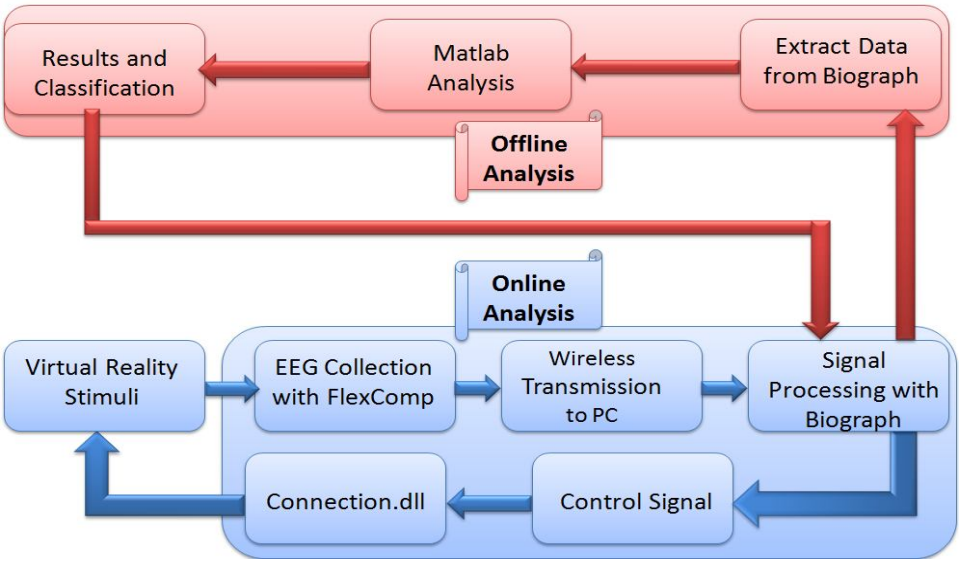

Figure 7-1: Overall system Flowchart

7.3. Equipment

7.3.1. Computer Specification

The Master computer was a HP xw4600 with Intel® Core™ 2 Duo 8400 processor, 3 GB DDR3 memory, 2.66 GHz with 1333 MHz Front Side Bus memory, 4 MB L2 cache memory, 300 GB hard disk space and CD/DVD writer. A17 inch display was used in the system. This computer was used to control the four virtual reality computers, as well as a platform to run the EEG acquisition software used in this project.
Since this computer is the master computer to control Virtual Reality computers, so in order to leave space for other research to be conducted in the virtual environment, we have chosen the offline analysis performed on a second computer. It's an LG with Intel® dual-Core™ E6500 processor, 4 GB DDR3 memory, 2.93 GHz, 931 GB hard disk space, CD/DVD writer and a 21 inch display.

7.3.2. Wireless EEG Equipment

The Flex Comp Infiniti™ encoder is a 10 channel, multi-modality device for real-time computerized biofeedback and data acquisition. It has 10 protected pin sensor inputs with two channels sampled at 2048 s/s and three channels sampled at 256

s/s. The Flex Comp Infiniti™ encoder is able to render a wide range of objective physiological signs used in clinical observation and biofeedback, including:

- Electromyography (EMG)
- Electrocardiography (ECG)
- Electroencephalography (EEG)
- Skin Conductance
- Skin Temperature

Figure 7-2: The FlexComp Infiniti™ encoder [90]

The sensors passed signals to the host computer via the microprocessor-controlled Flex Comp Infiniti™ encoder unit. The encoder samples the incoming signals, digitizes, encodes, transmits the sampled data, passes the data to the Tele-Infiniti CF (a telemetry option) and sends data via Bluetooth to a Bluetooth USB adapter [90]. Thought Technology products monitor and record physiological and mechanical signals, analyze information, and provide auditory and visual feedback [90]. Components and accessories from Thought Technology used in this study were the Flex Comp Infiniti™ encoder, Tele-Infiniti CF, EEG Cables Bipolar, Biograph Infinity, Channel Editor and Screen Editor, 10-20 Conductive Gel and Nu-prep EEG skin prepping gel. Electrodes were connected through extender cables. Blue, yellow and black colors mark the positive, negative and the neutral electrodes. The encoder is battery run and the technical specification of Flex Comp Encoder is provided in the annex. Many of the BCI researchers used up to 128 electrodes to collect EEG. As we were looking to get only the motor imagery, using two electrodes mounted bilaterally over the motor cortex was suitable enough for our experiments.

7.3.3. Virtual Reality ICUBE

The EON ICUBE™ is a PC based multi-sided immersive environment in which

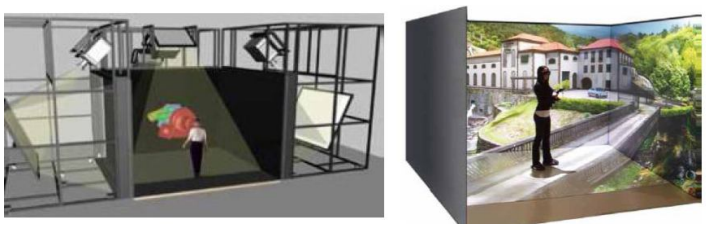

Figure 7-3 ICUBE [103]

participants are completely surrounded by virtual imagery and 3D sound. Stimuli were generated on four HP Z800 workstations and were rear-projected onto four Da-Lite Fast-Fold 10' wide x 7.5' wall-screen (one frontal , two lateral and one ground), from a distance of 4.10 m. The image was projected on the screens using four InFocus LP725 projector scanning at 75 Hz with a resolution of 3,072x768 ,2500 ANSI Lumens brightness and 2400:1 Contrast ratio. Stereoscopic active lightweight shutter glasses and position trackers are also installed, and the result is complete immersion of the user in a virtual world where objects float in space with high quality graphics. 12 infrared cameras (Optitrack) with trackers are implemented to monitor the user's position and orientation at 12hz sampling rate and are used to calculate a stereoscopic perspective view while allowing the user to freely move into and around the objects floating in space.

For the synchronization between the four computers, the master computer on the same network was used.

7.3.4. Virtual Reality Tunnel

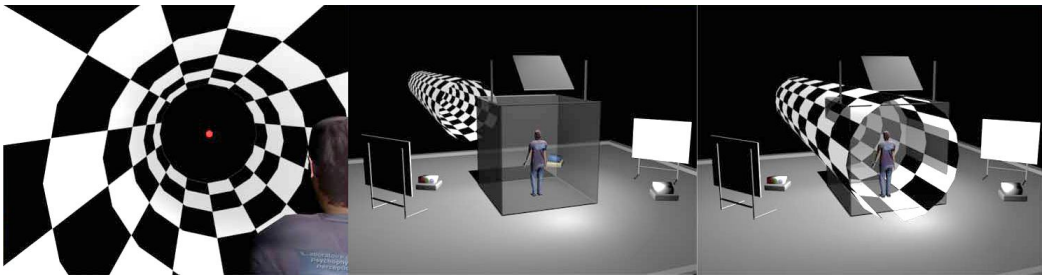

Figure 7-4: Virtual Reality Tunnel [76]

As a virtual environment, we had chosen the 3D Tunnel, static and moving in the Anterior-Posterior direction, within a Peripheral visual field condition (PF). The virtual tunnel respected all the aspects of a real physical tunnel (i.e., stereoscopy and size increase with proximity).

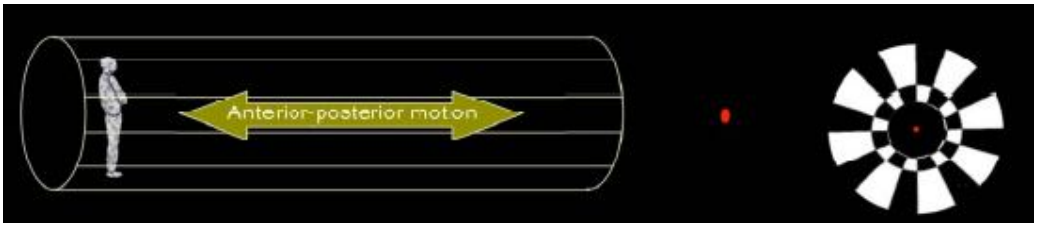

Figure 7-5: Peripheral visual field condition [76]

To program the tunnel, C++, OpenGL and VR Juggler were used. In order to create stereoscopic environment, we have presented two offset images separately to the left and right eye of the viewer in conjunction with shutter glasses which were controlled by an infrared transmitter that sends a timing signal that allows the liquid crystal layer of the glasses to alternately darken over one eye, and then the other, in synchronization with the refresh rate of the screen, being otherwise transparent. Meanwhile, the display alternately displays different perspectives for each eye [78]. These two-dimensional images are then combined in the brain to give the perception of 3-D depth. The tunnel was 3 m in diameter and 91 m long. Its front extremity was closed with a wall (subtending 2°) to reduce aliasing. Its back extremity was virtually located 7 m behind the subject [76]. A red fixation point (subtending 0.2°) was placed at the end of the tunnel at equal distance of the lateral wall. Stimuli were either static or dynamic moving at speed of 1.1 m/s. This velocity was perceived corresponding to normal gait. The equation of motion of the tunnel is

$$x(t)=A/2 \text{ Sin } (Vt+ ℓ) \qquad (20)$$

where A refers to the amplitude (in meters), V refers to the frequency (in hertz), and ℓ refers to the phase. In peripheral visual field conditions, proximal parts of the tunnel remained, while central parts were truncated and replaced by a black uniform field. The texture was a pattern of alternating black and white squares. The association of shape (cylinder), texture, and perspective provided a radial flow to the central visual field and a lamellar flow to the peripheral visual field. This optic flow structure is the one for which the visual system is very sensitive and consequently quite responsive with respect to the control of stance [76]. The squares were all the same size in the virtual world (corresponding to real-world conditions) but appeared smaller at distance due to perspective. Consequently, sensitivity of the visual system for spatial frequencies and cortical magnification were essentially accounted for by this naturalistic stimulation [76].

7.3.5. Biograph Software

Biograph Infinity 5.0 software from Thought Technology was used in this research. This software controls different activity like extracting EEG signals through

electrodes, digitizing and sending signals to the PC, filtering and processing data, separating signal into different frequency bands, Biofeedback …etc. Time synchronization of the start of stimulus slideshow and data collection also is achieved using features of the software. It can export time series data in plain text format for further analysis. It has a built-in notch filter which removes line noise from electricity systems [38]. The software has battery indicators to prevent loss of performance due to low battery voltage.

Biograph Infinity provides different data collection and analysis screens, but we created our own virtual channels and screens for the purpose of this research, using the Screen Editor, Script Editor and Channel Editor installed with Biograph.

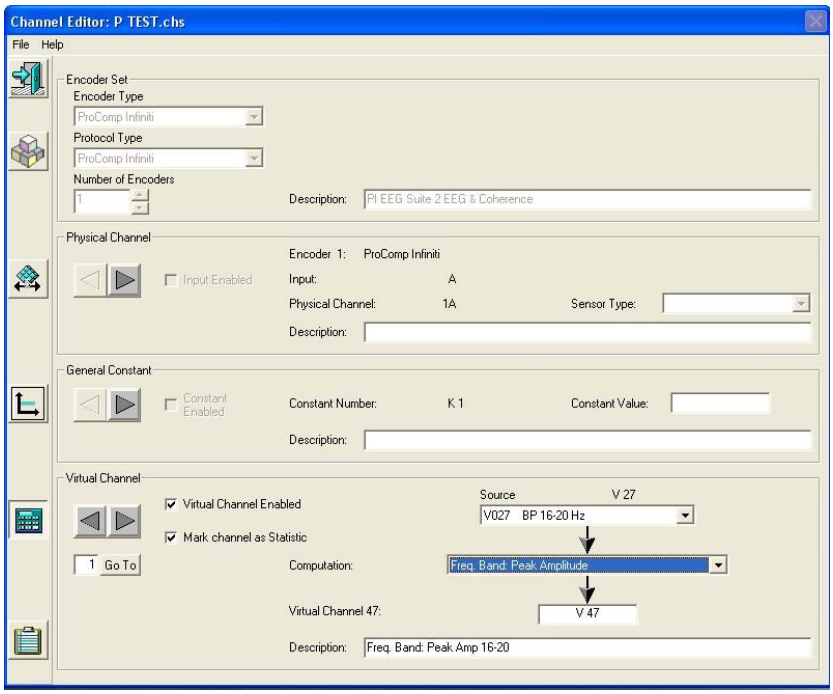

Figure 7-6: Channel Editor installed with Biograph

7.3.6. MATLAB

MATLAB (matrix laboratory) is a numerical computing environment and fourth-generation programming language. Developed by MathWorks, MATLAB allows matrix manipulations, plotting of functions and data, implementation of algorithms, creation of user interfaces, and interfacing with programs written in other

languages, including C++, Java, and FORTRAN, using different libraries called toolboxes [105].

7.4. Methodology and protocol

Table 7-1: Methodology and protocol

1 Session = 4 Runs	
1 Run = 80 trials	
1 Run=12 min	10 min pause

In the standard paradigm for the discrimination of two mental states, the experimental task was to imagine either forward or backward movement depending on a written command. 10 naïve subjects (mean age 25.6 ± 3.92), 9 males and 1 female participated in this experiment. They all signed a consent where they were explained the confidentiality and reliability of their data. They also received a compensation of 25 $ each session, total 50 $ for both.

The experiment included two sessions for each subject; data of session number one were labeled training data, and were used for offline analysis, while session number two data were labeled test data. Session two was performed in 2 days, where half of the trials were performed in day one and the second half was performed in day two. This split was to avoid fatigue and to allow learning. Session 2 data were considered as test data for online experiment based on the results from the first session. Each session contained 4 runs, and each run was 80 trials, which resulted in 320 trials in total, 160 trials for moving backward and 160 trials for moving forward. The number of trials was based on the Graz BCI paradigm, and to obtain enough trials for the averaging step. To be able to extract a good event-related potential, averaging the signals across the trials is one of the most common method, however a minimum number of 100 trials is required to be able to extract the time-locked event. The training trials were labeled -1.1 for forward and 1.1 for backward movement. The goal was to correctly label the test data by using a classifier developed from training data that maximizes the performance measure for the true test labels. For this

research we used 3 bipolar EEG Ag/Cl cup electrodes attached to the scalp bilaterally over the motor cortex in positions C3, Cz,C4 and bipolar at Pz, according to the 10-20 system. In order to place the electrodes, we first located the Inion.

On the posterior base of the skull, where the spine meets the skull, there is a small protrusion called the “inion”. It can be found by running the finger up the spine towards the skull, this is the location of Oz. Then we located the nasion which is the depression on the bridge of the nose, just below the brow and directly between both eyes. The line between these two points runs along the inter hemispheric fissure of the brain, so we marked a spot located at 50% of the distance between the nasion and the inion [90].

Figure 7-7: localizing EEG electrodes placements on the scalp [104]

Then we located the mandibular notch, where we placed a finger against the tragus, just anterior to the ear, and asked the subject to open their mouth. Our finger should find its way into a cavity, resting superior to the mandibular notch. The line that connects the left and right mandibular notches runs along the central sulcus of the brain (the space that separates the frontal and parietal lobes). So we marked a spot located at 50% of the distance between the left and right mandibular notches. It should intersect directly with the mark made between the front and back of the head. The intersection of these two lines is electrode location CZ.

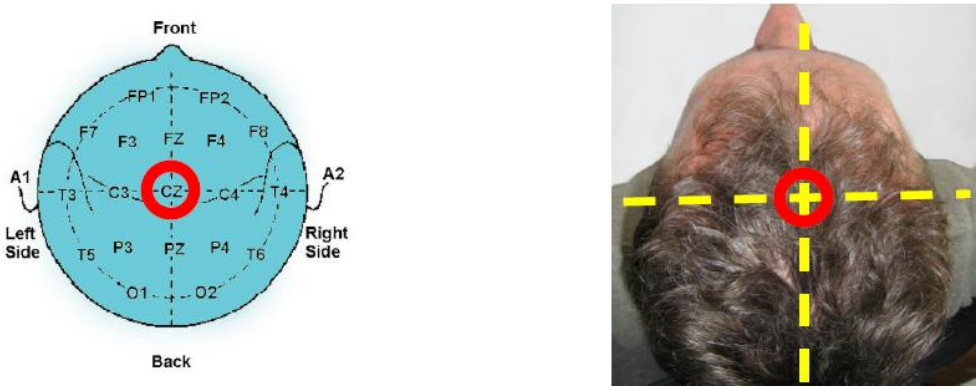

Figure 7-8: localizingCz electrode placement on the scalp [104]

Along the line between the mandibular notches, 20% of the total distance towards the left is location C3, and 20% towards the right is location C4.

Figure 7-9: localizing C3, C4 electrode placement on the scalp [104]

Then we separated the hair around the electrode site and a preparing gel in order to clean and remove sweat and dust.

Figure 7-10: Scalp preparation for EEG electrodes placements [104]

After that we added Ten20 paste onto the cup electrode, just enough to form a ball on the cup.

Figure 7-11: Attaching EEG electrode to the scalp [104]

Then we repeated the above preparation and placement steps on the ear lobes [90]:

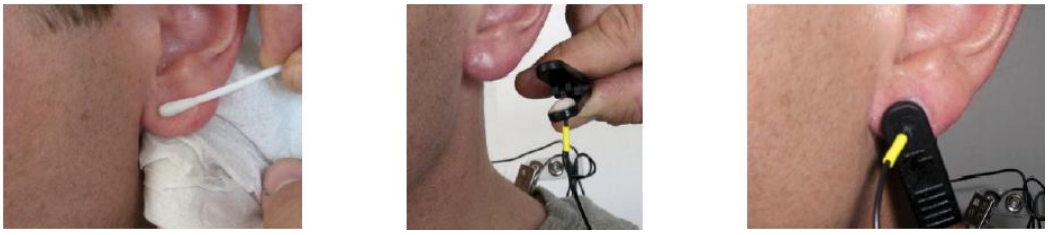

Figure 7-12: Attaching reference electrodes to the ear lobe [104]

Then we have asked the subject to stand in the ICUBE virtual environment device 50 cm away from the front screen, with the 3 EEG channels attached to his scalp over the motor cortex in positions C3, Cz and C4, where then we started the built up environment in ICUBE. The experiment paradigm starts at this point.

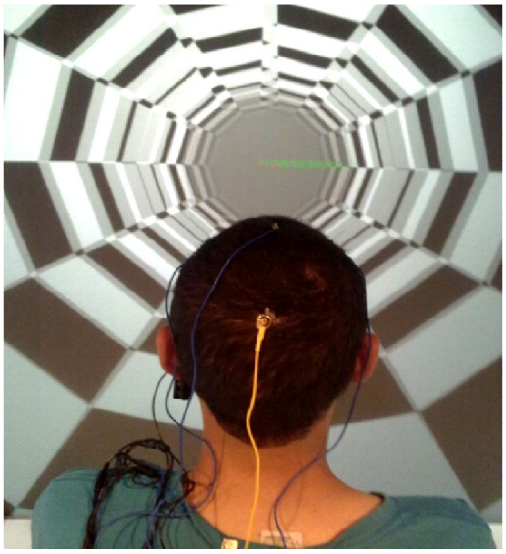

Figure 7-13 A subject in the tunnel

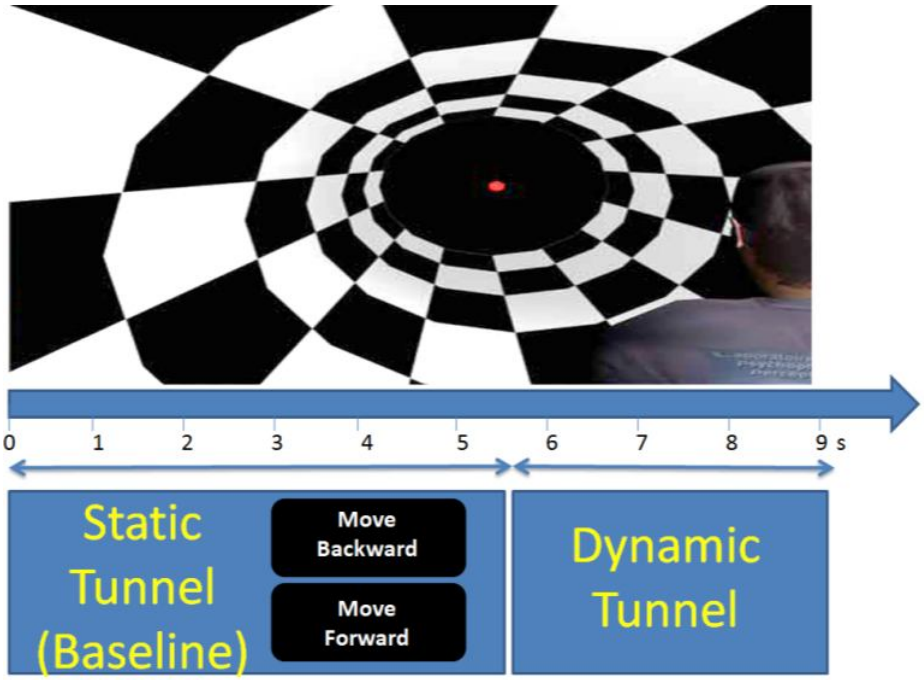

Figure 7-14: One trial Paradigm of the BCI in our research

The timing of the experiment was based on the standard Graz-BCI paradigm, where each trial was 9 sec long and started with 3 seconds of a static tunnel, in order to acquire a baseline EEG. Then for 2 sec the presentation of a written command " Move forward " or " Move Backward " randomly presented at the center of the screen, followed by 0.5 second of a static tunnel and then 3.5 seconds of dynamic tunnel (moving at the same requested direction). Depending on the direction requested, the subject was instructed to imagine moving in the tunnel, e.g., forward movement or backward movement, and to stop the imagination once the tunnel starts to move. In session 1, we used a dynamic tunnel to facilitate the task of motor imagery. However, in session 2, the dynamic tunnel represented a feedback for the subject because it moved in the same requested direction. The whole session duration was around one hour and a half including preparation and rest times. For start synchronization between the recordings and the paradigm start, a keyboard push-button prompt to start on the screen was used right before starting the paradigm of the experiment. However for the end synchrony, the recordings were set to be terminated after 48 minutes from the beginning of the recording.
Motor behavior and imagery (moving in virtual tunnel) can change the functional connectivity within the cortex and results in ERD/ERS of mu and central Beta rhythms , and motor imagery can modify the neuronal activity in the primary

sensory-motor areas in a very similar way as observable with a real executed movement [20],[68].

Signals were acquired with the thought technology Wireless EEG system, transmitted to the master workstation where Biograph was installed.

We designed a special platform for this experiment with the channel editor and the screen editor that comes with Biograph. Besides the two virtual channels for the EEG acquisition, we used many other virtual channels. Here are some of these virtual channels:

1- IIR Filter :

We used IIR filters algorithm (explained in 4.1.2 of this thesis) as butterworth bandpass filters of the 18_{th} order and sampling rate of 256 Hz, in order to filter the raw signal between 8-30 Hz [144],[14] and then this signal was band-pass filtered again to get the four main frequency bands:

1) Alpha band and μ rhythm between 8-12 Hz
2) SMR band between 12-15 Hz
3) Low and central beta band between 16-24 Hz
4) High beta band between 25-30 Hz

We chose the butterworth filter amongst other types of IIR filters in order to reduce the ripple effect of the signal, and the frequency bands were chosen according to the international classification of EEG signals as shown in 2.3.

2-Frequency band Total amplitude:

These algorithms determine the total amplitude value within a given band (PSD), and they take band power (which is the squared magnitudes of FFT) as an input. A 1-sec hanning window was chosen to give a frequency resolution of 1 Hertz/bin.

3-Time-Frequency Analysis:

Joint Time-Frequency Analysis provides the ability to analyze a signal in the time and frequency domains simultaneously, thus showing how the frequency spectrum of a signal changes over time with a coloured spectrogram. The algorithm was explained in 4.3.3.1. of this thesis. Performing a Short-time Fourier Transform (STFT) or time-frequency analysis was an obvious extension of this approach that permits an insight into the ERD /ERS by analysing the power variation with respect to time. The

difficulty with identifying time-frequency features is the inherent trade-off between the time and frequency resolution [79].

It is impossible to achieve a high degree of resolution in both the time and frequency domain of the short EEG segments and thus the domain of the feature that maximally identifies with the left or right trial must be prioritised. Due to the short epochs utilised in this system, the resolution in either domain was severely compromised. The STFT was estimated at a high spectrogram resolution of 1 second hanning windows in time with a 50% overlap, and 64 frequency bins. These settings were chosen to obtain a balanced time/frequency resolution and a lowest detectable frequency of 1 Hz.

4-Arithmetic Operations:

Multiplication for example was used to have the EEG samples squared, this operation along with the mean and standard deviation of the second 3, these were used later to be considered as coefficients of the formula used to compute the threshold over a band-power according to 4.2.1.1. and 6.1. as will be explained later. Subtraction was also used for the asymmetric ratio method.

These were the main virtual channels we have used to build our own platform for EEG analysis. The main screen instruments used in the designed platform were:

1- The bar graph :

The Bar Graph instrument offers the option of single or dual threshold-triggered feedback. Whenever a signal passes the threshold, a Boolean signal output 1 is triggered.

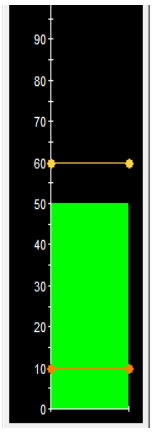

2-**The Line graph:**

We have used the line graph for displaying the filtered signals over time during the session recording or replaying.

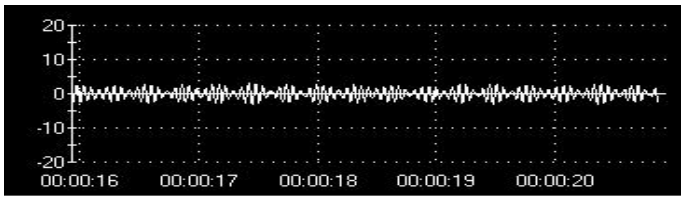

3-Time frequency instrument:

The time frequency instrument displays a colored spectrogram of the frequency domain in respect to the time.

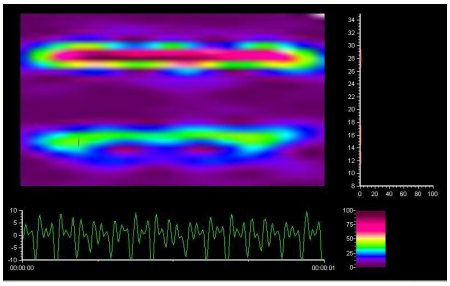

5- The Connection Instrument:

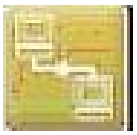

The Connection Instrument allows connecting and controlling an external software program (for example, a virtual reality application) by sending it signals from the BioGraph Infiniti system. The external application can be on the same computer as BioGraph or on a different computer that is in the same network as the BioGraph computer.

An interface file in xml format lists signals and associated commands, which were in this project: Move forward, Move backward. We modified The DLL file of our application used in this study, the virtual reality tunnel, in order to make the tunnel move forward or backward according to the Boolean signal it receives whenever the signal passes a threshold in Biograph. The xml file used for our application is provided in the annex.

After recording a session number 1 for a subject, and after applying the manual artifact removal algorithm within Biograph, clean data were exported to another computer for offline analysis.

Any recorded session in Biograph can be replayed using the “Replay Session" button in the software. Session data can be also exported into a text file via the button " Export Data ", where we can choose the type of data we want to export, as well as choosing the sampling rate, time period and duration and event markers if any were used, where alpha- numeric keys can be programmed to indicate an event when pressed when the session is being recorded.

For this application, we exported band-power signals at a sample rate of 256 Hz, and we exported the rest of the data at 8 Hz sampling rate.

The virtual tunnel application generated also a XML file which contains the event markers at second 3 of every trial, move backward and move forward.
These event markers correspond to the state of the tunnel presented In the ICUBE every time it's presented. These XML files along with the text files were imported to MATLAB for offline analysis.

7.5. Signal Pre-Processing

Most signal Pre-Processing parts was achieved within Biograph. As mentioned in 7.4., the bandpass IIR filters were used to filter the signal between 8-30 Hz and then were used to band-pass the signal in order to obtain 4 frequency bands:

- 8-12 Hz
- 12-15 Hz
- 16-24 Hz
- 25-30 Hz.

Artifact rejection was performed by Biograph during session recording and via an Artifact Auto-rejection mode. This algorithm removed automatically the parts of the recorded signal where the amplitude exceeds the normal EEG amplitude, which is in this case 20 μv. We also performed manual Artifact removal while replaying the session, where the parts of the signal with artifacts were removed. A notch filter provided by Biograph was also used to remove power line interference.
All of these algorithms results in clean signals ready to be exported to another application for offline analysis as mentioned before.
The last pre-processing part was to de-trend the signals [79]. The event-related potentials are relatively small compared to the total EEG spectrum, so in order to get a clean signal ready for processing, a baseline was averaged over a 1 sec window, 2 seconds prior to moving onset, and then mean baseline was subtracted the from every single trial. For each subject, an event-related potential template was generated, specific to each channel, feature and event, by ensemble averaging across the trials. The signal is now ready for processing and feature extraction.

7.6. Feature extraction and selection:

Most parts of the feature extraction phase were performed online within Biograph, where those features were used later for offline analysis. Only two were extracted offline. The features extracted are:

a. Time-Frequency Representation Spectrogram (online)
b. Frequency band Power (online) and ERD/ERS (offline)
c. Power Spectral Density and Asymmetrical ratio (online)
d. Auto-regression model (offline)

After importing the online features into MATLAB, data of every feature in every frequency band and for every task were averaged across all trials. We had 160 trials of motor imagery for moving forward in the tunnel and 160 trials of motor imagery for moving backward in the tunnel, and with an event marker for every position, labeled -1.1 for forward movement and 1.1 for backward. This resulted in a matrix of rows and columns, where each column represented a feature in a specific frequency band, and rows represented the features values at a specific time-point. Since we had 3 extracted features (BP, PSD, and PSD As.R), 4 frequency bands and 3 channels, this resulted in 32 columns of features. However, and since there were 48 minutes of recorded EEG (excluding breaks) from session 1 for each subject, this resulted in 23040 time-points if the sampling rate was 8hz, and 737280 time-points if the sampling rate was 256 Hz. This part of data was then used with the event markers to calculate the average signal across trials for every position, features and frequency band.

7.6.1. Time-Frequency Representation Spectrograms

The TFR (Time-Frequency Representation) was mainly used online so we can usually define the most active frequencies and their strengths during the mental task achieved by the participant in every single trial. Since the TFR spectrogram was computed online, we have replayed the session number one for every subject while looking at event markers in the text file provided, thus we were able to study the power spectrum in respect to time. TFR analysis was designed to handle the trade-

off between time and frequency by many methods. Biograph provided four of these methods: STFT, wigner-ville distribution, Gabor, Matching Pursuit**.** Each method offered its own benefits and trade-offs.

The STFT was the simplest and quickest of the four methods, but provided the poorest offline simultaneous time-frequency resolution of the four methods. However, the Matching pursuit, which adapted to the signal characteristics and localizes individual components, provided the best time-frequency resolution of all methods, but was more processing-intensive.

Since we had 48 minutes of EEG recordings, so a low intensively processing method was required, and here we chose the STFT method.

So, after an online visualization of the most active frequency bands during both tasks, we were ready to use the second method of signal processing for our BCI.

7.6.2. Band Power and ERD/ERS calculation

After extracting the band-power values calculated online for every channel and every frequency band, and after cleaning and averaging the data offline, we calculated the ERD/ERS time-course [35],[41]. This method is explained in 4.2.2. of this thesis. In order to calculate the ERD/ERS time course, we first calculated the average power in a reference interval [35] between second 2 and 3. Then we calculated the relative power change for the power of the movement versus the reference interval. These calculations resulted in signals templates with the ERD/ERS for each of the two tasks performed. We then selected the best two ERS/ERD that distinguished between the two tasks. This selection was based on the percentage change method, where we calculated the percentage change between the averaged backward/forward signals relative to forward, and on the feature points between second 4 and 6.5. The purpose was to find the maximum percentage change between the peaks of two templates' features of the averaged signals.

The best ERD/ERS of each task were later set up in Biograph as signal thresholds for session 2. This means that whenever the subject's EEG power signal passes threshold 1, the tunnel was triggered to move in forward direction, and whenever the EEG power signal passes threshold 2, the tunnel was triggered to move backward. This method was the only method tested online.

7.6.3. Power Asymmetrical ratio

Because the data have been filtered into 4 frequency bands, four Power Spectral Densities for each channel were calculated and then four power asymmetry ratios were calculated online within Biograph between electrodes C3-C4. All of the PSD features and the Asymmetrical Ratio features were later used for offline analysis.

7.6.4. Auto-regression models

We applied in this study two Auto-Regression methods to model the features calculated online (BP, PSD and PSD Asymmetrical Ratio), where the model coefficients were used later as features, and then fed into the classifiers. After importing the features to MATLAB, we modeled every single feature, in every frequency band and every channel; we modeled these with two different Auto-regression algorithms: AR burg method and ARX least squares method. To model these features, we tested and varied the model order (n_a as AR model order and n_a=n_b as ARX model orders) from 2 to 10 and a step value of 1, for the PSD and PSD asymmetrical ratio. The model orders for the BP features were varied from 2 to 30, with a step value of 1 between 2 and 8, and a step value of 2 between 8 and 30. These cut-offs were chosen based on the state-space model selection function that we had run over all of the previously extracted features [50].

One other parameter had to be set for the ARX; we set the exogenous input to be the template of averaged backward trials when modeling backward trials and the template of averaged forward trials when modeling forward trials, because averaging across trials assist in extracting the event-related potential hidden within the noise. We tested the auto-regression methods to investigate how well these estimated parameters could serve in distinguishing between forward and backward single trials, based on the number of model coefficients used. These methods are explained in 4.2.2.2 of this thesis. In this section, we saw that a large amount of features were extracted. These features are:

1. BP x 4 frequency bands x 3 channels (fs=256 Hz)
2. BP-ARX x 4 frequency bands x 3 channels x 18 model orders (fs=256 Hz)
3. BP-AR x 4 frequency bands x 3 channels x 18 model orders (fs=256 Hz)

4. PSD x 4 frequency bands x 3 channels (fs=8 Hz)
5. PSD-ARX x 4 frequency bands x 3 channels x 9 model orders (fs=8 Hz)
6. PSD-AR x 4 frequency bands x 3 channels x 9 model orders (fs=8 Hz)
7. As.R x 4 frequency bands x 2 channels (fs=8 Hz)
8. As.R-AR x 4 frequency bands x 2 channels x 9 model orders (fs=8 Hz)
9. As.R-ARX x 4 frequency bands x 2 channels x 9 model orders (fs=8 Hz)

So, in total, 824 features were extracted and presented to the classifiers, 380 at a sampling frequency of 8 Hz, and 444 at a sampling frequency of 256 Hz. The offline nature of this stage allowed us to run the tests on all of these features, so we can later select the features that achieved the best classification performance, which will be explained in the coming section. It is important to select the specific feature at the specific frequency band and channel which holds the most significant information that distinguish between the two tasks of the experiment, otherwise too many information will increase computation and results in poor classification due to the additional noise and redundant information.

7.7. Classification

This phase tested our previous offline calculations presented in 7.6. The LDA classifier and linear SVM were used to classify each feature of every single frequency band and every channel. LDA was used because it requires less training and computation compared with neural network based classifiers, where SVM was used because of the good generalization properties and its insensitivity to the curse of dimensionality. For the classification of band-power, we used the Diagonal LDA, where its only difference from the fisher LDA is that it computes the diagonal covariance matrix estimates. Later, we compared SVM and LDA performance in order to select the best classifier for this study. In linear SVM, we tested different values for the C factor in an exhausted search for the optimum C factor, where we varied the values exponently between $1.e^{-7}$ and $1.e^{2}$ with a step value of e^{-1}. The features were divided into 4 epochs, in order to investigate the optimum time (and thus feature points) that the imagery signal achieved the best classification accuracy

[92], thus decreasing the computation time. Various epochs were experimented based on a 0.5s increase. These epochs were:

1) Epoch 1: 4 – 5s
2) Epoch 2: 4 – 5.5s
3) Epoch 3: 4 – 6s
4) Epoch 4: 4 – 6.5s

However, we ran the search for the optimum C factor on the data of a randomly selected 50 % of the subjects, which means 5 subjects out of the 10 subjects we tested, and found $C=1.e^{-2}$ to give optimum results, so we assumed a generalization of this value for all subjects' data of this study. Consequently, we ran 36256 (824 features x 4 epochs x LDA + 824 features x 4 epochs x SVM 10 C factors) classification test for the session 1 data of 50 % of the subjects, and 6592 (824 features x 2 classifiers x 4 epochs) classification test for the session 1 data of the other 50 % subjects. All of these classifications were performed with 10-cross-validation and the positive rate calculation to test the classifications' performance. We wrote some MATLAB functions to perform theses analysis. The analysis time for this exhaustive search of the best feature that can distinguish between forward/backward tasks was around 30 hours for session 1 data of every subject of the first 50 % and 6 hours for each of the rest participants. We then selected the classifiers and features with the highest classification performance amongst all subjects, and re-ran the classification using the best features over pair of electrodes and then over three electrodes. We then selected the classifier that achieved the best classification performance and used this classifier on session 2 data and on run 4, where we used session 1 data to train the classifiers and the data of the session 2 run as test data, in order to simulate the online performance of the classifiers by labeling the test data, and thus giving the guess of the user's intention to navigate backward or forward in the virtual tunnel. The following section presents some of the results we obtained using all methods illustrated in 7.6.

7.8. Results and discussions

7.8.1. Online TFR

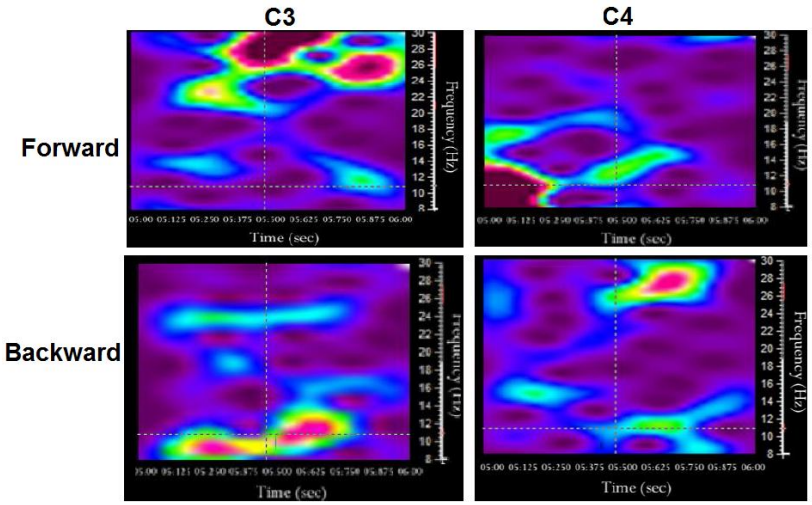

Figure 7-15 Online TFR over C3 and C4

Figure 7-15 displays four online TFRs from the experiment with subject 3. These TFRs were taken between second 5 and second 6, which means that the first half second of the TFR represents half a second before motor imagery termination, where the second half second of the TFR represents half a second after the motor imagery termination. The first column displays TFR for electrode C3 and the second column displays the TFR for electrode C4. The first row refers to the TFR when the subject was instructed to imagine a forward movement, where the second row refers to the TFR when the subject was instructed to imagine a backward movement. During the forward movement, we can clearly see the α-ERD, but once the motor imagery was terminated, a large and a remarkably strong β ERS appeared over C3 and lasted for few milliseconds. On the other hand, the α-ERD appeared also during the backward movement over C3, however, and right after terminating the backward motor imagery, a small and strong β ERS appeared over C4 and lasted for few milliseconds. This suggested that we had a lateralization of signals for motor imagery forward and backward movements, where the right motor cortex showed higher activity for

backward movement versus the left motor cortex, which in turn showed also a higher activity for the forward movement.

7.8.2. Online Band-Power ERD/ERS Biofeedback

After the offline calculation of the ERD/ERS time-course on 12 band-powers (4 frequency bands x 3 channels), we found that there was no difference between the two tasks in the alpha and SMR frequency bands and for all channels.
We also found that motor imagery of forward and backward movement didn't change power at Cz, neither within the alpha band at C3, which corresponded to results found by researchers in [16]. The next result presents the β-ERS at channels C4 and C3 respectively, and at the frequency band 25-30 Hz.

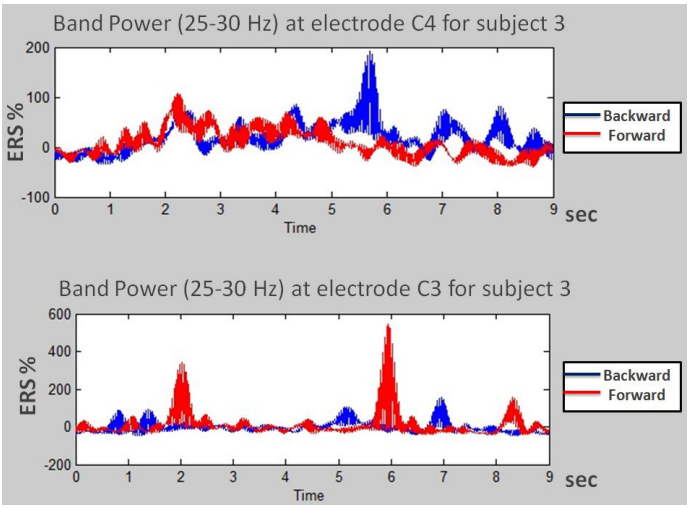

Figure 7-16 β-ERS at channels C4 and C3 respectively, and at the frequency band 25-30 Hz for subject 3

This upper figure shows a remarkable backward ERS that starts right after the termination of the movement imagery and peaked with a 200 % and after about 200 msec. The template illustrates no overlap with the forward signal which appears to be equal to baseline, with a correlation of 0.31. This supports the results researchers in [77] had found, that the right motor cortex and during the motor imagery of moving backward, showed a remarkably higher activation than the motor imagery of moving forward. The lower figure shows exactly the inverse results. At the left motor cortex, the motor imagery of forward movement, resulted in an activation of the left brain motor cortex area, with a remarkable ERS that started 200 ms after the

movement offset, and peaked with a 600 % after about 300 msec. which means after 500 msec. of the termination of the motor imagery. This template illustrates no overlap with the forward signal which appears to be equal to baseline, with a correlation of 0.28. Thus, motor imagery of moving backward would relatively highly activate the motor cortex of the right brain hemisphere, while motor imagery of moving forward would activate the motor cortex of the left brain hemisphere. This result supports our hypothesis 3, that motor imagery of forward-backward movement can activate the motor cortex the same way a strong optic flow does. The two ERS values were later set up in Biograph as signal thresholds to form a control signal for an online Biofeedback test in session 2. The first ERS value was for transition from idling to "move forward" state, while the second one was for transition from idling to "move backward" state. So, the backward threshold was set on the BP of the frequency band 25-30 Hz over channel C4 according to the following equation:

$$Th_b = MEAN + 6 \times STDEV \qquad (21)$$

Where Th is the threshold, b refers to backward, $MEAN$ is the power calculated in a reference interval and $STDEV$ is the standard deviation. The *STDEV* coefficient was calculated according to the ERS time-course, and was selected based on a value that would yield a maximal separation between the standard deviations from the mean baseline of the two tasks, and was set to 3 standard deviations each, i.e. 3 negative standard deviations from the mean for the task that had the higher curve and 3 positive standard deviations from the mean for the task that had the lower curve. For subject 7, we calculated two negative standard deviations from the mean of the averaged backward signal over C4, and calculated its ERS time-course, and found that it was close to 3 standard deviations from the mean baseline. We then repeated that for the forward and found that it was 2 standard deviations from the mean baseline. So we selected the value 6 based on 2 $STDEV_{backward}$ + 1 $STDEV_{safety\ for\ backward}$ + 3 $STDEV_{forward}$.

This formula means that whenever the power over the motor cortex of the right hemisphere exceeds and passes a threshold of 6 standard deviations from the baseline, i.e. activation over C4 resulting from the motor imagery of backward

movement, this would trigger the virtual reality tunnel with a Boolean that induces the tunnel to move in the backward direction. Similarly, the same setting was used as a threshold over the motor cortex of the left brain hemisphere, which means that whenever the power over the motor cortex of the left hemisphere passes a threshold of 6 standard deviations from the baseline, i.e. activation over C3 resulting from the motor imagery of forward movement, this would trigger the virtual reality tunnel with a Boolean that induces the tunnel to move in the forward direction. If the instruction was to move in either direction or the subject failed to generate the correct pattern, where the signal of the opposite instruction exceeds its threshold, the tunnel was triggered to move accordingly. We tested this method online on subject 3. The session 2 consisted of four runs, where the same paradigm was used but with two differences. The first difference was that in session 2, the subject was instructed to stop the motor imagery right after the command " Move Forward " or " Move Backward " offset, i.e. at second 5 of the trial, instead of stopping the motor imagery once the tunnel moves. This modification was performed based on the ERS results. Since the ERS peaked at 200-500 ms of the motor imagery offset for both tasks, this modification of terminating the motor imagery at second 5 would let the beta power to rebound and then peak at second 5.5. The Interface between Biograph and our virtual tunnel was programmed that whenever the signal passed the threshold at second 5.5 and only at this point, the Boolean was sent to trigger the tunnel to move in either direction. The second difference was that the signal was acquired at a sampling rate of 8 Hz and was smoothed out by averaging 3 consecutive samples (with a moving average) in order to produce a smooth Control Signal (CS). Session 2 was performed in 2 different days, of the same week. The following table shows the results for subject 3, where accuracy equals the success rate, which is the proportion of correct hits of a task amongst the total number of events of the same task.

Table 7.2 results of the ERS Biofeedback for subject 3

Subject 3	Run 1	Run 2	Run 3	Run 4	Run 4 Av. Accuracy
Backward	27.5	62.5	87.5	87.5	83.75
Forward	72.5	47.5	47.5	80	

The following chart plots the Biofeedback results for subject 3:

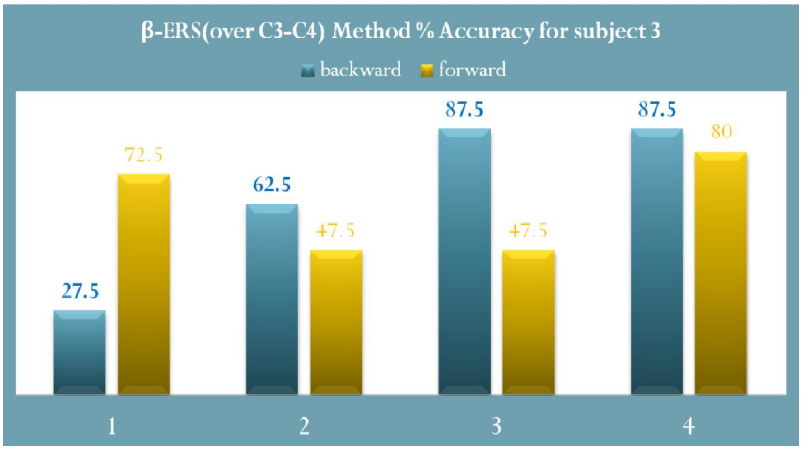

Figure 7-17 Beta-ERS (over C3 and C4) method accuracy results for subject3

At run1 of session 2 as depicted by figure 7.5, we can see a remarkable bias toward the forward imagery movement versus the backward imagery movement, where the subject was able to control the forward movement with a success of 72.5 %, versus a success of 27.5 % to control the backward movement. At run2, the subject tried to put much more effort to control the backward movement with a success rate of 62.5 %, but failed to sustain the same strength to control the forward movement with a success rate that dropped to 47.5 %, and this could be seen as a learning curve to control the forward-backward movement. Subject 3 continued the learning curve at another day, and continued to develop his mental strategy and learn to control the backward movement, where he achieved a success rate of 87.5 % for backward control, but he was still working with a total bias to the backward control versus forward control which achieved a success rate of 47.5 %. Finally, and after 96 minutes of training, subject 3 succeeded the learning strategy and succeeded in sustaining a success rate of 87.5 % for the backward control, and in the same time, regained the strength and mental strategy required for forward control. This learning curve supported our hypothesis 2. This online biofeedback was totally performed using ERS band-power over the high β frequency band (25-30 Hz). Amongst the 10 subjects we tested, 7 showed the same ERS pattern at the high β frequency band, and 3 subjects showed the same pattern but with a central β-ERS (16-24 Hz). These were subject 2, 6 and 9. All patterns had also different ERS values for both forward and backward motor imagery. The results of the online β-ERS Biofeedback for the ten subjects tested are listed in the table below:

Table 7.3 the results of the online beta-ERS biofeedback across all subjects

subject	Run1		Run2		Run3		Run4		Av.Run4
	Backward	Forward	Backward	Forward	Backward	Forward	Backward	Forward	
1	27.5	60	52.5	47.5	42.5	77.5	70	72.5	71.25
2	47.5	77.5	65.5	62.5	77.5	72.5	87.5	82.5	85
3	27.5	72.5	62.5	47.5	87.5	47.5	87.5	80	83.75
4	12.5	77.5	57.5	57.5	42.5	57.5	47.5	62.5	55
5	25	85	47.5	52.5	77.5	85	72.5	92.5	82.5
6	22.5	82.5	47.5	52.5	67.5	77.5	77.5	87.5	82.5
7	75	80	67.5	85	62.5	92.5	50	77.5	63.75
8	22.5	62.5	52.5	62.5	47.5	87.5	77.5	92.5	85
9	30	77.5	67.5	47.5	77.5	82.5	72.5	82.5	77.5
10	37.5	72.5	52.5	42.5	62.5	87.5	72.5	82.5	77.5
AV	32.75	74.75	57.3	55.75	64.5	76.75	71.5	81.25	76.37
STDEV	17.53	8.11	7.91	12.25	16.02	14.24	13.44	9.07	10.1

The purple highlighted subjects are the subjects that showed a central β-ERS, where the yellow highlighted figures are the highest success rates achieved in this experiment. From the last column of this table, which is plotted below, we can see that 50 % of the subjects were able to achieve accuracy of more than 80 % and after a total of 96 minutes of training, 48 without feedback and 48 with feedback.

Figure 7-18 Run 4 average accuracy for all subjects

To study the average performance of the subjects during the four runs of the biofeedback, we plotted the average success rates of every task at each run and across all subjects.

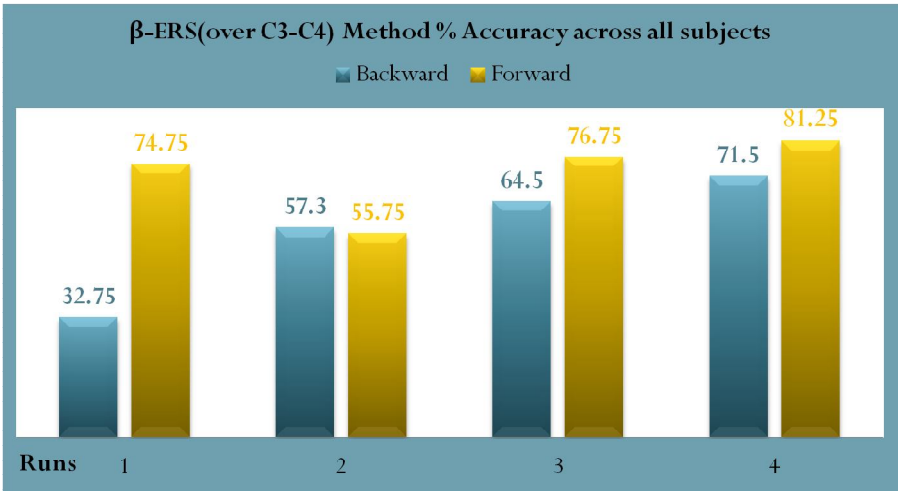

Figure 7-19 Beta-ERS method accuracy across all subjects

The template shows an expected bias toward forward control versus backward control in run1. We have also applied the T-test to interpret the results, where we applied the intra-subjects T-test on the pair of the two tasks in every single run. The subjects had significantly more trouble to control the tunnel movement using motor imagery to the back more than the forward motor imagery ($r_{b1\text{-}f1}$=0.191, t=-7.434, dof=9, p<0.001) because walking forward is an easy automated task for the brain, however, moving backward would require more strength and concentration, and would require also learning to develop a special mental strategy in order to alter the brain waves to produce the correct control signal. So the success rate for the backward control was 32.75 % ± 17.53 versus 74.75 % ± 8.11 for forward control. Most of the subjects in run 2 put much effort into the backward-control strategy learning versus the forward control, where the bias was inverted toward the backward control, which its success rates were improved, accompanying a drop in the success rate of the forward control, in average success rate of 57.3 % ± 7.91 for backward control versus 55.75 % ± 12.25 for forward control ($r_{b2\text{-}f2}$=414, t=0.426, p<1). The next day and in run3, the backward control continued to improve gradually in a so-like linear learning curve, where the forward control was regained ($r_{b3\text{-}f3}$=-0.181, t=-1.663, p<0.2). We think that was because this run was performed in a different day, and so the brain was back to achieve a high success rate for its automated task, the forward control, but sustained the learning and mental strategy he developed for the backward control, and continued to develop it more, to achieve

a higher success rate of 64.5 % ±16.02, where the forward control was regained with a success rate of 76.75 % ± 14.24. In run 4, the subjects' brains continued to develop the mental strategy for the backward control, where a remarkable improvement took place to increase the success rate with only 71.5 % ± 13.44, where the forward control stabilized with slight improvement ($r_{b4\text{-}f4}$=603, t=-2.864, p<0.02). So we can say that the biofeedback induced a learning curve to control the backward navigation in virtual reality ($r_{b1\text{-}b4}$=-0.184, $t_{b1\text{-}b4}$=-5.109, p<0.05), in contrast to the forward navigation in virtual reality ($t_{f1\text{-}f4}$=-1.816,p> 0.1), where in this biofeedback, the learning curve started with a bias toward the naturally automated forward control versus backward control, then the backward control improved gradually with a so-like linear learning curve, however the forward control was lost in run 2, but regained then stabilized at run 3 and 4. We have applied ANOVA to the results for statistical comparisons. As a consequence of the numerous planned comparisons required in the first phase of this study, the Greenhouse-Geisser as well the Huynh-Feldt corrections were applied to interaction tests in order to control for random outcomes in this context. The ANOVA revealed a significant intra-subject main effect of 'Task' (F=26.085, dof=1, p<0.01), a significant effect of 'Runs' (F=17.204, dof=3, p<0.001) and a significant 'Runs' × 'Task' interaction (F=14.085, dof=3, p<0.01), and also revealed a significant inter-subject main effect(F=978.355, dof=1, p<0.001).

7.8.3. Offline analysis for feature selection

This section presents all experimental classification results over session 1 data that we obtained in this study. These results will be briefly presented, due to the high amount number of classification tests we ran, but they will be discussed in detail.

All features that achieved a classification accuracy of less than 60 % were considered bad classification features. This value was selected as 10 % above chance. We started to run classification over all features extracted from each electrode separately, in order to find and select the feature that would yield to the best classification accuracy from one single EEG channel, so we could later use it for classification of the session 2 data, and thus, the BCI would use only one EEG channel. However, all features within α and SMR band and all PSD features fall in this range, when the classification accuracies fall between 30 and 55 %. Some of the tables showing these

results are provided in the annex. This depicted that using a single EEG channel for this study would yield to poor classification results. Then we ran classifications over pairs of channels and then over the features from all 3 channels together. Again, all features within α and SMR band yielded poor classification results, and this depicted that the ERD-classifier couldn't be used for the purpose of our research. However, when running classifications over the power spectral density asymmetrical ratio features between C3 and C4 (extracted from Biograph), the classifier showed a good classification performance over the higher β band for subjects who showed a strong ERS within this band, and also showed good classification results over the central β band for subjects who showed a strong activity within this band. To investigate the best classification in terms of epochs, the graph below shows the results obtained across all subjects, when we ran the classification of power spectral density asymmetrical ratio between C3-C4 within the β band.

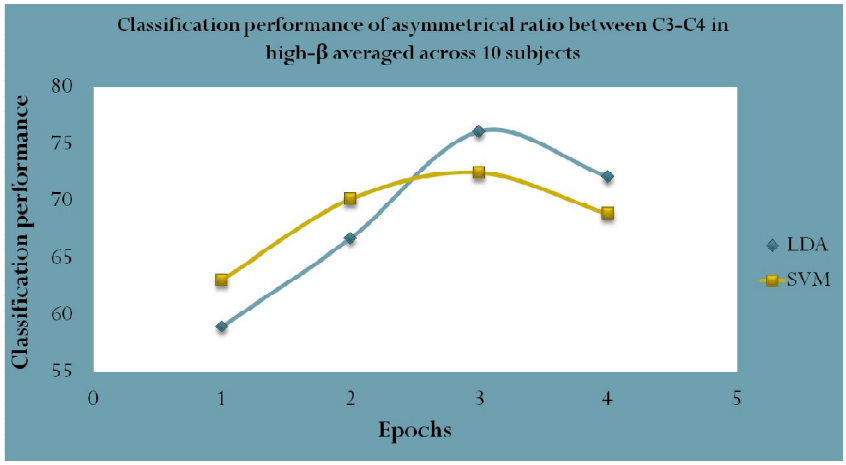

Figure 7-20 Classification of power spectral density asymmetrical ratio between C3-C4 within the β band varied with epochs and averaged across 10 subjects

All classifications showed that the epoch that achieved the highest classification accuracy was epoch 3, i.e. the classifier gave poorer results when classifying the ERD, and better results when classifying the ERS. However, the classifiers' performance was attenuated at epoch 4; we think that this was due to the visual effect the dynamic tunnel added to the event-related potential.

To investigate the best classification results in terms of the C factor, the following table shows the results obtained across all subjects, when we ran the SVM

classification of power spectral density asymmetrical ratio between C3-C4 within the β band, and varied the C factor between different values.

Table 7.4 PSD classification with SVM when varying C factor

C factor	SVM
1.00E-07	58.75
1.00E-06	61.98
1.00E-05	64.23
1.00E-04	66.02
1.00E-03	68.5
1.00E-02	70.21
1.00E-01	68.25
1.00E+00	69.875
1.00E+01	59.44
1.00E+02	57.67

It's obvious that the highest accuracy was achieved using the value $1.e^{-02}$ for the C factor. All results that will be presented next are presented within epoch 3 and with a C factor of $1.e^{-02}$. Figure 7-21 displays the cut-offs and range to select to model the PSD As.R and BP features, where the best range for the band-power features was 2-25, and 2-9 for the asymmetrical ratio features. So, we chose a bit wider range to accommodate ranges from all features.

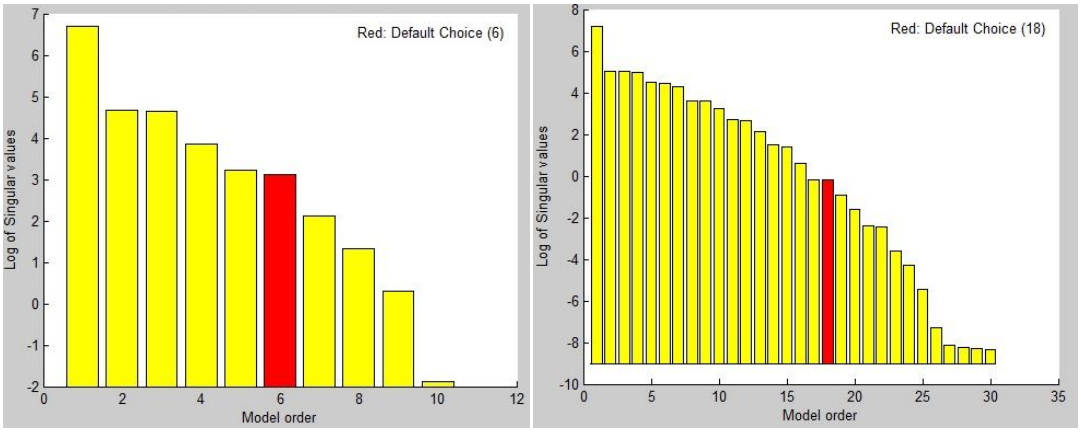

Figure 7-21 state-space model order selection for β-PSD As.R on the left and β-BP on the right

The table below shows the classification accuracy for the power spectral density asymmetrical ratio over C3-C4 over β band for subject 3, varied with model orders.

Table 7.5 Classification results for PSD asymmetrical ratio over beta band varying with model order for subject 3

Classification results for β-PDS –ASR						
Model order	Feature		AR		ARX	
	LDA	SVM	LDA	SVM	LDA	SVM
2	76.11	70.21	73.45	69.24	74.77	71.2
3	74.68	71.02	71.08	68.02	68.19	67.34
4	76.02	69.875	69.24	62.875	57.36	62.5
5	75.28	69.34	65.89	58.45	56.875	61.07
6	73.25	70.5	67.875	66.25	55.05	72.45
7	76.09	68.25	69.02	66.25	63.41	66.14
8	75.44	69.73	65.5	63.73	62.12	65.25
9	73.375	70.14	59.36	68.12	60.75	64.24
10	76	68.66	59.36	66.83	57.21	61.18

We can see from the table that the LDA classifier gave a higher value 6 % accuracy than the SVM, but the classification drops remarkably when the features were modeled in both AR and ARX methods, which tells that these models were modeling noise but not the actual feature. Even though, model order 2 gave the best results amongst other orders. Thus, using the PSD asymmetrical ratio as a feature gave better results than using their model coefficients as features. The classification accuracy for most subjects is close to this indicating that the AR method is poor at predicting upcoming forward and backward movements. A pure guess would offer the same chances of accurate classification. From the previous results, we can also see that we can't rely on one single EEG channel to predict the upcoming forward-backward movement, and that we need at least two EEG channels to achieve an average accuracy of over than 75 %. The next table compares between the session 1 offline classification accuracy over the PSD asymmetrical ratio and the session 2 online Band-Power Biofeedback for all subjects.

Table 7.6 comparisons between session 1 offline classification over beta band and the session 2 online biofeedback for all subjects

Subject	LDA	SVM	AR-LDA	AR-SVM	ARX-LDA	ARX-SVM	BP
1	74.50	68.57	72.79	69.44	73.38	73.71	71.25
2	76.84	71.85	77.63	70.84	75.29	67.84	85.00
3	80.44	78.88	78.88	75.82	78.88	76.50	83.75
4	73.38	67.75	74.91	66.50	73.38	72.13	55.00
5	69.79	65.35	64.50	65.00	68.88	66.69	82.50
6	69.50	67.16	68.25	69.91	71.47	68.38	82.50
7	79.82	71.07	73.38	60.75	77.52	70.69	63.75
8	77.54	72.47	74.50	75.57	75.60	77.57	85.00
9	81.54	71.69	75.29	71.69	76.50	70.07	77.50
10	77.79	67.32	74.35	66.85	76.85	68.44	77.50
AV	76.11	70.21	73.45	69.24	74.77	71.20	76.38
STDEV	4.23	3.89	4.24	4.66	3.02	3.72	10.13

So, using 2 channels BCI, only 20% of the subjects achieved a classification accuracy of 80-82 %, and 60 % achieved classification accuracy of 70-80 %. However, for the Band-Power online Biofeedback, 50 % of the subjects achieved classification accuracy of 80-85 %. We can also see that the average classification accuracy for both methods were almost the same. The next table displays the classification accuracy for the Band-Power 25-30 Hz over C3,C4 and Cz, where the second and the fifth column shows the results when the features where classified with LDA and SVM respectively, and the other columns shows the results when the Band-Power models' coefficients were classified using the same two classifiers and when varying the model order from 2 to 30.

Table 7.7 classification of beta band-power from 3 EEG channels varied with model order for subject 3

Model Order	LDA			SVM		
	LDA	AR	ARX	SVM	AR	ARX
2	69.38	66.56	65.63	65	67.81	65.31
3	70.62	68.13	69.06	68.44	67.19	67.81
4	71.56	60.62	59.69	65.63	67.81	71.56
5	71.25	70.94	66.56	64.69	64.69	66.25
6	71.88	66.56	67.81	65	69.38	71.25
7	71.88	68.13	66.25	70.62	69.69	70.31
8	71.25	68.13	72.5	70	73.75	67.5
10	71.25	69.38	69.38	73.12	74.69	69.69
12	70.94	67.5	68.75	73.75	75.94	68.44
14	70.62	68.75	69.38	74.69	70.94	64.69
16	70.94	70.31	69.06	70.31	69.38	67.5
18	71.88	69.38	69.69	71.25	69.69	66.87
20	71.25	67.19	69.38	68.13	71.25	68.13
22	70	69.38	69.06	72.5	67.5	69.38
24	70.31	67.81	70	69.38	69.06	69.06
26	70.62	68.13	69.06	71.25	70.31	69.69
28	71.25	68.75	69.69	67.19	68.75	67.19
30	70.62	67.19	70	67.81	69.38	69.38

The table displays that Band-Power auto-regression modeling gave almost the same results the Band-Power features gave, however, only the AR model of order 12 when classified with SVM, showed slightly higher classification accuracy. So, in order to compare the performance of classification between all methods and averaged across all subjects, the next graph displays a sort-of equal classification accuracy (~ 76%) over the β-ERS for the online Biofeedback using 2 EEG channels (session 2), the Power Spectral Density Asymmetrical ratio with LDA classifier using 2 EEG channels (session 1) and the Band-Power when classified with SVM using 3 EEG channels (session 1), where the modeled features were modeled with the best model orders.

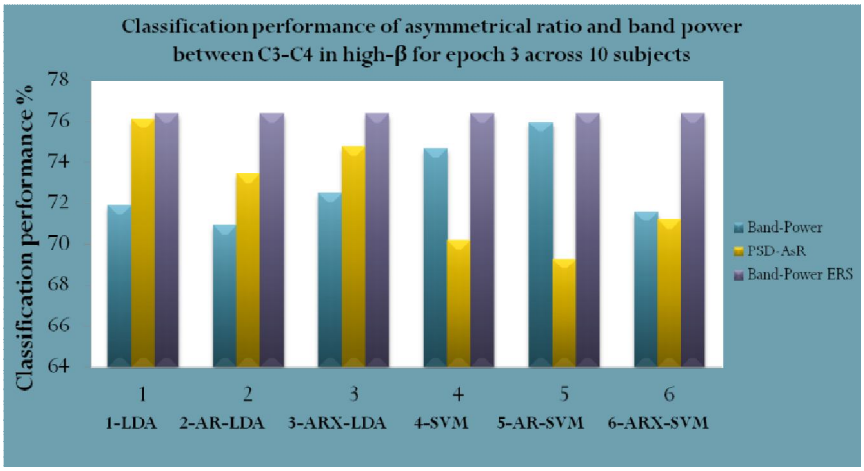

Figure 7-22 classification accuracy over β-ERS for the online Biofeedback using 2 EEG channels (session 2), the Power Spectral Density Asymmetrical ratio with LDA classifier using 2 EEG channels (session 1) and the Band-Power modeled with AR_{burg} when classified with SVM using 3 EEG channels (session 1)

After the classification of the session 1 data, we selected the features that yielded the best classification accuracy, which were in our case:

1-β-Power spectral density asymmetrical ratio between C3 and C4 with LDA classifier

2-β-Band-Power modeled with AR_{burg} over C3, C4 and CZ with SVM classifier

These data were used as training data to train the classifiers, and used the session 2 data to test the classifiers, in a so-like simulation of the classifier performance when implemented online. The results are displayed in the table below.

Table 7.8 Session 2 classification results for PSD asymmetrical ratio between C3-C4 classified with LDA, Band-Power from C3-C4-CZ modeled with AR_{burg} and classified with SVM, and Band-Power online biofeedback for all subjects

	PSD As.R		BP		Biofeedback
subject	session 1	session 2	session 1	session 2	
1	74.5	78.3	75.98	79.34	71.25
2	76.84	83.25	77.36	83.43	85
3	80.44	78.74	79.29	84.67	83.75
4	73.38	78.5	78.44	79.06	55
5	69.79	75.5	74.825	82.81	82.5
6	69.5	73.84	67.09	75.31	82.5
7	79.82	79.44	75.56	79.86	63.75
8	77.54	80.22	82.12	84.06	85
9	81.54	80.63	76.76	74.68	77.5
10	77.79	81.02	76.34	75.93	77.5
AV	76.11	78.94	76.3765	79.915	76.38
STDEV	4.23	2.71	3.89	3.74	10.13

It is remarkable that with the AR-modeled Band-Power features, the average accuracy over all subjects was close to 80 %, with an increase of approximately 4 % from the online Biofeedback.

Chapter 8

Conclusions & future Works

8.1. ERS-BCI

This thesis described the results of an evaluation of an asynchronous BCI application conducted with 10 subjects. We studied performances of human learning and machine learning BCI in a two-session paradigm that lasted 48 minutes each, using 3 EEG channels and trying to find the minimum number of electrodes that could achieve the highest performance. Subjects interacted with strong Virtual Reality stimuli and were asked to control their forward-backward navigation in a virtual tunnel by using imagined forward-backward movements. Results of this project, as well as previous psychophysical results showed that the motor cortex was activated bilaterally when backward-forward movements were imagined, and thus a single EEG channel couldn't be used to control a virtual reality application with these imagined movements. This result was remarkable within the TFR extracted online. The TFR was able to show the ERS activity for both tasks, and this was due to the lateralization of the tasks over the two sides of the motor cortex. The high frequency resolution of the TFR helped in the determination of the subject-specific band where the ERS occurred right after termination of the motor imagery. On the other hand, when using two EEG channels and applying the human learning and biofeedback training, the ERD couldn't be used to train the subjects, so the training was used over the β-ERS band-power features. All of the subjects were able to control their navigational direction within the tunnel, but with an averaged accuracy of 76 %. The subjects found the backward control a harder task to achieve (the average accuracy for backward control was 50-70% versus ~64-84% for forward control). They all started the feedback sessions with a bias toward the forward control, which depicted that using backward imagined movement was not an easy task to control, and thus was not a feasible task to use in a motor imagery BCI. In session 2 training, some of the participants asked for a reference on their performance, like a feedback of the strength of their signals, so they would be able to know how to improve their

mental strategies, consequently we think that the lack of a continuous feedback contributed to the bad performance of some participants. It was well proven that the continuous feedback facilitates the learning stage to operate a BCI, so if we had used a continuous feedback on form of signal strength, maybe this could have helped in improving performance of the subjects. Most of the subjects found session one boring, yet they all found session two more attractive and challenging since it was themselves who were controlling the tunnel. At the first two runs, and when participants couldn't achieve a good performance, they were tired due to 24 minutes of mental activity, and they were frustrated of not being able to control the tunnel, and, that's why splitting up session 2 to be performed in two days helped the participants to relax, get their strength back, and overcome the frustration. So, maybe by using continuous feedback in session one and shortening this session, the participants would have found it less boring, they would have been more motivated and their performance would have been improved with less time. During the experiments, the participants commented on the fact that being in the stand-up position in the tunnel gave a realistic feeling of moving within the dynamic tunnel, and provided them with a more realistic motor imagery, even though it was tiring. The selected stimuli were strong enough to help the participants generate the correct motor imagery task. In regards to machine learning, the band-power features modeled with AR and classified with SVM, as well as the well-known and widely used power spectral asymmetrical ration with LDA classifier gave slight better results than human learning methods, with an average classification accuracy of almost 80 %. Using auto-regression modeling over the band power features helped in decreasing the number of features over one channel, but increased the required number of channels, where good classification accuracy was obtained only when using band-power features from three channels, however these methods decreased the computation time. The use of the AR modeling method to extract the ERS from the background EEG was shown to be a good method and boosted the SNR of the event-related potential's ERS, but showed very poor results when used to extract the ERD. However, this technique didn't improve classification accuracy when applied over the PSD asymmetrical ratio features comparing to the features themselves, and also showed poor results when used over PSD features in order to extract both ERD and

ERS. This was because the PSD features were originally extracted features, holding both the event-related potentials amidst and mixed with the background EEG noise, and that the ERS template generated by the PSD, was too vague to be detected and extracted by the AR. On the other hand, the ARX failed also to extract the event related potentials when modeling the PSD for the same previous reason, but provided better results when modeling the band-power features. In this project, the exogenous input used was the ensemble averaged templates of the backward-forward trials, so the factor that raised sensitivity to the exogenous input in this project was the subject-specific template. The complexity of the task, the imagined forward-backward movement, generated ERD templates that were similar for both tasks, which made this complexity a contributor factor to the poor results the AR and ARX provided when modeling certain features. However, the ERS templates were quite different, especially bilaterally, even though the results didn't vary remarkably with order higher than 8. Results suggested that a further investigation and understanding of the creation of the exogenous input is needed to improve the ARX performance. Finally, the SVM and LDA both proved to be very good classifiers for the forward-backward motor imagery features, however, using SVM was much more complicated due to the parameters that need to be set up and selected to get the best classification results. Using only LDA would have saved a lot of time since the results were similar. In this project, we only used linear classifiers, since they are the simplest to use. Perhaps polynomial and Gaussian classifiers would have provided better results, but would have required more analysis time to set their parameters and search for the optimum parameter that would yield to best classification performance. The classifiers weren't implemented online, even though the interface codes were already provided by Thought Technology, this was due to the investigation nature of this study. Since motor imagery of backward movement required higher strength to achieve and control, another strategy to improve the BCI control is to assign an easier imagery task to control the backward navigation in the tunnel. Biofeedback training with two electrodes and machine learning with three electrodes provided almost same performance, however, using more than three EEG channels may have had improved the classification performance, but is still a trade off to use fewer channels. Finally, the online merge of human learning and machine

learning techniques would improve the performance and capabilities to control the BCIs.

8.2. Future work

We think that BCI era has started to merge into our daily lives and that the advances in BCI research are evolving.

There are currently new findings in cognitive neurophysiology, psychophysics, neural engineering and brain connectors mapping that are leading into a better understanding of the functionality of the human brain which leads to a better EEG source activity control, which would help us in any future work in the BCI domain especially in the overall design level. As future work, we are looking into designing EEG caps and electrodes with new ergonomic designs so where they will be much easier to wear with fewer electrodes and the electrodes will require less contact gel. Another part of the BCI we are looking to develop is the signal processing part, where we are looking to develop new algorithms of artifact removal in a way that will make the signal cleaner and more efficient to be treated. New parameters and algorithms will be developed for the feature extraction and selection phase, like the pattern recognition algorithms, which will lead into new state of the art BCI that uses new concepts, rather than ERS or SSVEP. Furthermore, of the most important algorithms we are looking to develop are the machine learning and classification methods, in a way that would help us to recognize multi-tasks signals, rather than the binary tasks recognition used in this project. The BCI would then be used in a very wide application field, if several mental tasks were recognized. On the other hand, when we were performing the test over subjects, all subjects claimed that they felt more comfortable operating the BCI when they were provided with a feedback in form of controlling their navigation direction in the tunnel in session 2, where in session 1 they had the feelings that they were just “passive operators”. After the second run of session2, some of our subjects asked if they could have their performance displayed on the screen, so they would know how well they were doing and should they improve their mental strategy to control the tunnel. Most of the subjects were also wondering if there were easier protocols to follow for someone to

learn operating a BCI. So, as a future work, we are looking to develop new paradigms and protocols that would facilitate operating the BCI with less training, as well as finding ways to provide the subjects a feedback of their signals' strength in form of bars that would be displayed over the screen, and maybe the 3D technique would be used for more attractive and realistic interaction. The development of displaying a feedback of the operator's control signals, as well as the feedback in form of the controlled task, may lead in the future to use audio/visual and somato-sensory feedback, which may also, facilitates training and usability.

Error detection and response verification will take also a big part in our future work, in order to reduce the response time of the signal so it can be more close to real time. Immersive virtual environments are becoming a crucial demand in the BCI world, so by developing new scenes and environments, we will be able to conduct new treatment and rehabilitation methods for many psychological and pathological disorders, and may be by integrating the BCI to control not only virtual environments, but also to control robots and rehabilitation gadgets.

Since BCI is a multidisciplinary field, nowadays, a new Master Degree academic program is taking place in the universities: Brain Computer Interface Engineering. The next few years should see the deployment of variety of these devices and their ongoing development to help improve the lives of so many people [56].

References

[1]. Alexandra Constantine, " A Brain-Computer Interface for the Classification of Motor Imagery", B.A. Thesis from UNIVERSITY Williamstown, Massachusetts, U.SA., 2007

[2]. Allison BZ, Brunner C, Kaiser V, Muller-Putz GR, Neuper C, Pfurtscheller G., "Toward a hybrid brain-computer interface based on imagined movement and visual attention", J Neural Eng 7(2): 26007, 2010.

[3]. Allison BZ, Leeb R, Brunner C, Muller-Putz GR, Bauernfeind G, Kelly JW, Neuper C., "Toward smarter BCIs: extending BCIs through hybridization and intelligent control", J Neural Eng 9(1): 013001, 2012.

[4]. Al chalabi B., Msadi M., Hbobati M.K., “Portable wireless EEG”, pre-B.Sc. thesis, University of Damascus, 2009.

[5]. Bashashati A, Fatourechi M, Ward RK, Birch GE., "A survey of signal processing algorithms in brain-computer interfaces based on electrical brain signals", J Neural Eng 4(2): R32-57, 2007.

[6]. Bayliss, J.D.; , "Use of the evoked potential P3 component for control in a virtual apartment," Neural Systems and Rehabilitation Engineering, IEEE Transactions on , vol.11, no.2, pp.113-116, June 2003

[7]. Bayliss, J.D.; Ballard, D.H.; , "A virtual reality testbed for brain-computer interface research," Rehabilitation Engineering, IEEE Transactions on , vol.8, no.2, pp.188-190, Jun 2000

[8]. Bernhard Graimann, Brendan Allison, Gert Pfurtscheller, “Brain-Computer Interfaces: A gentle introduction”, in “Brain computer Interfaces: revolutionizing human computer interaction”, springer, 2011.

[9]. Birbaumer, N.; Kubler, A.; Ghanayim, N.; Hinterberger, T.; Perelmouter, J.; Kaiser, J.; Iversen, I.; Kotchoubey, B.; Neumann, N.; Flor, H.; , "The thought translation device (TTD) for completely paralyzed patients," Rehabilitation Engineering, IEEE Transactions on , vol.8, no.2, pp.190-193, Jun 2000

[10]. Borroni P, Montagna M and Cerri G, Baldissera F, Cyclic time course of motor excitability modulation during the observation of a cyclic hand movement, Brain Res, vol. 1065, (no. 1-2) ,pp. 115-24, 2005

[11]. Brosseau-Lachaine, O., Casanova, C., Faubert, J. ,Infant sensitivity to radial optic flow fields during the first months of life. Journal of Vision, 8(4):5, 1-14, 2008

[12]. Brosseau-Lachaine, O., Faubert, J., Casanova, C. ,Functional sub-regions for optic flow processing in the posteromedial lateral suprasylvian cortex of the Cat. Cerebral Cortex, 11, 989-1001, 2001

[13]. Bufalari, S.; Mattia, D.; Babiloni, F.; Mattiocco, M.; Marciani, M.G.; Cincotti, F.; , "Autoregressive spectral analysis in Brain Computer Interface context," Engineering in Medicine and Biology Society, 2006. EMBS '06. 28th Annual International Conference of the IEEE , vol., no., pp.3736-3739, Aug. 30 2006-Sept. 3 2006

[14]. C. Guger, G. Edlinger, W. Harkam, I. Niedermayer, and G. Pfurtscheller, How many people are able to operate an EEG-based brain-computer interface (BCI)?, IEEE Trans. on Neural Sys. and Rehab., 11(2):145–147, 2003

[15]. Cho, B.H.; Lee, J.M.; Ku, J.H.; Jang, D.P.; Kim, J.S.; Kim, I.Y.; Lee, J.H.; Kim, S.I.; , "Attention Enhancement System using virtual reality and EEG biofeedback," Virtual Reality, 2002. Proceedings. IEEE , vol., no., pp.156-163, 2002

[16]. Christa Neuper, Michael Wörtz, Gert Pfurtscheller, " ERD/ERS patterns reflecting sensorimotor activation and deactivation", In: Christa Neuper and Wolfgang Klimesch, Editor(s), Progress in Brain Research, Elsevier, 2006, Volume 159, Pages 211-222,(http://www.sciencedirect.com/science/article/pii/S0079612306590144)

[17]. Deng, J.; He, B.; , "Classification of imaginary tasks from three channels of EEG by using an artificial neural network," Engineering in Medicine and Biology Society, 2003. Proceedings of the 25th Annual International Conference of the IEEE , vol.3, no., pp. 2289- 2291 Vol.3, 17-21 Sept. 2003

[18]. DENNISJ. McFARLAND, A. TODDLEFKOWICZ, and JONATHAN R.WOLPAW, " Design and operation of an EEG-based brain-computer interface with digital signal processing technology", Behavior Research Methods, Instruments, & Computers, 1997.29 (3).337-345

[19]. Desney Tan and Anton Nijholt, "Brain-Computer Interfaces and Human-Computer Interaction", in *Human–Computer Interaction Series*, Springer London, 2010

[20]. Dong Ming; Changcheng Sun; Longlong Cheng; Yanru Bai; Xiuyun Liu; Xingwei An; Hongzhi Qi; Baikun Wan; Yong Hu; Luk, K.D.K.; , "ICA-SVM combination algorithm for identification of motor imagery potentials," Computational Intelligence for Measurement Systems and Applications (CIMSA), 2010 IEEE International Conference on , vol., no., pp.92-96, 6-8 Sept. 2010

[21]. Edlinger, G.; Holzner, C.; Guger, C.; Groenegress, C.; Slater, M.; , "Brain-computer interfaces for goal orientated control of a virtual smart home environment," Neural Engineering, 2009. NER '09. 4th International IEEE/EMBS Conference on , vol., no., pp.463-465, April 29 2009-May 2 2009

[22]. Ernst Niedermeyer, Fernando Lopes da Silva, "Electroencephalography. Basic principles, Clinical Applications and Related Fields", 3rd edition, Williams & Wilkins Baltimore, 1993

[23]. F. Lotte, "Brain-Computer Interfaces for 3D Games: Hype or Hope?", Foundations of Digital Games (FDG'2011), pp. 325-327, 2011

[24]. F. Lotte, "Study of Electroencephalographic Signal Processing and Classification Techniques towards the use of Brain-Computer Interfaces in Virtual Reality Applications", PhD Thesis from the National Institute of Applied Sciences (INSA) Rennes, 2008

[25]. F. Lotte, A. Lécuyer, C.T. Guan, "Towards a Fully Interpretable EEG-based BCI", 4th International Brain-Computer Interface meeting, 2010

[26]. F. Lotte, A. Van Langhenhove, F. Lamarche, T. Ernest, Y. Renard, B. Arnaldi, A. Lécuyer, "Exploring Large Virtual Environments by Thoughts using a Brain-Computer Interface based on Motor Imagery and High-Level Commands", Presence: teleoperators and virtual environments, vol. 19, no. 1, pp. 54-70, 2010

[27]. F. Lotte, C.T. Guan, "An Efficient P300-based Brain-Computer Interface with Minimal Calibration Time", Assistive Machine Learning for People with Disabilities symposium (NIPS'09 Symposium), 2009

[28]. F. Lotte, M. Congedo, A. Lécuyer, F. Lamarche, B. Arnaldi, "A Review of Classification Algorithms for EEG-based Brain-Computer Interfaces", Journal of Neural Engineering, 4, R1-R13, 2007 - featured article - highlights of 2007

[29]. F. Lotte, Y. Renard, A. Lécuyer, "Self-paced Brain-Computer Interaction with Virtual Worlds: a Quantitative and Qualitative Study 'Out of the Lab'", 4th International Brain-Computer Interface Workshop and Training Course, pp. 373-378, 2008

[30]. Fabiani GE, McFarland DJ, Wolpaw JR, Pfurtscheller G.," Conversion of EEG activity into cursor movement by a brain-computer interface (BCI)", IEEE Trans Neural Syst Rehabil Eng 12(3): 331-8, 2004.

[31]. Fan Yang; Weidong Chen; Bian Wu; Yu Qi; Jianxun Luo; Yu Su; Jianhua Dai; Xiaoxiang Zheng; , "An adaptive BCI system for virtual navigation," Information Science and Engineering (ICISE), 2010 2nd International Conference on , vol., no., pp.64-68, 4-6 Dec. 2010

[32]. Friedrich EV, McFarland DJ, Neuper C, Vaughan TM, Brunner P, Wolpaw JR.," A scanning protocol for a sensorimotor rhythm-based brain-computer interface", Biol Psychol 80(2): 169-75, 2009.

[33]. Fruitet J, McFarland DJ, Wolpaw JR., "A comparison of regression techniques for a two-dimensional sensorimotor rhythm-based brain-computer interface", J Neural Eng 7(1): 16003, 2010.

[34]. Fujisawa, J.; Touyama, H.; Hirose, M.; , "EEG-based navigation of immersing virtual environment using common spatial patterns," Virtual Reality Conference, 2008. VR '08. IEEE , vol., no., pp.251-252, 8-12 March 2008

[35]. G. Pfurtscheller and F. H. Lopes da Silva, "Event-related EEG/MEG synchronization and desynchronization: basic principles", Clinical Neurophysiology, 110(11):1842–1857, 1999.

[36]. G. R. Müller-Putz, R. Scherer, M. Billinger, A. Kreilinger, V. Kaiser, C. Neuper, “Proceedings of the 5th International Brain-Computer Interface Conference 2011”, Graz University of Technology, Austria, September 22-24 2011

[37]. Gert Pfurtscheller, Robert Leeb, Josef Faller and Christa Neuper," Brain-Computer Interface Systems used for Virtual Reality Control ", In Kim J.-J. (Ed.) Virtual Reality, InTech, 2011

[38]. Golam Mohammad Moshiuddin Aurup, " User Preference Extraction from Bio-Signals: An Experimental Study ",M.Sc. Thesis from Concordia University ,Montreal, Quebec, Canada, 2011

[39]. Holzner, C.; Guger, C.; Edlinger, G.; Gronegress, C.; Slater, M.; , "Virtual Smart Home Controlled by Thoughts," Enabling Technologies: Infrastructures for Collaborative Enterprises, 2009. WETICE '09. 18th IEEE International Workshops on , vol., no., pp.236-239, June 29 2009-July 1 2009

[40]. J. Faller et al ., " An application framework for controlling an in a desktop-based virtual environment via a software SSVEP brain-computer interface", Presence, 19(1):25–34, 2010.

[41]. J. Kalcher, G. Pfurtscheller, " Discrimination between phase-locked and non-phase-locked event-related EEG activity", Electroencephalography and Clinical Neurophysiology, Volume 94, Issue 5, Pages 381-384, May 1995

[42]. J.A. Pineda et al., “Learning to Control Brain Rhythms: Making a Brain-Computer Interface Possible,” IEEETrans. Neural Systems and Rehabilitation Eng., vol. 11, no. 2, pp. 181-184, 2003

[43]. Joseph D . Bronzino ,"The Biomedical Engineering Handbook", Second Edition, p-p 253-256,CRC Press, 1999

[44]. Kayagil, T. A., O. Bai, et al., "A binary method for simple and accurate two-dimensional cursor control from EEG with minimal subject training." Journal of Neuroengineering and Rehabilitation 6, 2009

[45]. Krusienski DJ, Grosse-Wentrup M, Galan F, Coyle D, Miller KJ, Forney E, Anderson CW., " Critical issues in state-of-the-art brain-computer interface signal processing", J Neural Eng 8(2): 025002, 2011.

[46]. Krusienski DJ, McFarland DJ, Wolpaw JR.,"An evaluation of autoregressive spectral estimation model order for brain-computer interface applications", Conf Proc IEEE Eng Med Biol Soc 1,

[47]. Krusienski DJ, Schalk G, McFarland DJ, Wolpaw JR, "A mu-rhythm matched filter for continuous control of a brain-computer interface", IEEE Trans Biomed Eng 54(2): 273-80, 2007.

[48]. Krusienski DJ, Wolpaw JR.," Brain-computer interface research at the wadsworth center developments in noninvasive communication and control", Int Rev Neurobiol 86,

[49]. L. George, F. Lotte, R. Viciana Abad, A. Lécuyer, "Using Scalp Electrical Biosignals to Control an Object by Concentration and Relaxation Tasks: Design and Evaluation", 33rd Annual International Conference of the IEEE Engineering in Medicine and Biology Society (EMBC'11), pp. 6299-6302, 2011

[50]. Ljung L., “System Identification toolbox: User’s Guide”, Mathworks inc., 2008

[51]. Lécuyer, F. Lotte, R. Reilly, R. Leeb, M. Hirose, M. Slater, “Brain-Computer Interfaces, Virtual Reality, and Videogames”, IEEE Computer, vol. 41, no. 10, pp 66-72, 2008

[52]. Lee, P.-L.; Wu, C.-H.; Hsieh, J.-C.; Wu, Y.-T.; , "Visual evoked potential actuated brain computer interface: a brain-actuated cursor system," Electronics Letters , vol.41, no.15, pp. 832- 834, 21 July 2005

[53]. Leeb R, Friedman D, Muller-Putz GR, Scherer R, Slater M, Pfurtscheller G.," Self-paced (asynchronous) BCI control of a wheelchair in virtual environments: a case study with a tetraplegic", Comput Intell Neuroscience, 2007

[54]. Leeb, R.; Pfurtscheller, G.; , "Walking through a virtual city by thought," *Engineering in Medicine and Biology Society, 2004. IEMBS '04. 26th Annual International Conference of the IEEE* , vol.2, no., pp.4503-4506, 1-5 Sept. 2004.

[55]. Li Ke; Junli Shen; , "Classification of EEG signals by ICA and OVR-CSP," Image and Signal Processing (CISP), 2010 3rd International Congress on , vol.6, no., pp.2980-2984, 16-18 Oct. 2010

[56]. Mak JN, Wolpaw JR, "Clinical Applications of Brain-Computer Interfaces: Current State and Future Prospects", IEEE Rev Biomed Eng 2, 2010

[57]. Martinez, Pablo; Hovagim Bakardjian,; Andrzej Cichocki,. "Fully online multicommand brain-computer interface with visual neurofeedback using SSVEP paradigm.(Research Article)." Computational Intelligence and Neuroscience. Hindawi Publishing Corp. 2007

[58]. McFarland DJ, Krusienski DJ, Wolpaw JR, "Brain-computer interface signal processing at the Wadsworth Center: mu and sensorimotor beta rhythms", Prog Brain Res 159,

[59]. McFarland DJ, Miner LA, Vaughan TM, Wolpaw JR, "Mu and beta rhythm topographies during motor imagery and actual movements", Brain Topogr 12(3): 177-86, 2000.

[60]. McFarland DJ, Sarnacki WA, Wolpaw JR, "Electroencephalographic (EEG) control of three-dimensional movement", J Neural Eng 7(3): 036007, 2010.

[61]. McFarland DJ, Wolpaw JR., "Brain-Computer Interfaces for Communication and Control", Commun ACM 54(5): 60-66, 2011.

[62]. McFarland DJ, Wolpaw JR., " Sensorimotor rhythm-based brain-computer interface (BCI): model order selection for autoregressive spectral analysis", J Neural Eng 5(2): 155-62, 2008.

[63]. Mcolin Cameron, "EXCEL 2007: Multiple Regression", Dept. of Economics, Univ. of California, retrieved from : http://cameron.econ.ucdavis.edu/excel/ex61multipleregression.html

[64]. McFarland, D.J.; Wolpaw, J.R.; , "Sensorimotor rhythm-based brain-computer interface (BCI): feature selection by regression improves performance," Neural Systems and Rehabilitation Engineering, IEEE Transactions on , vol.13, no.3, pp.372-379, Sept. 2005

[65]. Padmasai, Y.; Subba Rao, K.; Raghavendra Rao, C.; Sita Jayalakshmi, S.; , "Analysis of EEG Using Principal Component Approach," Electronics, Circuits and Systems, 2007. ICECS 2007. 14th IEEE International Conference on , vol., no., pp.134-137, 11-14 Dec. 2007

[66]. Palaniappan, R.; Paramesran, R.; Nishida, S.; Saiwaki, N.; , "A new brain-computer interface design using fuzzy ARTMAP," Neural Systems and Rehabilitation Engineering, IEEE Transactions on , vol.10, no.3, pp.140-148, Sept. 2002

[67]. Panicker, R.C.; Puthusserypady, S.; Ying Sun; , "An Asynchronous P300 BCI With SSVEP-Based Control State Detection," Biomedical Engineering, IEEE Transactions on , vol.58, no.6, pp.1781-1788, June 2011

[68]. Pfurtscheller G, Brunner C, Schlogl A, Lopes da Silva FH.,"Mu rhythm (de)synchronization and EEG single-trial classification of different motor imagery tasks", Neuroimage 31(1): 153-9, 2006.

[69]. Pfurtscheller G, Muller-Putz GR, Schlogl A, Graimann B, Scherer R, Leeb R, Brunner C, Keinrath C, Lee F, Townsend G, Vidaurre C, Neuper C," 15 years of BCI research at Graz University of Technology: current projects", IEEE Trans Neural Syst Rehabil Eng 14(2): 205-10, 2006.

[70]. Pfurtscheller G, Neuper C, Andrew C, Edlinger G., "Foot and hand area mu rhythms", Int J Psychophysiol 26(1-3): 121-35, 1997.

[71]. Pfurtscheller et al. , "EEG based discrimination between imagination of right and left hand movement", EEG clin NeuroPhysio 103(6): 642-51, 1998

[72]. Pfurtscheller G, Neuper C., "Motor imagery activates primary sensorimotor area in humans", Neurosci Lett 239(2-3): 65-8, 1998.

[73]. Pfurtscheller G., "Graphical display and statistical evaluation of event-related desynchronization (ERD)", Electroencephalogr Clin Neurophysiol 43(5): 757-60, 1978.

[74]. Pfurtscheller J, Rupp R, Muller GR, Fabsits E, Korisek G, Gerner HJ, Pfurtscheller G., "[Functional electrical stimulation instead of surgery? Improvement of grasping function with FES in a patient with C5 tetraplegial", Unfallchirurg 108(7): 587-90, 2005.

[75]. Pfurtscheller, G.; Neuper, C.; , "Motor imagery and direct brain-computer communication," Proceedings of the IEEE , vol.89, no.7, pp.1123-1134, Jul 2001

[76]. Piponnier, J.-C., Hanssens, J.-M., Faubert, J. ,Effect of visual field locus and oscillation frequencies on posture control in an ecological environment. Journal of Vision, 9(1):13, 1-10, 2009

[77]. Ptito, M., Kupers, R., Faubert, J., Gjedde, A. ,Cortical representation of inward and outward radial motion in man. NeuroImage., 14, 1409-1415, 2001

[78]. R F Hellbaum,T L Turner, "LC shutter glasses provide 3-D display for simulated flight", Information Display Magazine, Vol. 2, Issue 9, Sept. 1986

[79]. Raymond Carl Smith, " Electroencephalograph based Brain Computer Interfaces", M.Sc. Thesis from UNIVERSITY COLLEGE DUBLIN, Dublin, Ireland, 2004

[80]. Riechmann, H.; Hachmeister, N.; Ritter, H.; Finke, A.; , "Asynchronous, parallel on-line classification of P300 and ERD for an efficient hybrid BCI," Neural Engineering (NER), 2011 5th International IEEE/EMBS Conference on , vol., no., pp.412-415, April 27 2011-May 1 2011

[81]. Robert Leeb, Volker Settgastb, Dieter Fellnerb,c, Gert Pfurtschellera, "Self-paced exploration of the Austrian National Library through thought", International Journal of Bioelectromagnetism, Vol. 9, No.4, pp. 237 - 244, 2007

[82]. Samuel Vara Prasada Raju, G. Rajendra Kumar, D. Santhosh Kumar, "A Real Time EEG Signals for Brain and Computer Interface", IJECT Vol. 2, Issue 4, Oct . - Dec ., 2011.

[83]. Scherer R, Lee F, Schlogl A, Leeb R, Bischof H, Pfurtscheller G., "Toward self-paced brain-computer communication: navigation through virtual worlds", IEEE Trans Biomed Eng 55(2 Pt 1): 675-82, 2008.

[84]. Scherer R, Muller GR, Neuper C, Graimann B, Pfurtscheller G., "An asynchronously controlled EEG-based virtual keyboard: improvement of the spelling rate", IEEE Trans Biomed Eng 51(6): 979-84, 2004.

[85]. Sheikh H, McFarland DJ, Sarnacki WA, Wolpaw JR., "Electroencephalographic(EEG)-based communication: EEG control versus system performance in humans", Neurosci Lett 345(2): 89-92, 2003.

[86]. Shih JJ, Krusienski DJ, Wolpaw JR., "Brain-computer interfaces in medicine", Mayo Clin Proc 87(3): 268-79, 2012.

[87]. Sosa, O.A.P.; Quijano, Y.; Doniz, M.; Chong-Quero, J.E.; , "BCI: A historical analysis and technology comparison," Health Care Exchanges (PAHCE), 2011 Pan American , vol., no., pp.205-209, March 28 2011-April 1 2011

[88]. Sterman, M. B., D. A. Kaiser, et al. (1996). "Spectral analysis of event-related EEG responses during short-term memory performance." Biofeedback and Self-Regulation 21(4): 367-367.

[89]. Tatum, W. O., Husain, A. M., Benbadis, S. R., "Handbook of EEG Interpretation" Demos Medical Publishing, 2008

[90]. Thought technology, Flex comp infinity Hardware manual, retrieved on 6th sept. 2011, www.thoughttechnology.com

[91]. Townsend G, Graimann B, Pfurtscheller G., " A comparison of common spatial patterns with complex band power features in a four-class BCI experiment", IEEE Trans Biomed Eng 53(4): 642-51, 2006.

[92]. Townsend, G.; Graimann, B.; Pfurtscheller, G.; , "Continuous EEG classification during motor imagery-simulation of an asynchronous BCI," *Neural Systems and Rehabilitation Engineering, IEEE Transactions on* , vol.12, no.2, pp.258-265, June 2004

[93]. Vaughan TM, McFarland DJ, Schalk G, Sarnacki WA, Krusienski DJ, Sellers EW, Wolpaw JR., "The Wadsworth BCI Research and Development Program: at home with BCI", IEEE Trans Neural Syst Rehabil Eng 14(2): 229-33, 2006.

[94]. Vaughan TM, Wolpaw JR, Donchin E., " EEG-based communication: prospects and problems", IEEE Trans Rehabil Eng 4(4): 425-30, 1997.

[95]. Vuckovic, A. (2009). "Non-invasive BCI: how far can we get with motor imagination?" Clinical neurophysiology : official journal of the International Federation of Clinical Neurophysiology 120(8): 1422-1423

[96]. Wolpaw JR, McFarland DJ, Neat GW, Forneris CA., "An EEG-based brain-computer interface for cursor control", Electroencephalogr Clin Neurophysiol 78(3): 252-9, 1991.

[97]. Wolpaw JR, McFarland DJ, Vaughan TM., "Brain-computer interface research at the Wadsworth Center", IEEE Trans Rehabil Eng 8(2): 222-6, 2000.

[98]. Wolpaw JR, McFarland DJ., "Control of a two-dimensional movement signal by a non invasive brain-computer interface in humans", Proc Natl Acad Sci U S A 101(51): 17849-54, 2004.

[99]. Wolpaw JR., "Brain-computer interfaces as new brain output pathways", J Physiol 579(Pt 3): 613-9, 2007.

[100]. Yi-Hung Liu; Jui-Tsung Weng; Zhi-Hao Kang; Jyh-Tong Teng; Han-Pang Huang; , "An improved SVM-based real-time P300 speller for brain-computer interface," Systems Man and Cybernetics (SMC), 2010 IEEE International Conference on , vol., no., pp.1748-1754, 10-13 Oct. 2010

[101]. Yuanqing Li; Jinyi Long; Tianyou Yu; Zhuliang Yu; Chuanchu Wang; Haihong Zhang; Cuntai Guan; , "An EEG-Based BCI System for 2-D Cursor Control by Combining Mu/Beta Rhythm and P300 Potential," Biomedical Engineering, IEEE Transactions on , vol.57, no.10, pp.2495-2505, Oct. 2010

[102]. http://www.mathworks.com/help/bioinfo/ug/support-vector-machines-svm.html

[103]. http://eonreality.com/brochures/eon_icube_ld.pdf

[104]. EEG suite, thought technology Ltd., *http://www.thoughttechnology.com*

[105]. http://en.wikipedia.org/wiki/MATLAB

Appendix A: XML code

```
<?xml version="1.0"?>
- <TargetApplication>
    <Title>BCITunnel</Title>
    <Snapshot>BCITunnel.bmp</Snapshot>
    <Path>C:\BCI\bcitunnel.exe</Path>
    <Arguments>BCITunnel.exe</Arguments>
  - <Action>
      <ID>0</ID>
      <Description>Move forward</Description>
    </Action>
  - <Action>
      <ID>1</ID>
      <Description>Move backward</Description>
    </Action>
</TargetApplication>
```

Appendix B: Flex-comp infinity technical specifications

FlexComp Infiniti Encoder (SA7550)

Size (approx.)	130mm x 95mm x 37mm (5.1″ x 3.7″ x 1.5″)
Weight (approx.)	200g (7oz)
Power Source	4AA batteries, single use alkaline or NiMh Rechargeable
Supply Voltage	3.6V – 6.5V (fiber optic), minimum 4.0V (Compact Flash)
Battery Life, Alkaline cells	30h typical, 20h minimum
Low-battery warning	20 – 30 minutes of battery life remaining
Sensor supply voltage	7.260V ± 2mV
ADC output	14bits
Full-scale input range, DC	2.8V±1.696V
LSB magnitude	207µV
Encoder channel bandwidth (3dB) and sample rate	DC – 512Hz @ 2048 samples/second DC – 64Hz @ 256 samples/second DC – 64Hz @ 200 samples/second DC – 8Hz @ 32 samples/second DC – 8Hz @ 20 samples/second
Anti-aliasing Filter	5th order Butterworth
Alias rejection	30dB typical
DC gain accuracy	±0.5% (initial, or after self-calibration)
DC offset	±3LSB (initial, or after self-calibration)
Overall system accuracy	5%
Offset drift, calibration temperature ±10C	±5 LSB
Encoder noise	150µV RMS, 1mV p-p typical, offset removed

EEG-Z Sensor (SA9305Z)

Size (Approx.)	37mm x 37mm x 12mm (1.45″ x 1.45″ x 0.45″)
Weight (approx.)	25g (1oz)
Input Impedance	10GΩ in parallel with 10pF
Signal Input Range	0 –200µV
Sensitivity	$<0.1\mu V_{RMS}$
CMRR	>130dB
Channel Bandwidth	2Hz – 1kHz
Accuracy	$\pm0.3\mu V_{RMS}$, ±5% of reading @10°C to 40°C

Appendix C: Additional results in the BCI study

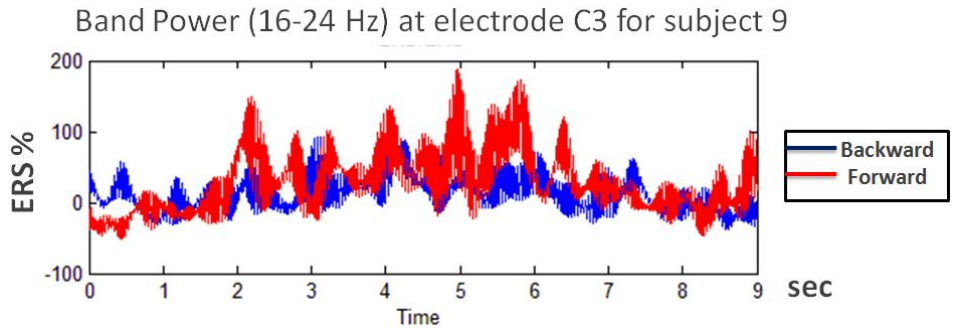

Session1	β -PSD ASSYMMETRICAL RATIO C3-C4						β- BAND-POWER OVER Cz						BP
			AR		ARX				AR		ARX		
Subject	LDA	SVM	LDA	SVM	LDA	SVM	LDA	SVM	LDA	SVM	LDA	SVM	
1	74.50	68.57	72.79	69.44	73.38	73.71	53.38	49.25	57.50	58.13	60.75	62.38	71.25
2	76.84	71.85	77.63	70.84	75.29	67.84	59.50	50.00	60.95	60.38	61.25	62.38	85.00
3	80.44	78.88	78.88	75.82	78.88	76.50	50.00	48.50	46.25	50.88	57.13	58.38	83.75
4	73.38	67.75	74.91	66.50	73.38	72.13	57.63	50.00	58.63	62.63	60.50	46.75	55.00
5	69.79	65.35	64.50	65.00	68.88	66.69	58.50	56.25	53.38	63.07	58.77	59.50	82.50
6	69.50	67.16	68.25	69.91	71.47	68.38	51.00	50.63	63.75	63.00	63.63	63.63	82.50
7	79.82	71.07	73.38	60.75	77.52	70.69	53.13	54.25	55.63	58.44	53.69	54.68	63.75
8	77.54	72.47	74.50	75.57	75.60	77.57	55.63	50.33	50.07	56.41	58.13	59.98	85.00
9	81.54	71.69	75.29	71.69	76.50	70.07	57.00	47.50	54.50	60.50	52.50	64.82	77.50
10	77.79	67.32	74.35	66.85	76.85	68.44	59.50	50.00	48.82	57.52	58.38	63.57	77.50
AV	76.11	70.21	73.45	69.24	74.77	71.20	55.53	50.67	54.95	59.10	58.47	59.61	76.38
STDEV	4.23	3.89	4.24	4.66	3.02	3.72	3.47	2.63	5.51	3.74	3.40	5.43	10.13